

CONCENTRATION DEPENDENT ^1H -NMR CHEMICAL SHIFTS OF QUINOLINE
DERIVATIVES

Adam Beck

A Thesis Submitted to the
University of North Carolina Wilmington in Partial Fulfillment
of the Requirements for the Degree of
Master of Science

Department of Chemistry and Biochemistry

University of North Carolina Wilmington

2007

Approved by

Advisory Committee

Chair

Accepted by

Dean, Graduate School

TABLE OF CONTENTS

ABSTRACT	iii
ACKNOWLEDGEMENTS	v
LIST OF TABLES	vi
LIST OF FIGURES	vii
INTRODUCTION	1
RESULTS AND DISCUSSION	19
Overview	19
Synthesis	20
Ring Position	36
Monomers vs. Dimers	44
Functional Hinge Groups	49
Computational Dipoles	51
CONCLUSION	56
EXPERIMENTAL	59
Synthesis of Aliphatic Monoester and Diester Quinoline Analogs	60
Synthesis of Aliphatic Monoether and Diether Quinoline Analogs	66
Synthesis of Benzyl Monoether and Diether Quinoline Analogs	74
Synthesis of Benzoyl Monoester and Diester Quinoline Analogs	79
Synthesis of Unsymmetrical Diesters	82
Synthesis of Aliphatic Monoamides	85
REFERENCES	87
APPENDIX	89

ABSTRACT

Quinolines are an important group of heterocyclic compounds that are found in many biologically active natural products and synthetic molecules. The non-exchangeable hydrogens of quinolines have been shown to have unusual concentration dependent chemical shift changes in $^1\text{H-NMR}$ studies. It is proposed that these changes are due to dipole-dipole and π - π interactions between two or more quinolines. The approach used to investigate the inter- and intramolecular π - π interactions of the quinoline protons in solution was to synthesize quinoline monomers and dimers substituted at the 6 and 8 positions and compare their concentration dependent chemical shifts of their aromatic protons. The quinoline dimers with C_3 , C_6 and C_{10} tethers were evaluated with respect to the substitution location, length of tether and functional group attaching the tether and the quinoline ring.

The concentration dependent chemical shifts ($\Delta\delta/\Delta C$) of the quinoline protons on the 6-substituted diquinoline diesters were smaller than those of the equivalent 6-monoesters. However, the 8-substituted diquinoline diesters had similar chemical shifts compared to the 8-monoesters. This data is consistent with the 6-substituted dimers being able to stack intramolecularly in an anti-parallel conformation. The $\Delta\delta/\Delta C$ of the 6-substituted diethers and the 8-substituted diethers were similar to their respective 6 and 8-substituted monoethers. This shows that while the position of the substituent contributes to inter- and intramolecular interactions, it is not the only determining factor. The 6-substituted monoethers supported $\pi - \pi$ stacking in an anti-parallel conformation with longer ether linkages creating more steric interference. The 8-substituted monoethers also supported π

– π stacking in an anti-parallel conformation with longer ether linkages hindering intermolecular lateral movement between rings.

ACKNOWLEDGEMENTS

I would like to thank Dr. Seaton for her guidance during this research. I feel I have learned a great deal in my experience here and attribute that to her knowledge, patience and understanding that makes her a truly great mentor. I would also like to Dr. Mitra for his contributions to this research and his thought provoking questions has always helped drive the motivation behind this work. From teaching labs to presenting at national conferences, the last two and a half years in graduate school has been a very unique challenge, which I will not forget.

Thank you Dr. Martin for your assistance to me and helping me to understand the computational aspect of this work I have discussed. I appreciate your willingness to make time for me when I had questions. Thank you Dr. Varadarajan for your help with my questions on synthesis and your insightful explanations, I found your Physical Organic class to be very valuable. I also need to thank Heather McCreery and Charisse Stephens for being so supportive and keeping me motivated when I needed it; you are both great friends.

I appreciate the opportunities given to me by the Chemistry Department and have enjoyed working with and around the faculty. There is no question as to why this department is as highly ranked as it is year after year as one of the top institutions. I am very happy that the environment created in this department was not a competitive one, but supportive and cooperative.

LIST OF TABLES

Table	Page
1. Synthesis of 6-substituted quinoline monoester and diesters (2 , 2a-c).....	21
2. Synthesis of 8-substituted quinoline monoester and diesters (4 , 4a-c).....	22
3. Synthesis of 6-substituted quinoline monoether and diethers (5a-f).....	23
4. Synthesis of 8-substituted quinoline monoether and diethers (6a-e).....	24
5. Synthesis of 6-benzyl and benzoyl monomers and dimers (7 , 7a , 8 , 8a-c).....	25
5. Synthesis of 8-benzyl and benzoyl monomers and dimers (9 , 9a , 10 , 10a-c).....	26
7. Synthesis of 6/8-unsymmetrical diester diquinolines (11a , 11b , 11c).....	27
8. Synthesis of 6-substituted quinoline monoamide (13)	27
9. Synthesis of 8-substituted quinoline monoamide (15).....	27
10. NMR assignments for monoester 2 using COSY and NOE data.....	28
11. NMR assignments for diester 2a using COSY and NOE data.....	29
12. NMR assignments for monoether 5a using COSY and NOE data.....	30
13. NMR assignments for diester 5e using COSY and NOE data.....	31
14. Comparison of calculated dipoles as semi-empirical, molecular orbital and density functional theory, values shown for selected 6 and 8-substituted mono and diquinoline derivatives.....	52

LIST OF FIGURES

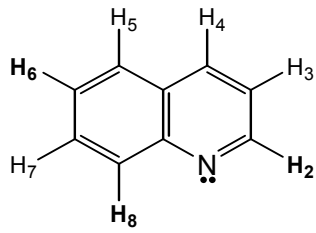
Figure	Page
1. Structures of Quinoline and the anti-malarial drug, Quinine	2
2. Anchoring of biomolecules onto a carbon nanotube through π bond interactions of aromatics. ¹	5
3. Polyarene transition metal complexes utilizing aromatic stacking to show intermolecular contact. ² A single polyarene d^8 Pd molecule and a multilayer polyarene d^8 Pd complex are shown.....	5
4. Molecular clip shown features a rigid diether aromatic scaffold ³ , constraining the opening of the clip to 10 Å. The lower diagram shows it in closed form, making the complex with <i>p</i> -dinitrobenzene. The distance between one side of the host and the guest molecule is 3.8 Å.....	10
5. Proposed molecular clips shown feature flexible linkers. 6-Diester diquinoline (A) shown with C ₆ linker complexing with <i>p</i> -dichlorobenzene. 6-Diether diquinoline (B) shown with C ₆ linker complexing with tetrachlorobenzene.	10
6. Electrostatic surface potential maps of aromatic systems showing their respective polarizabilities. 1,5-dialkoxynaphthalene is shown to display high degree of electron richness within the ring system, whereas 1,4,5,8-naphthalenetetracarboxylic diimide displays strong electropositive character in its center....	12
7. Simple conformational geometries of quinoline monomers and dimers (no tether is shown for dimers). Quinolines are aligned point-to-point with the arrow along the z-axis. The proposed anti-parallel stacking model (ii) is aligned with crossing dipoles. The ¹ H-NMR investigation of quinoline derivatives in solution represents an average of these conformations.....	14
8. Conformations of tethered quinoline dimers, accepted (A) and non-accepted (B). The tethered conformation of the 8-dimer is not allowed due to steric strain. Specific functional groups on the linkers are not shown in this case.....	18
9. (A) Stacked ¹ H-NMR plots showing the $\Delta\delta$ for the aromatic protons through a range of concentrations (0.5 M – 0.16 M in CDCl ₃) on 8-monoester 4 . (B) $\Delta\delta$ vs. Δ Concentration to yield slopes for aromatic protons on 8-monoester 4 . The $\Delta\delta/\Delta C$ slopes for the all products are shown in Appendix 1-12.....	33
10. $\Delta\delta/\Delta C$ for quinoline protons on 6- and 8- quinoline analogs. Both dimers shown have C ₁₀ hydrocarbon tethers and diester linkages. Both monomers are acetyl acetate esters.	35

11. Concentration dependence for proton H4 of monoquinoline derivative products. 6-Quinoline monomers are shown in blue (front) and 8-quinoline monomer are shown in red (back). The absolute values are shown on the Z-axis for the scale of $\Delta\delta/\Delta C$	38
12. A series of 6-substituted quinoline rings showing favorable anti-parallel conformation with shorter ether linkages: (A-D) 6-monoethers 5a-c, 8 . A series of 8-substituted quinoline rings showing favorable anti-parallel conformation with longer ether linkages: (E-H) 8-monoethers 6a-c, 10	39
13. Concentration dependence for proton H4 of symmetrical and unsymmetrical diester quinoline derivatives. The H4 proton on the 6-quinoline rings are shown in blue (front) and H4 proton on the 8-quinoline ring are shown in red (back). For corresponding tethers with hydrocarbon tethers, the number of carbon atoms is shown (<i>n</i>). The absolute values are shown on the Z-axis for the scale of $\Delta\delta/\Delta C$	42
14. Area specific plots of $\Delta\delta/\Delta C$ for proton H4 of symmetrical and unsymmetrical diester quinoline derivatives vs. the equivalent monomer. (A) C ₆ -tethered diesters. (B) C ₁₀ -tethered diesters. (C) Phthalate diesters. All plots show significantly reduced $\Delta\delta/\Delta C$ for 4H of the 8-quinoline ring on unsymmetrical products.....	43
15. Concentration dependence for proton H4 of monoquinoline vs. diquinoline products. Dimers are shown in blue (front) and monomers are shown in red (back). For corresponding tethers with hydrocarbon tethers, the number of carbon atoms in the tether is shown (<i>n</i>). The absolute values are shown on the Z-axis for the scale of $\Delta\delta/\Delta C$	47
16. Concentration dependence for proton H4 of diquinoline derivatives. 6-Quinoline dimers are shown in blue (front) and 8-quinoline dimer are shown in red (back). For corresponding tethers with hydrocarbon tethers, the number of carbon atoms is shown (<i>n</i>). The absolute values are shown on the Z-axis for the scale of $\Delta\delta/\Delta C$. 8-Quinoline benzyl diether (para) and diether (n=3) were not synthesized.....	48
17. (A) Concentration dependence for aromatic protons on the 6-quinoline monomer and dimers: 2, 2a, 5b, 5e . (B) Concentration dependence for the aromatic protons on the 8-quinoline monomer and dimers: 4, 4a, 6b, 6d . The alkyl diesters and diethers have a C ₆ linker and the absolute values are shown on the y-axis for the scale of $\Delta\delta/\Delta C$	50
18. Electrostatic potential maps for 6 and 8-quinoline monomers (2, 4, 5b, 6b). Structures were geometry optimized at the semi-empirical / AM1 level followed by a single point HF / 6-31G** calculation. Dipole calculations were recorded at both levels for comparison, indicated by arrows. Calculations were performed on Titan (ver 1.0.1., 1999) by Wavefunction and Schrodinger, Inc.....	54
19. X-Ray crystal structure of 6-substituted diquinoline diester: 2c	55

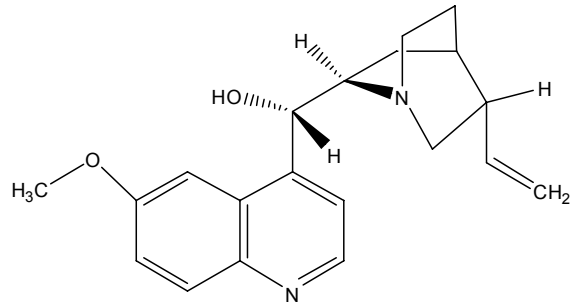
INTRODUCTION

Quinolines (Figure 1) are an important group of heterocyclic compounds that are used extensively as intermediates in the synthesis of many biologically active natural products and synthetic compounds.⁴⁻⁸ Quinine (Figure 1) is a natural product which was used for many years for the treatment of malaria.⁹ Several synthetic analogs of quinine, such as Chloroquine[®] and Amodiaquine[®] and Mefloquine[®] are also powerful drugs for the treatment of malaria.¹⁰ Currently, the interruption of heme detoxification in the red blood cell is the most conventional theory of quinoline derived drug treatments of parasitic infections such as malaria.¹¹ Quinoline based heterocycles also have medicinal uses in the treatment of lupus, arthritis and HIV related illnesses, however the mechanisms behind these activities are not well known.¹² A better understanding of quinolines role when interacting with biological systems could help determine these mechanisms and which intermolecular forces are influencing them.

Certain quinoline derivatives are also able to bind metals, such as zinc and copper, and are being tested for use as probes for metals in natural waters and in treatment of medical disorders, such as Alzheimer's disease, which involve accumulation of metal ions in tissues.¹³ The synthesis of new metal complexes with quinoline derived antibacterial compounds are important in order to understand their drug-metal ion interactions and because of their potential applications in pharmaceuticals. The solution chemistry of fluorescent quinoline-based zinc probes, for example, could benefit from an understanding of interactions of quinoline with itself and with the metal.¹⁴



Quinoline



Quinine

Figure 1: Structures of quinoline and the anti-malarial drug, quinine.

Nuclear magnetic resonance spectroscopy (NMR) illustrates how quinoline molecules interact with other molecules in solution. ¹H-NMR provides information about the chemical environment each hydrogen atom of the molecule experiences. Through NMR studies, it has been observed that interaction of quinoline derivatives with each other results in interesting concentration dependent NMR behavior, which is proposed to arise through aromatic stacking interactions.¹⁵ These concentration dependent chemical shift changes differ significantly from chemical shift variations that are temperature or solvent dependent. It is important to understand the forces that are behind this stacking behavior and how much they contribute to the solution structure and the overall interaction energy.

Aromatic stacking in quinoline is based on the self-associative properties of the nonpolar heterocyclic ring system and does not involve H-bonding. The nature of these interactions that affect the intermolecular stabilization is not defined, nor is the extent to which the π - π stacking effect determines the three dimensional structure of the associated molecules. However, aromatic stacking has been found to contribute to the behavior of molecules in fields related to biochemistry, coordination chemistry and nanotechnology. For instance, it has been shown that aromatic stacking may play an important role in sugar binding by membrane transport proteins, such as the hydrophobic face to face stacking of the galactopyranosyl ring between Trp 151 and Cys 148 providing interhelix support in the protein LacY.¹⁶ Aromatic stacking has been shown computationally to be highly correlated to H-bonding between the nitrogen (N3) and oxygen atoms of cytosine, within the DNA double helix.¹⁷ The majority of studies done on aromatic stacking use an aqueous environment to represent biological conditions. It is widely reported that, in

aqueous solutions, hydrogen bonding and the hydrophobic effect both play a large role in explaining why stacking occurs. There is evidence that intramolecular heteroaromatic attractions in an aqueous systems are strongly due to the dipoles or multipoles located in the molecule.¹⁸ In aprotic nonpolar solutions of neutral molecules, the effect of H-bonding is limited to the solute molecules so that the hydrophobic effect is minimized. Thus the noncovalent inter- and intramolecular interactions such as dipole-dipole, electrostatic and London dispersion forces become more important in aprotic, nonpolar solutions. The dipole moments of different quinoline derivatives can vary significantly,¹⁹⁻²¹ therefore conformations based on dipole-dipole interactions are subject to placement of various substituents on the quinoline rings.

Noncovalent forces are also being more thoroughly investigated and applications are being developed based on π -stacking. An example of one application is the immobilization of biomolecules onto carbon nanotubes,¹ where the anchoring system used is based on the noncovalent π -bond interactions (Figure 2). Using noncovalent forces in this way is beneficial to the structural and electronic integrity of the nanotubes, even though the electron transport character is highly dependent on the π -bound molecule.²²

Furthermore, π - π interactions have helped determine structural features of polyarene transition metal compounds,² as in some d^8 Pd complexes (Figure 3). Also, the design of multilayer aromatic systems have been aided by the addition of specific metals, such as the anthracene-silver (I) complex.²³

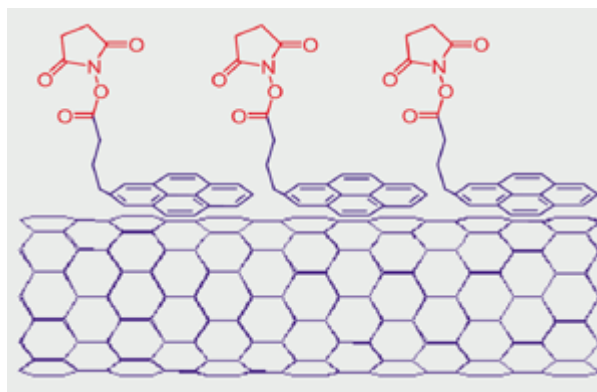


Figure 2: Anchoring of biomolecules onto a carbon nanotube through π bond interactions of aromatics.¹

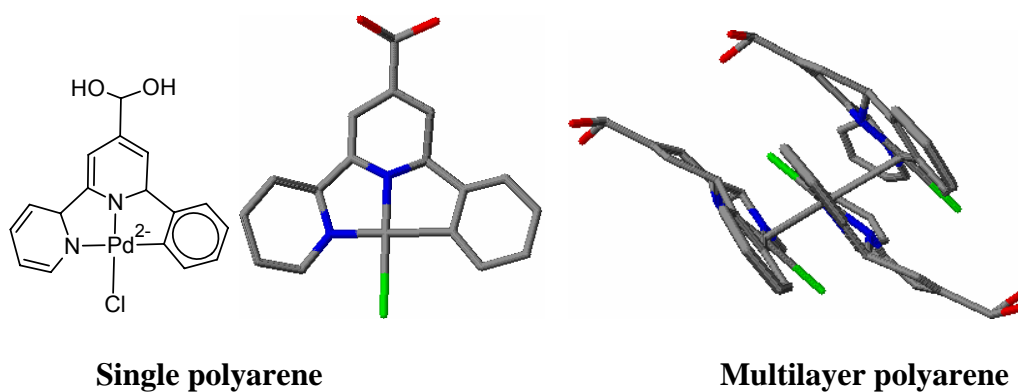


Figure 3: Polyarene transition metal complexes utilizing aromatic stacking to show intermolecular contact.² A single polyarene d⁸ Pd molecule and a multilayer polyarene d⁸ Pd complex are shown.

In the field of supramolecular chemistry, structures are formed around noncovalent bonding interactions, in which many multi-aromatic complexes exist. There are many potential applications regarding the use of supramolecular dimers, such as encapsulation and complexation through host-guest interactions. Most dimers in this field to date have been based on the use of hydrogen bonding and coordination with metals.²¹ There have been many studies on π - π stacking^{15,24-26} and dipole-dipole interactions^{20,21,27} in supramolecular complexes, but very few experiments have been designed around these forces. One recent study investigates the intramolecular interactions within 1,8-diacridylnaphthalene *N,N'*-dioxides as a clathrate host and a variety of guest molecules, which proposes that guest molecules with larger dipoles have more electrostatic repulsion resulting in a higher degree of instability between the host-guest complex.²⁰ This is, perhaps, because there are questions concerning which π - π stacking models are applicable, depending on the conditions of the experiment. The entropically favorable contributions that arise from the aggregation of π systems in aqueous solution are minimized in organic solvents. This is supported by the number of observations that report an offset face to face stacking arrangement, whereas the solvophobic model predicts a maximum overlap of π - π interactions.²⁸ It is possible that an electron donor-acceptor type of action is taking place, but this implies that inter- or intramolecular charge transfer complexes have formed, which do not completely describe the lowest energy conformations of the monomers and dimer. There is also an atomic charge model which predicts that π - π interactions between any two molecules may be based on the attraction of opposing atomic charges, favoring electrostatic interactions. While this can not be completely ruled out, it has been shown computationally that this model did not

favor any conformation over another.²⁸ This narrows the attraction forces down to dipole-dipole, electrostatics and van der Waals interactions, which are also influenced by each other.

It is difficult to predict the amount of electrostatic influence that is contributed from polar, aprotic solvents to the overall interaction energy. If it is true that van der Waal forces that are derived from overlapping π orbitals can donate significantly to the $\pi - \pi$ interaction energy, then they should strongly determine the geometry of aromatic stacking in a direct face-to face arrangement in order to maximize overlap. However, in the case of the benzene dimer and substituted benzene dimers, the most computational favorable stacking conformation is an offset facial conformation and sometimes a edge to face conformation.²⁹ This would lead to the geometry being controlled by the dipole interactions or electrostatic contribution, since benzene has no dipole, but does not limit the magnitude of the attraction in π system to just these two forces.

Additional examples of the role of $\pi - \pi$ stacking come from a sub section of supramolecular chemistry where molecular clips or tweezers have been designed (Figure 4), originally from derivatives of caffeine.³⁰ These derivatives serve the purpose of binding with a guest molecule or binding intermolecularly with themselves and forming much larger supramolecules. Molecular clips work on the principle of forming noncovalent bonds through the tips of the receptor part of the molecule. The process of forming novel host-guest complexes or clathrates is important because it may provide a different method for separation or purification of molecules with high selectivity, and is relatively simple and economic. The host-guest molecule approach is designed around the noncovalent binding of one planar molecule that is electron rich with an electron poor

molecule, or usually binding of charged species, such as ions or metals. There is evidence that electron rich aromatics, used as molecular clips, will complex with electron-deficient aromatic substrates (Figure 4), using π - π and CH- π interactions.³ It has been proposed that the size and shape of the space between the clips plays a large role in how well it will bind to its guest and that the more van der Waals contact surface there is between the host and guest, the stronger the complexation will be.³¹

There are three components to a dimer or “molecular clip” to consider: the two aromatic portions supplying the π - π interactions, the linker that tethers them together and the point of functionality at which the aromatic section connects to the linker. The rigidity of the linker module is thought to enhance host-guest complexation. In fact, the concept of guest binding to molecular tweezers was based on three main elements: 1) a tether that prevents self-association, 2) a plane to plane distance of about 7 Å between the receptors, and 3) a tether that keeps the receptors in a syn conformation.³⁰ However, an inflexible linker limits the host molecule to binding strongly with only a very limited species of guest. A linker with strict rigidity is not mandatory, yet in order to maintain favorable π - π interactions, molecular clips with flexible linkers may not be able to overcome the energy hurdle to conform to a sterically unfavorable position if the conformation of the folded dimer is entropically unfavorable.³²

Tethered quinolines with flexible linkers may also have binding capabilities, either intramolecularly between rings or intramolecularly with a guest molecule. It is difficult to predict how different functional groups on the hydrocarbon tethers will influence the ability of the quinoline dimer to form host-guest complexes in solution. For example, the diester linkage (Figure 5 – **A**) may be more sterically hindered than its ether counterpart

(Figure 5 – **B**), which may prevent tweezer formation. The functional group also affects the electron richness of the host quinoline rings, but provides no basis for predictions made on favorable complexes since the overall contributions made by these interactions are not well defined.

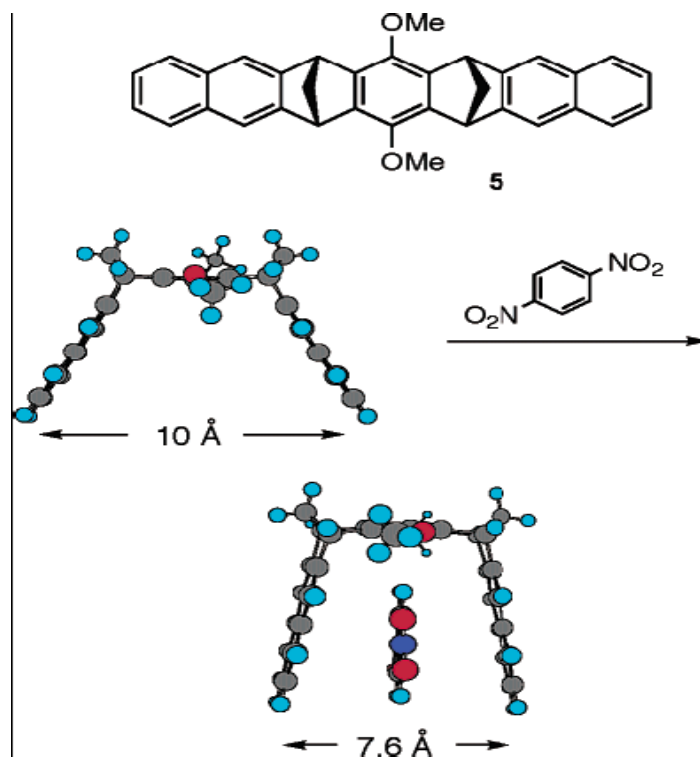


Figure 4: Molecular clip shown features a rigid diether aromatic scaffold³, constraining the opening of the clip to 10 Å. The lower diagram shows it in closed form, making the complex with *p*-dinitrobenzene. The distance between one side of the host and the guest molecule is 3.8 Å.

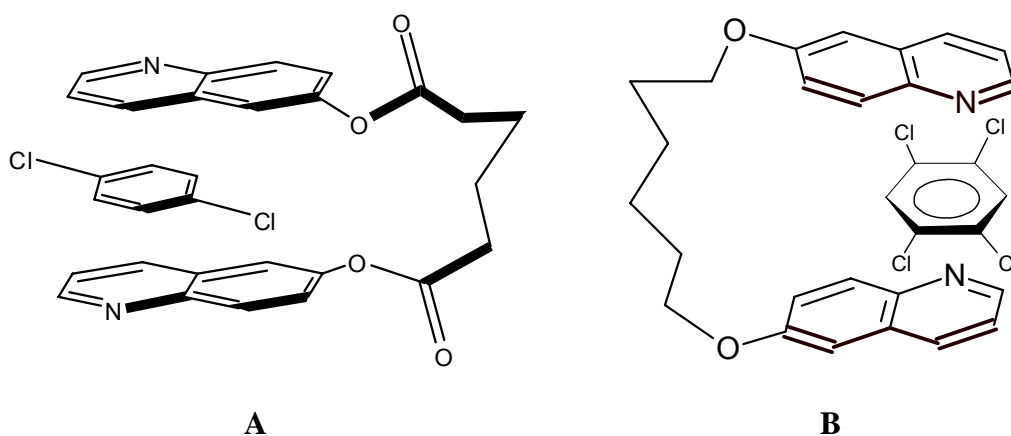


Figure 5: Proposed molecular clips shown feature flexible linkers. 6-Diester diquinoline (A) shown with C₆ linker complexing with *p*-dichlorobenzene. 6-Diether diquinoline (B) shown with C₆ linker complexing with tetrachlorobenzene.

Many supramolecular compounds exist in a crystalline state where the inter- and intramolecular interactions are more evident.^{31,33,34} In solution, a variety of conditions may exist (polarity, H-bonding, electrostatics) which affect the properties of monomers and dimers that interact with each other. In polar solvents, the two competing theories for self association are based on electrostatics and the hydrophobic effect. It has been reported that there is an increase in association constants as the polarity of the solvent increases, which is in favor of the hydrophobic effect, but the electrostatic contributions are still mentioned to be significant.³ In other words, the electrostatic interactions are proposed to play a large role in controlling the stacking geometry or the conformation of the foldimer. This stacking conformation of the dimer molecule is also thought to determine the magnitude of desolvation in aqueous solution. If the electrostatic interactions significantly contribute to the solution state structure of these aromatic systems, then it is important to look at the electrostatic potential maps for aromatic dimers compounds under investigation (Figure 6). A visualization of the electrostatic potential map of a compound is helpful to determine where chemical reactions might take place and the theoretical disbursement of electrons over the molecular surface.

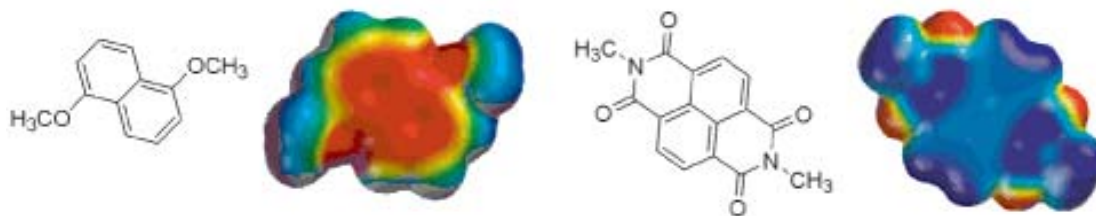


Figure 6: Electrostatic surface potential maps of aromatic systems showing their respective electrostatic potentials. 1,5-Dialkoxynaphthalene is shown to display high degree of electron richness within the ring system, whereas 1,4,5,8-naphthalenetetracarboxylic diimide displays strong electropositive character in its center. Calculated using semi-empirical AM1 method for simple visual comparison. (*Shown without permission*).³

It is proposed that in addition to π - π stacking interactions, electrostatic or dipole-dipole interactions both play a role in concentration dependent behavior of quinolines. It is also proposed that, in solution, one quinoline ring stacks on top of another, so that the each nitrogen is across from the carbon at the H-4 position of the opposing ring¹⁵ in the face-to-face anti-parallel conformation (Figure 7 – **ii**). The dipoles of the quinoline rings are in opposite directions in this conformation. There are three other face-to-face stacking conformations which might play a role in the association of quinoline molecules in solution (Figure 7 – **i, iii, iv**). The π - π interactions may behave differently depending on the conformation of the quinolines in solution. There are several other models that illustrate various conformations of stacking behavior (Figure 7). One such model shows simple quinoline monomers experience face-to-face interactions where the nitrogen of the pyridine ring is opposite to the nitrogen of the second pyridine ring in a slightly offset position (**iv**). Interactions to yield configurations where the benzene ring is over the pyridine ring of quinoline (Figure 7 – **v, vi**), as parallel nitrogen stacking (**i, iii**) or t-shaped (**vii, viii**) might also be possible, although, the t-shaped structures do not fit the NMR data of various substituted quinolines.¹⁵ The lone pair of electrons on individual quinolines would add to the shielding effect experienced by the neighboring H-4 proton, thus giving it a lower chemical shift than protons: H-3, H-5, H-6, and H-7. In an anti-parallel stack, an upfield chemical shift would be noticed by the H-4 proton, which is located spatially across from the nitrogen on the opposing ring. Thus, for H-4 protons stacked in anti-parallel conformations (**ii, iv**), higher concentration solutions contain a higher proportion of stacked quinolines, which results in lower chemical shifts, as is observed.¹⁵

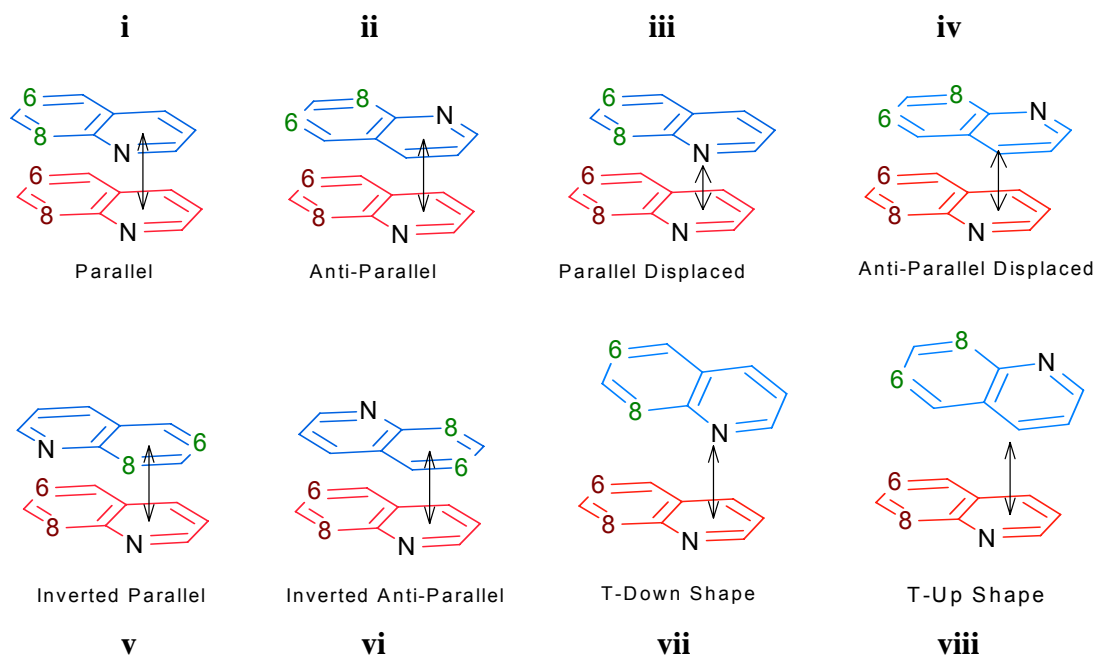


Figure 7: Simple conformational geometries of quinoline monomers and dimers (no tether is shown for dimers). The ends of each arrow indicate the alignment of the quinoline rings, with respect to each other, along the z-axis. The proposed anti-parallel stacking model (**ii**) is aligned with crossing dipoles. The $^1\text{H-NMR}$ investigation of quinoline derivatives in solution represents an average of these conformations.

Concentration dependent chemical shifts of quinoline protons have been documented^{15,24,35}, yet the reason for these shifts is not fully understood. In NMR samples, at low concentrations, quinoline monomers should act independently of each other, whereas at high concentrations, protons on the quinoline experience a different magnetic field because of the proposed stacking interactions and display different NMR patterns. If quinolines could be tethered together, so that the quinoline rings would stack intramolecularly, then the chemical environment of quinoline dimer protons should not change significantly and should be much less concentration dependent. In this case, the behavior of tethered quinolines should help elucidate the solution state structure of quinolines.

Our research was designed to look for evidence to distinguish between the inverted (Figure 7 - **v**, **vi**) and the non-inverted (**i**, **ii**, **iii**, **iv**) conformations of quinoline dimers. Energy calculations on pyridine molecules have shown an energetically favorable conformation of anti-parallel displaced pattern³⁶ (Figure 7 - **iv**), where the nitrogen of one pyridine is directly over the H-4 of the second pyridine ring. This pattern may also contribute to the solution structure of our quinolines and be prevalent in our study of diquinoline analogs. Distinguishing experimentally between face-to-face and displaced geometries as well as quantifying the percent contribution of each conformer is beyond the scope of this research.

One experimental approach to trying to distinguish between possible stacking models is to synthesize tethered quinolines (Figure 8) and analogous monomers, and investigate concentration dependence by ¹H-NMR of quinoline monomers and dimers. Whether the tethered quinolines are able to self associate will depend on the position on

the ring where they have been tethered. The stacking of tethered quinolines is dependent upon three conditions: 1) the position on the ring where the chain is attached, 2) the length of the connecting hydrocarbon chain and 3) the functional group connection between the ring and the chain. The simple quinolines are not hindered from stacking with another quinoline and displaying concentration dependent chemical shifts. It is proposed that quinoline dimers, which are able to interact inter- and intramolecularly, would not behave similar to their equivalent monomers. If intramolecular interactions are favorable, then the extent of concentration dependent shifts should be lower than for simple quinolines or tethered quinolines where intramolecular stacking is not possible. However, if the stacked conformation is favorable, there would be only a small dependence on concentration when two quinolines are tethered together so that they fold into the stackable conformation. However, when linked by a hydrocarbon chain of suitable length, quinolines can stack inter- or intramolecularly. As shown in Figure 7, models shown in non-inverted conformations **i-iv** that have quinolines connected through a tether of 5-14 atoms at C-2, C-3, C-6 and C-7 positions could stack intramolecularly, but could not in the inverted conformations **v-viii** because the linker would experience too much strain to wrap around the dimer complex. However, quinolines connected at C-4, C-5 and C-8 positions on the ring should only be able to stack in parallel conformations (Figure 7 - **i, iii, v**) so that the H-8 protons are not in a cross ring location to each other.

The goal of this research was to determine the behavior or solution structure of heterocyclic aromatic compounds in solution, specifically regarding π - π intramolecular stacking. The proposed method to evaluate this behavior was to synthesize multiple quinoline dimers and monomers that could be used to compare three main variables, each

of which could ease or hinder ring stacking. The products synthesized vary in 1) the ring position of the substituent, 2) the length of hydrocarbon tethering chain and 3) the hinge functional group connecting the hydrocarbon linker to the aromatic rings. Comparison of the $^1\text{H-NMR}$ chemical shifts of the monomer and dimer products, through a range of concentrations, was used to evaluate their behavior.

A hydrocarbon tether may allow (Figure 8 - **A**) or hinder (Figure 8 - **B**) intramolecular stacking of quinolines. In order to determine the extent that the hydrocarbon chain length hinders the interaction of the two quinoline structures, tethered quinoline derivatives containing C_3 , C_6 and C_{10} linkers were compared. The hinge group, which connects the hydrocarbon chain to the aromatic, may function to facilitate stacking or prevent it through steric strain, but may also change the electrostatic nature and the overall dipole of the molecule. In this study, ester and ether hinge functional groups were compared, as well as amides.

The monomer analogs were used as a control in the comparison to the diquinoline products. It is proposed that the monomers would show a greater change in chemical shift as a function of concentration, whereas dimer analogs capable of intramolecular stacking would show a smaller change in chemical shift since their intramolecular stacking is not concentration dependent.

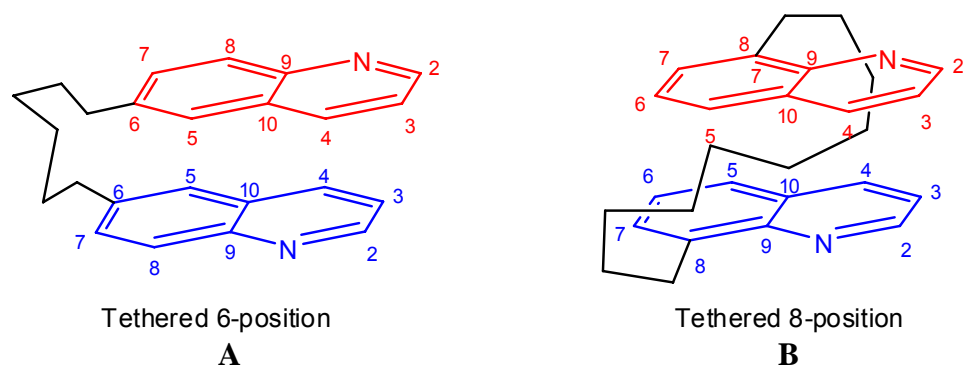


Figure 8: Conformations of tethered quinoline dimers, accepted (**A**) and non-accepted (**B**). The tethered conformation of the 8-dimer is not allowed due to steric strain. Specific functional groups on the linkers are not shown in this case.

RESULTS AND DISCUSSION

Overview

To account for the effect of chain length, location of substituent and functional hinge group on the stacking abilities of tethered quinolines in solution, a series of over 30 quinoline derivatives were synthesized (Tables 1-7, **1-12c**). Products were purified by flash column chromatography (FCC) for $^1\text{H-NMR}$ studies to compare the effect of ring position, functional groups and chain lengths on concentration dependent chemical shifts. Molecular models predicted that dimers substituted in the 6- position would be able to conform to a planar anti-parallel aromatic stacking conformation (Figure 8 - **A**), whereas dimers in the 8- position would not, due to strain (Figure 8 - **B**).

The basis for this investigation on concentration dependence is founded on opposing dipole-dipole interactions that favor an anti-parallel conformation, which display $\pi - \pi$ stacking behavior. The 6 and 8 positions were chosen because substituents attached to these positions would be less likely to interfere with the dipole moment of the quinoline, specifically the pyridine section of the molecule and also because of synthetic considerations and availability of starting materials. Preliminary computational studies performed at low levels give variable results and thus may not accurately represent the dipole moment for the compounds studied. Also, the molecular dipole moment may not provide a complete explanation of these $\pi - \pi$ interactions since these dimerized compounds contain multiple dipoles or multipoles. However, it is reasonable to assume that dipole-dipole interactions contribute favorably to stacking amongst quinoline derivatives since it dipole-dipole interaction energies are significantly larger than electrostatic effects or van der Waal forces.

Synthesis

A considerable amount of effort was put into synthesizing, purifying and characterizing the quinoline monomers and dimers reported in this study. For the esters, a solution of 6-hydroxyquinoline (**1**) or 8-hydroxyquinoline (**2**) and triethylamine was reacted with a monoacid chloride or diacid chloride under argon to yield its respective monoester or diester products (Table 1 – **2-2c**, Table 2 - **4-4c**). For the ethers, a solution of **1** or **2** and potassium carbonate was reacted with an alkyl halide or alkyl dihalide under argon to yield its respective monoether or diether compounds (Table 3 – **5a-5f**, Table 4 – **6a-6e**). For the benzoyl esters, a solution of **1** or **2** and triethylamine was reacted with benzoyl chloride or phthalyl dichloride under argon to yield its respective benzoate monoester or phthalate diester products (Table 5 – **7-7a**, Table 6 - **9-9a**). For the benzyl ethers, a solution of **1** or **2** and potassium carbonate was reacted with benzyl chloride or xylylene dichloride under argon to yield its respective benzyl monoether or diether compounds (Table 5 – **8-8c**, Table 6 - **10-10c**). All products were purified by acid/base extractions followed by flash column chromatography and, in some cases, crystallization. The purified compounds were recovered in moderate to good yield (36-83%).

All protons of each compound were assigned using 1D and 2D NMR experiments including COSY and NOE. The carbon signals of each compound were assigned using a combination of the ^{13}C -NMR data and the heteronuclear single quantum and multiple bond correlations (HSQC, HMBC). As examples, the protons and carbons for select monomers and dimers (**2**, **2a**, **5a**, **5e**) were assigned using this method (Tables 10-13).

Table 1: Synthesis of 6-substituted quinoline monoester and diesters.

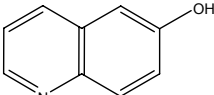
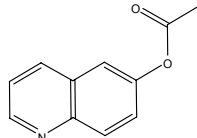
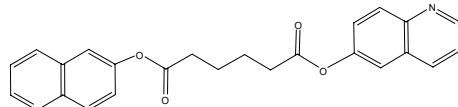
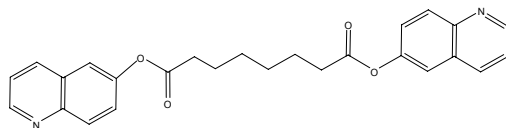
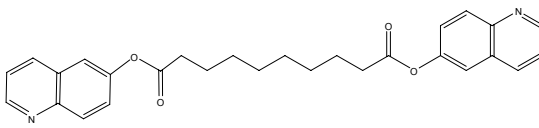
#	Quinoline Reagent	Synthesis Route	Quinoline Product	#
1		$\xrightarrow[\text{Et}_3\text{N, CH}_2\text{Cl}_2, 25\text{ C, 16 hrs}]{\text{CH}_3\text{CO-Cl}}$		2
		$\xrightarrow[\text{Et}_3\text{N, CH}_2\text{Cl}_2, 25\text{ C, 20 hrs}]{\text{Cl-CO(CH}_2)_4\text{OC-Cl}}$		2a
		$\xrightarrow[\text{Et}_3\text{N, CH}_2\text{Cl}_2, 25\text{ C, 22 hrs}]{\text{Cl-CO(CH}_2)_6\text{OC-Cl}}$		2b
		$\xrightarrow[\text{Et}_3\text{N, CH}_2\text{Cl}_2, 25\text{ C, 25 hrs}]{\text{Cl-CO(CH}_2)_8\text{OC-Cl}}$		2c

Table 2: Synthesis of 8-substituted quinoline monoester and diesters.

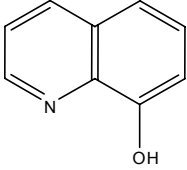
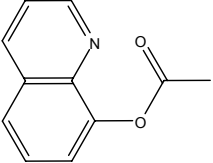
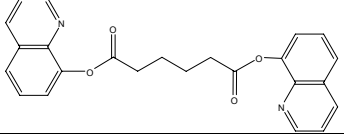
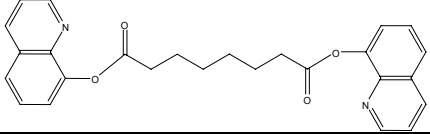
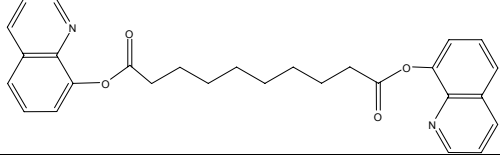
#	Quinoline Reagent	Synthesis Route	Quinoline Product	#
3		$\xrightarrow[\text{Et}_3\text{N, CH}_2\text{Cl}_2]{\text{CH}_3\text{COCl}}$ 25 C, 24 hrs		4
		$\xrightarrow[\text{Et}_3\text{N, CH}_2\text{Cl}_2]{\text{Cl-CO(CH}_2)_4\text{OC-Cl}}$ 25 C, 32 hrs		4a
		$\xrightarrow[\text{Et}_3\text{N, CH}_2\text{Cl}_2]{\text{Cl-CO(CH}_2)_6\text{OC-Cl}}$ 25 C, 22 hrs		4b
		$\xrightarrow[\text{Et}_3\text{N, CH}_2\text{Cl}_2]{\text{ClCO(CH}_2)_8\text{OCCI}}$ 25 C, 16 hrs		4c

Table 3: Synthesis of 6-substituted quinoline monoether and diethers.

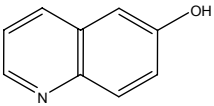
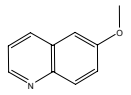
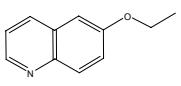
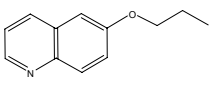
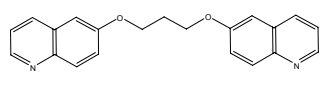
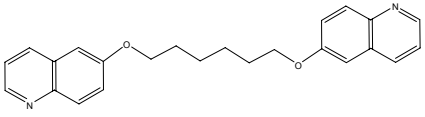
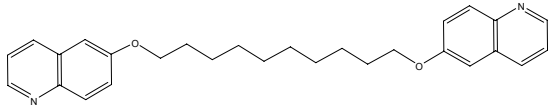
#	Quinoline Reagent	Synthesis Route	Quinoline Product	#
1		$\xrightarrow{\text{ICH}_3}$ NaH, 20% DCM / DMF 25 C, 24 hrs		5a
		$\xrightarrow{\text{ICH}_2\text{CH}_3}$ NaH, DMF 25 C, 24 hrs		5b
		$\xrightarrow{\text{ICH}_2\text{CH}_2\text{CH}_3}$ NaH, DMF 25 C, 18 hrs		5c
		$\xrightarrow{\text{Br}-(\text{CH}_2)_3-\text{Br}}$ K ₂ CO ₃ , DMF 97 C, 24 hrs		5d
		$\xrightarrow{\text{Br}-(\text{CH}_2)_6-\text{Br}}$ K ₂ CO ₃ , DMF 65 C, 24 hrs		5e
		$\xrightarrow{\text{Br}-(\text{CH}_2)_{10}-\text{Br}}$ K ₂ CO ₃ , DMF 90 C, 20 hrs		5f

Table 4: Synthesis of 8-substituted quinoline monoether and diethers.

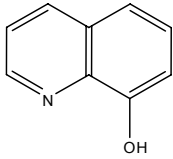
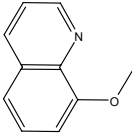
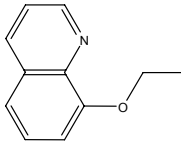
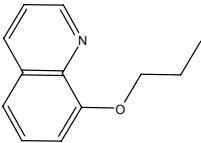
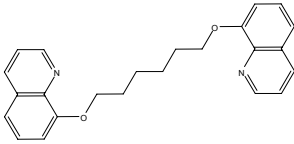
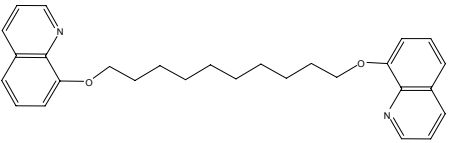
#	Quinoline Reagent	Synthesis Route	Quinoline Product	#
3		$\xrightarrow[\text{NaH, THF}]{\text{ICH}_3}$ 25 C, 16 hrs		6a
		$\xrightarrow[\text{NaH, THF}]{\text{ICH}_2\text{CH}_3}$ 25 C, 12 hrs		6b
		$\xrightarrow[\text{NaH, DMF}]{\text{ICH}_2\text{CH}_2\text{CH}_3}$ 25 C, 4 hrs		6c
		$\xrightarrow[\text{K}_2\text{CO}_3, \text{DMF}]{\text{I}-(\text{CH}_2)_6-\text{I}}$ 95 C, 21 hrs		6d
		$\xrightarrow[\text{K}_2\text{CO}_3, \text{DMF}]{\text{I}-(\text{CH}_2)_{10}-\text{I}}$ 95 C, 16 hrs		6e

Table 5: Synthesis of 6-substituted quinoline benzoyl monoester and diesters. Synthesis of 6-substituted quinoline benzyl monoether and diethers.

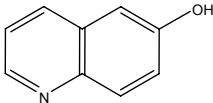
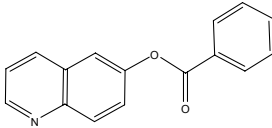
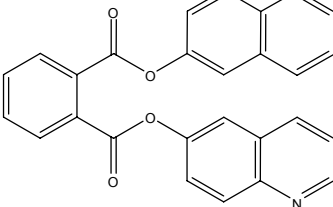
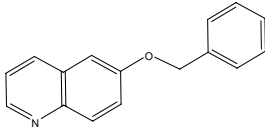
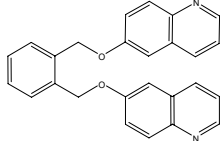
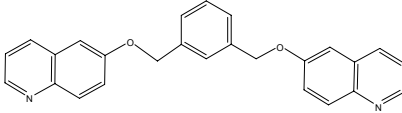
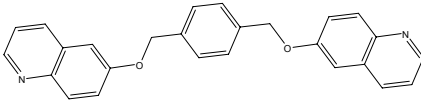
#	Quinoline Reagent	Synthesis Route	Quinoline Product	#
1		$\xrightarrow{\text{C}_7\text{H}_5\text{ClO}}$ $\text{N}(\text{Et})_3$, 50% DCM / DMF 25 C, 18 hrs		7
		$\xrightarrow{\text{C}_8\text{H}_4\text{Cl}_2\text{O}_2}$ $\text{N}(\text{Et})_3$, 80% DCM / DMF 25 C, 14 hrs		7a
		$\xrightarrow{\text{C}_7\text{H}_7\text{Br}}$ K_2CO_3 , DMF 25 C, 18 hrs		8
		$\xrightarrow{\text{C}_8\text{H}_8\text{Br}_2}$ K_2CO_3 , DMF 25 C, 12 hrs		8a
		$\xrightarrow{\text{C}_8\text{H}_8\text{Br}_2}$ K_2CO_3 , DMF 25 C, 14 hrs		8b
		$\xrightarrow{\text{C}_8\text{H}_8\text{Br}_2}$ K_2CO_3 , DMF 25 C, 10 hrs		8c

Table 6: Synthesis of 8-substituted quinoline benzoyl monoester and diesters. Synthesis of 8-substituted quinoline benzyl monoether and diethers.

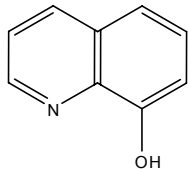
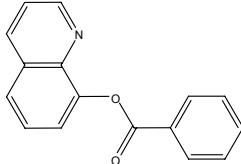
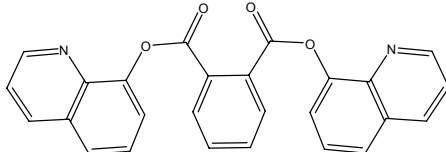
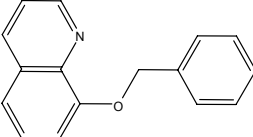
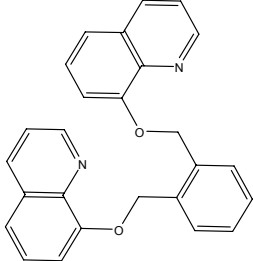
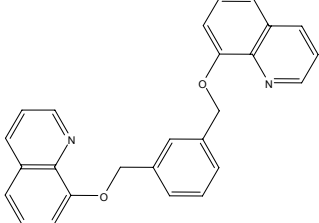
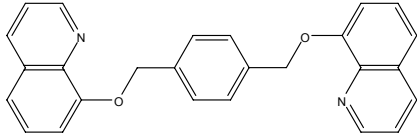
#	Quinoline Reagent	Synthesis Route	Quinoline Product	#
3		$\xrightarrow{\text{C}_7\text{H}_5\text{ClO}}$ N(Et) ₃ , 50% DCM / DMF 25 C, 18 hrs		9
		$\xrightarrow{\text{C}_8\text{H}_4\text{Cl}_2\text{O}_2}$ N(Et) ₃ , 80% DCM / DMF 25 C, 14 hrs		9a
		$\xrightarrow{\text{C}_7\text{H}_7\text{Br}}$ K ₂ CO ₃ , DMF 50 C, 72 hrs		10
		$\xrightarrow{\text{C}_8\text{H}_8\text{Br}_2}$ K ₂ CO ₃ , DMF 50 C, 72 hrs		10a
		$\xrightarrow{\text{C}_8\text{H}_8\text{Br}_2}$ K ₂ CO ₃ , DMF 50 C, 72 hrs		10b
		$\xrightarrow{\text{C}_8\text{H}_8\text{Br}_2}$ K ₂ CO ₃ , DMF 25 C, 10 hrs		10c

Table 7: Synthesis of 6/8-unsymmetrical diester diquinoline products

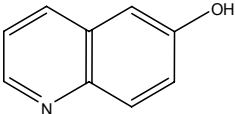
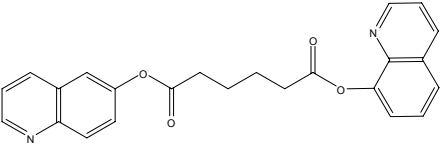
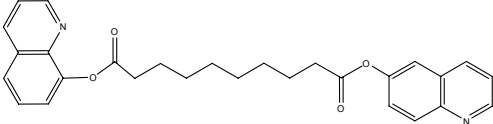
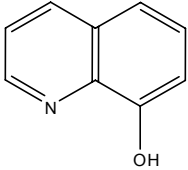
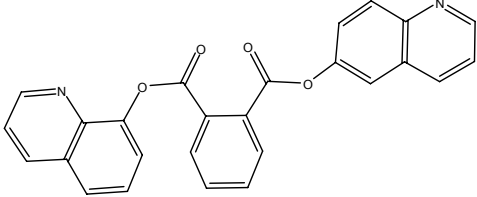
#	Quinoline Reagent	Synthesis Route	Quinoline Product	#
1		$\xrightarrow[\text{Et}_3\text{N, CH}_2\text{Cl}_2, 25\text{ C, 22 hrs}]{\text{Cl-CO(CH}_2)_6\text{OC-Cl}}$		11a
		$\xrightarrow[\text{Et}_3\text{N, CH}_2\text{Cl}_2, 25\text{ C, 16 hrs}]{\text{ClCO(CH}_2)_8\text{OCCl}}$		11b
3		$\xrightarrow[\text{N(Et)}_3, 80\% \text{ DCM / DMF}, 25\text{ C, 14 hrs}]{\text{C}_8\text{H}_4\text{Cl}_2\text{O}_2}$		11c

Table 8: Synthesis of 6-substituted quinoline monoamide.

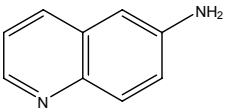
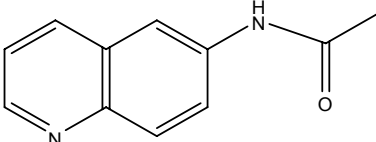
#	Quinoline Reagent	Synthesis Route	Quinoline Product	#
12		$\xrightarrow[\text{Et}_3\text{N, CH}_2\text{Cl}_2, 25\text{ C, 26 hrs}]{\text{CH}_3\text{CO-Cl}}$		13

Table 9: Synthesis of 8-substituted quinoline monoamide.

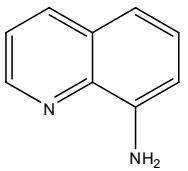
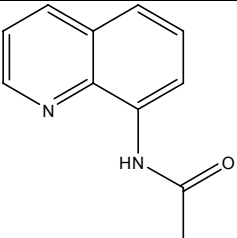
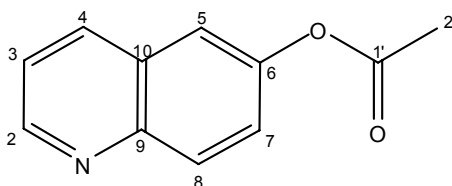
#	Quinoline Reagent	Synthesis Route	Quinoline Product	#
14		$\xrightarrow[\text{Et}_3\text{N, CH}_2\text{Cl}_2, 25\text{ C, 26 hrs}]{\text{CH}_3\text{CO-Cl}}$		15

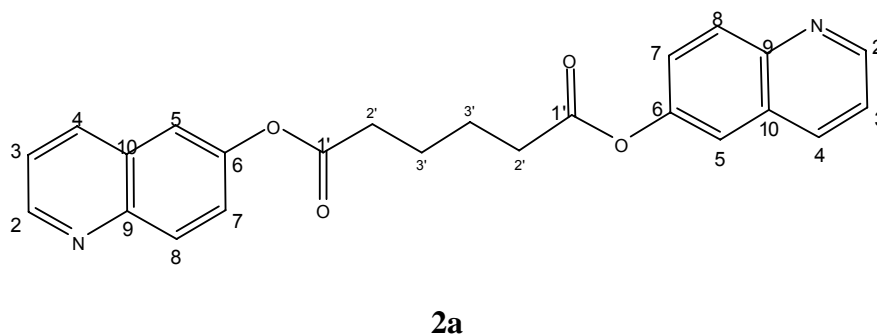
Table 10: Assignments of NMR data for monoester **2** using correlation and NOE spectroscopy.



2

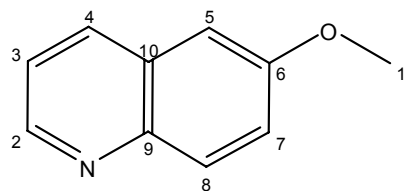
Position	δ ^1H (ppm)	Int.	Mult.	J (Hz)	δ ^{13}C (ppm)	COSY $^1\text{H} \rightarrow ^1\text{H}$	HMBC $^1\text{H} \rightarrow ^{13}\text{C}$	NOESY $^1\text{H} \rightarrow ^1\text{H}$
2	8.88	1H	<i>d</i>	4.2	31.52	H-3	C-4; C-9	H-3
3	7.37	1H	<i>dd</i>	8.2, 4.2	121.74	H-2; H-4	C-10	H-2; H-4
4	8.08	1H	<i>d</i>	8.2	131.21	H-3	C-2; C-5; C-9	H-3; H-5
5	7.55	1H	<i>d</i>	2.3	118.57	-	C-4; C-7	H-4
6	-	-	-	-	148.62	-	-	-
7	7.46	1H	<i>dd</i>	9.1, 2.3	124.88	H-8	C-5; C-9	H-8
8	8.12	1H	<i>d</i>	9.1	135.96	H-7	C-6; C-10	H-7
9	-	-	-	-	146.44	-	-	-
10	-	-	-	-	128.67	-	-	-
1'	-	-	-	-	169.32	-	-	-
2'	2.30	3H	<i>s</i>	-	31.52	-	C-1'	-

Table 11: Assignments of NMR data for diester **2a** using correlation and NOE spectroscopy.



Position	δ ^1H (ppm)	Int.	Mult.	J (Hz)	δ ^{13}C (ppm)	COSY $^1\text{H} \rightarrow ^1\text{H}$	HMBC $^1\text{H} \rightarrow ^{13}\text{C}$	NOESY $^1\text{H} \rightarrow ^1\text{H}$
2	8.88	1H	<i>dd</i>	4.0, 1.2	150.28	H-3	C-4; C-9	H-3
3	7.36	1H	<i>dd</i>	8.4, 4.0	121.62	H-2; H-4	C-10	H-2; H-4
4	8.07	1H	<i>d</i>	8.4	135.79	H-3	C-2; C-5; C-9	H-3; H-5
5	7.56	1H	<i>d</i>	2.4	118.41	-	C-4; C-7	H-4
6	-	-	-	-	148.45	-	-	-
7	7.47	1H	<i>dd</i>	9.2 2.4	124.71	H-8	C-5; C-9	H-8
8	8.12	1H	<i>d</i>	9.2	131.07	H-7	C-6; C-10	H-7
9	-	-	-	-	146.29	-	-	-
10	-	-	-	-	128.53	-	-	-
1'	-	-	-	-	171.71	-	-	-
2'	2.72	2H	<i>t</i>	4.8	34.01	H-3'	C-3'	H-3'
3'	1.95	2H	<i>p</i>	3.6	24.26	H-2'	C-1'; C-2'	H-2'

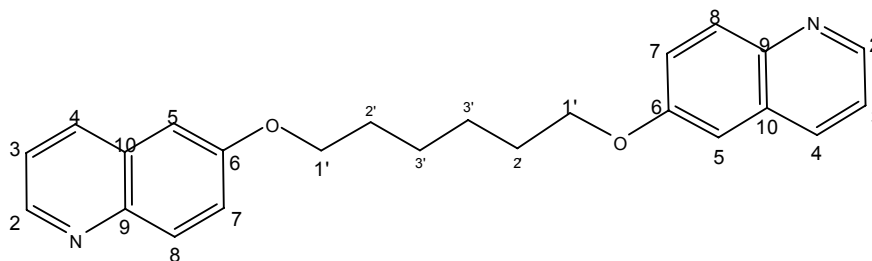
Table 12: Assignments of NMR data for monoether **5a** using correlation and NOE spectroscopy.



5a

Position	δ ^1H (ppm)	Int.	Mult.	J (Hz)	δ ^{13}C (ppm)	COSY $^1\text{H} \rightarrow ^1\text{H}$	HMBC $^1\text{H} \rightarrow ^{13}\text{C}$	NOESY $^1\text{H} \rightarrow ^1\text{H}$
2	8.75	1H	<i>dd</i>	4.2, 1.2	148.45	H-3	C-4; C-9	H-3
3	7.34	1H	<i>dd</i>	8.4, 4.2	121.98	H-2; H-4	C-10	H-2; H-4
4	8.04	1H	<i>dd</i>	8.4, 1.2	134.44	H-3	C-2; C-5; C-9	H-3; H-5
5	7.05	1H	<i>d</i>	2.8	106.33	-	C-4; C-7	H-4
6	-	-	-	-	157.21	-	-	-
7	7.37	1H	<i>dd</i>	9.2, 2.8	123.01	H-8	C-5; C-9	H-8
8	7.99	1H	<i>d</i>	9.2	130.94	H-7	C-6; C-10	H-7
9	-	-	-	-	145.22	-	-	-
10	-	-	-	-	129.10	-	-	-
1'	3.97	3H	<i>s</i>	-	55.80	-	-	H-5

Table 13: Assignments of NMR data for diether **5e** using correlation and NOE spectroscopy.

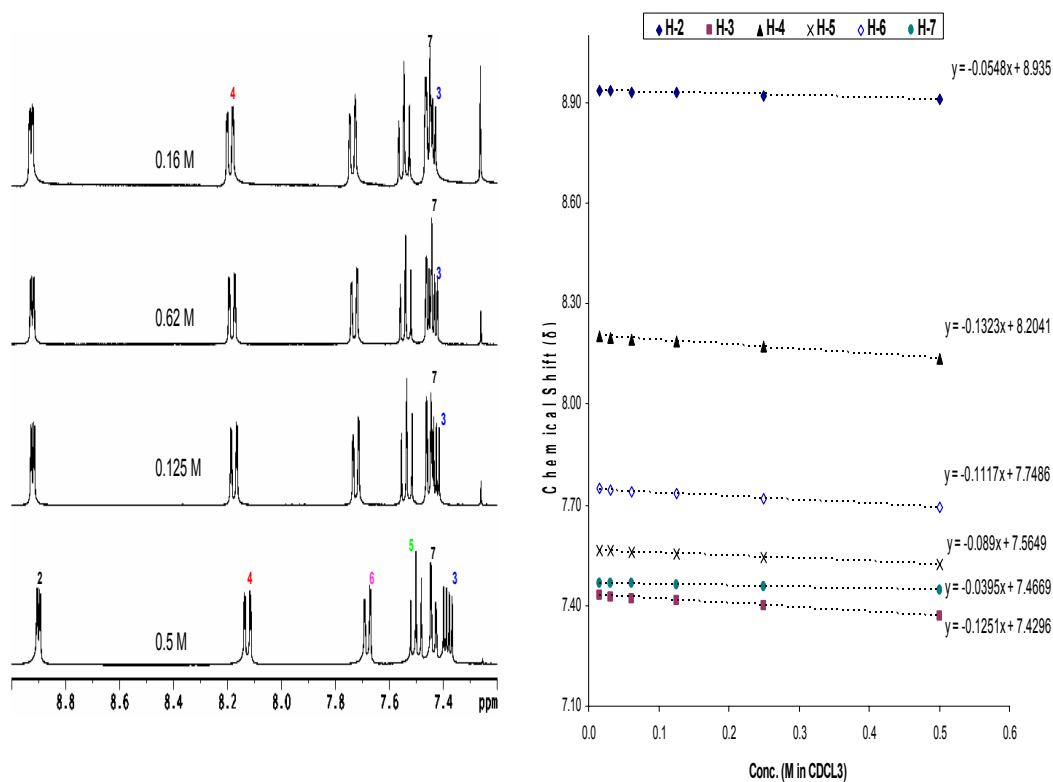
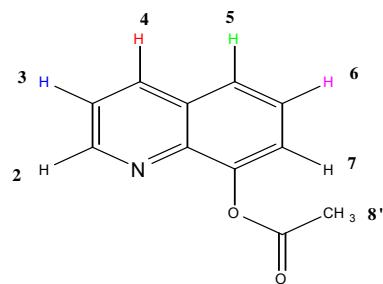


5e

Position	δ ^1H (ppm)	Int.	Mult.	J (Hz)	δ ^{13}C (ppm)	COSY $^1\text{H} \rightarrow ^1\text{H}$	HMBC $^1\text{H} \rightarrow ^{13}\text{C}$	NOESY $^1\text{H} \rightarrow ^1\text{H}$
2	8.76	1H	<i>dd</i>	4.2, 1.2	147.98	H-3	C-4; C-9	H-3
3	7.34	1H	<i>dd</i>	8.2, 4.2	121.51	H-2; H-4	C-10	H-2; H-4
4	8.03	1H	<i>dd</i>	8.2, 1.2	130.92	H-3	C-2; C-5; C-9	H-3; H-5
5	7.06	1H	<i>d</i>	2.7	105.98	-	C-4; C-7	H-4
6	-	-	-	-	157.37	-	-	-
7	7.37	1H	<i>dd</i>	9.1 2.7	122.74	H-8	C-5; C-9	H-8
8	7.99	1H	<i>d</i>	9.1	134.98	H-7	C-6; C-10	H-7
9	-	-	-	-	144.43	-	-	-
10	-	-	-	-	129.51	-	-	-
1'	4.11	2H	<i>t</i>	6.4	68.27	-	-	H-2'; H-3'; H-5; H-7
2'	1.92	2H	<i>m</i>	-	29.29	H-3'	C-1'; C-3'	H-1'; H-3'
3'	1.64	2H	<i>m</i>	-	26.10	H-2'	C-1'; C-2'	H-1'; H-2'

For concentration dependent studies, NMR spectra of each product were acquired at varying concentrations in CDCl_3 . The ^1H -NMR spectra (Figure 9 - **A**) of the 8-monoester **4** shows that as the monomer concentration decreases, many of the aromatic protons experience a downfield shift, but to different degrees, indicating that the less stacking interactions the quinolines experience, the less shielded the protons become. To examine the environment of individual protons, the chemical shift for each aromatic hydrogen in each compound were analyzed from ^1H -NMR data (Appendix 1-12). The plot of the chemical shift of each proton over a range of concentrations (0.5 M – 0.16 M) showed a linear relation (Figure 9 - **B**). The slope of the regression line represents the change in chemical shift / change concentration ($\Delta\delta/\Delta C$). The plot of $\Delta\delta/\Delta C$ for all the aromatic protons for a quinoline compound helps describe stacking the behavior of these molecules in solution (Figure 10).

If the anti-parallel displaced model (Figure 7 – **ii**) is applied, then the H-4 proton for the 8-monoester **4**, while stacked, would experience the highest electron density from the opposing nitrogen and therefore, would yield the highest degree of change in chemical shift, as concentration changes ($\Delta\delta/\Delta C = -0.13$, H-4, Figure 9 - **B**). The H-6 proton also experiences a relatively high ($\Delta\delta/\Delta C = -0.11$), which may be explained by the electron-withdrawing oxygens of the ester group on the opposing ring of the dimer. The quinoline monoesters and monoethers (**2**, **4**, **5a**, **6a**) were used as a basis with which to compare the quinoline dimers, so that the change in chemical shift for each aromatic proton versus a change in concentration could be measured. The absolute values of these slopes were applied to help compare and enhance the visual representation of the $\Delta\delta/\Delta C$ values.



A

B

Figure 9: (A) Stacked ¹H-NMR plots showing the $\Delta\delta$ for the aromatic protons through a range of concentrations (0.5 M – 0.16 M in CDCl₃) on 8-monoester 4. (B) $\Delta\delta$ vs. Δ Concentration to yield slopes for aromatic protons on 8-monoester 4. The $\Delta\delta/\Delta C$ slopes for the all products are shown in Appendix 1-12.

As the concentration varies, protons on the 6-diquinoline diester (**2c**, Table 1) product had a much lower $\Delta\delta/\Delta C$ than the 6-quinoline monoester **2**. However, this difference is not as significant between the shifts of the 8-diquinoline diester (**4c**, Table 1) and the 8-monoester **4**. Even with a C₁₀ linker, the 8-tethered diester **4c** was not able to show the self associative properties as much as the 6-tethered analog **2c** based on decreased $\Delta\delta/\Delta C$ values. This shows that the parallel conformations (Figure 7 - **i**, **iii**, **v**), which should be able to stack intramolecularly if tethered at the 8-position, do not contribute significantly to concentration dependent behavior.

Specifically, the H-4 proton of the 6-diester **2c** ($\Delta\delta/\Delta C = -0.057$) showed a 38% decrease in $\Delta\delta/\Delta C$ when compared to the H-4 proton of the 6-monoester **2** ($\Delta\delta/\Delta C = -0.093$). Whereas, the H-4 of the 8-diester **4c** ($\Delta\delta/\Delta C = -0.126$) showed only a 5% decrease in $\Delta\delta/\Delta C$ when compared to the H-4 proton of the 8-monoester **4** ($\Delta\delta/\Delta C = -0.132$). The 8-substituted quinolines (**4**, **4c**) showed greater concentration dependent shifts than did the 6-linked analogs (**2**, **2c**), perhaps because of reduced steric hindrance, as discussed later. Even though the differences are significant, the results for the C₁₀ tethered ester quinolines showed both dimers (**2c**, **4c**) had lower $\Delta\delta/\Delta C$ than the ester monomers (**2**, **4**), if only just slightly for the 8-substituted analogs. In almost all cases, protons H3, H4 and H5 have shown the same pattern, with proton H4 having the largest concentration dependence. Many subsequent figures are represented in comparison using just the H4 proton.

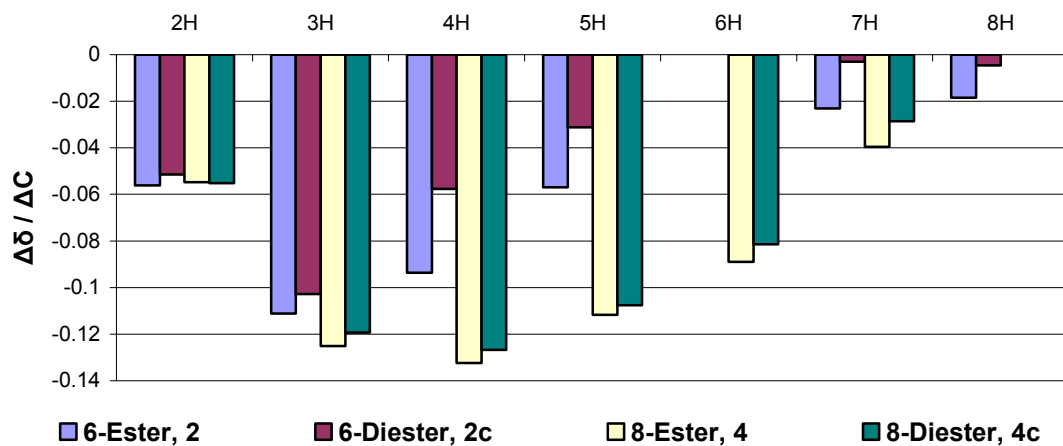


Figure 10: $\Delta\delta/\Delta C$ for quinoline protons on 6- and 8- quinoline analogs. Both dimers shown have C_{10} hydrocarbon tethers and diester linkages. Both monomers are acetyl acetate esters.

Ring Position

For all monomer products, the larger $|\Delta\delta/\Delta C|$ absolute values correspond to higher concentration dependence. Monoquinoline derivatives that have higher concentration dependence would be more likely to self associate or provide evidence of intermolecular π - π stacking. The concentration dependent data for the 6 and 8 substituted monoethers show an interesting pattern (Figure 11). In the proposed anti-parallel stacking conformation (Figure 7 – ii), the concentration dependence of the 6-monoethers increase as the substituents become smaller, suggesting a larger steric hindrance prevents this π - π stacking conformation. Specifically, the $\Delta\delta/\Delta C$ for the 6-monoethers (**5a**, **5b**, **5c**, **8**) decrease with size of the substituents [$\Delta\delta/\Delta C$'s = (methyl) -0.1054, (ethyl) -0.0821, (propyl) -0.0737 and (benzyl) -0.056, respectively]. Whereas, the $\Delta\delta/\Delta C$ of the 8-monoethers (**6a**, **6b**, **6c**, **10**) increase as the substituents become larger [$\Delta\delta/\Delta C$'s = (methyl) -0.0652, (ethyl) -0.0716, (propyl) -0.0722 and (benzyl) -0.1126, respectively]. An explanation of this is that in the anti-parallel conformation of 8-substituted monoether quinolines, the larger the substituent, the more they are held into position by reducing lateral movement. Models of selected quinoline rings were geometry optimized at the molecular mechanics level (MM+) and support these observations of intermolecular π - π stacking in the anti-parallel conformation (Figure 12).

The 6-acetyl monoester **2** also shows less concentration dependence compared to the 8-acetyl monoester **4**, which supports the notion of the steric hindrance from substituents at the 6 and 8 positions. The comparison of acetyl and benzoyl ester products for both 6 and 8 monoquinoline derivatives showed the benzoyl monoesters were more concentration dependent than the acetyl esters (Figure 11). It is possible that

the introduction of electron poor aromatic benzoyl rings contribute to the π - π stacking energies, most likely through the stacking of alternating electron rich and electron poor rings.

However, the 6-quinoline acetamide **12** shows a much greater concentration dependence than its 8-quinoline counterpart **14**, which can be explained through the specific H-bonding character of the amide. If the 6-quinoline acetamide is stacked in an anti-parallel position, the amide proton is able to hydrogen bond with the carbonyl of the opposing amide; this is not as likely for the 8-quinoline acetamide because the carbonyl is competing with the inter- and intramolecular hydrogen bonding from the pyridine nitrogen. However, the investigation into these types of amide groups was not pursued due to poor solubility of the diquinoline diamide products. At this time, it is important to point out that the $^1\text{H-NMR}$ data was collected at room temperature and the chemical shifts are not due to a single geometry, but an average of low energy conformations. It is clear that the solution state structure in nonpolar, aprotic solvents is controlled by multiple forces, including dipole-dipole, electrostatic interactions and London dispersion forces at the inter and intramolecular level.

Monomers, H4

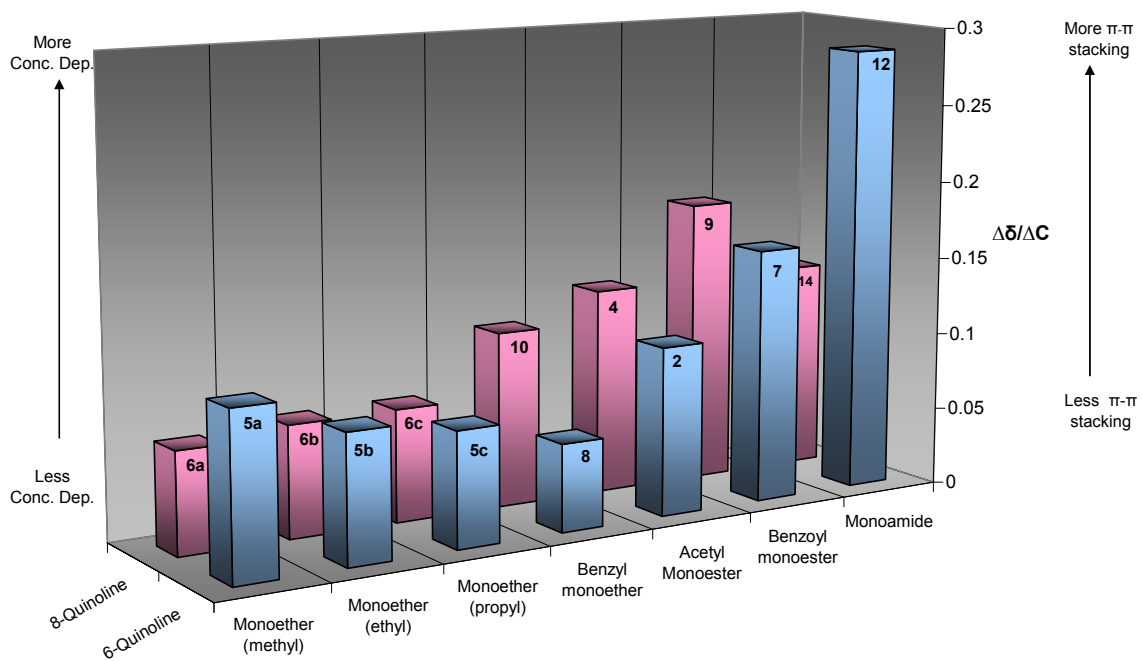


Figure 11: Concentration dependence for proton H4 of monoquinoline derivative products. 6-Quinoline monomers are shown in blue (front) and 8-quinoline monomer are shown in red (back). The absolute values are shown on the Z-axis for the scale of $\Delta\delta/\Delta C$.

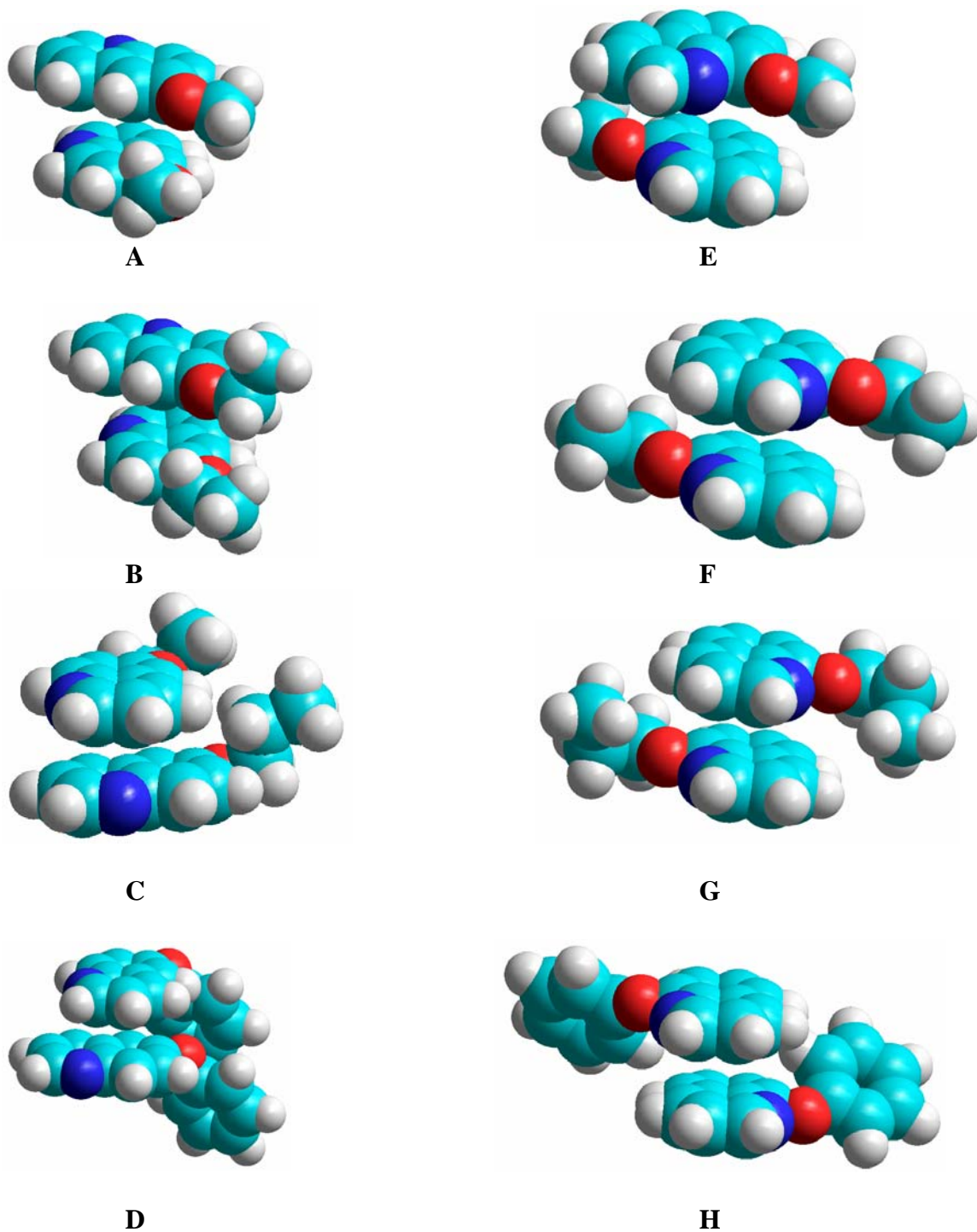


Figure 12: A series of 6-substituted quinoline rings showing favorable anti-parallel conformation with shorter ether linkages: (A-D) 6-monoethers **5a-c**, **8**. A series of 8-substituted quinoline rings showing favorable anti-parallel conformation with longer ether linkages: (E-H) 8-monoethers **6a-c**, **10**.

Since in solution there would be an average of several geometrical conformations, it stands to reason that stacking between two quinolines will not always be in the anti-parallel or face-to-face configuration, but it would be impossible to distinguish protons in each conformation or on each ring since the chemical shift is due to the average environment the proton experiences. In order to overcome this problem of symmetry, unsymmetrical diester dimers, where one ring is tethered to the 6-position and the other ring in the 8-position, were synthesized and their concentration dependence was measured and compared to their symmetrical counterparts (Figure 12). The $\Delta\delta/\Delta C$ of the unsymmetrical alkyl tethered dimers was less than their corresponding symmetrical dimers, most significantly for the H4 proton on the 8-substituted quinoline ring (Figure 14 – **A, B**). The concentration dependence for 4H of the symmetrical benzoyl diester **7a** (4H, $\Delta\delta/\Delta C = -0.0888$) showed a 45% decrease from the dependence of the 6-benzoyl monoester **7** (4H, $\Delta\delta/\Delta C = -0.1625$). The concentration dependence on the 6-substituted quinoline ring of the unsymmetrical phthalate diester **11c** (4H, $\Delta\delta/\Delta C = -0.0971$, Figure 14 - **C**) was similar to the symmetrical phthalate diester **7a** with a 40% decrease. In contrast, the symmetrical diester **9a** (4H, $\Delta\delta/\Delta C = -0.1446$) displayed only a 21% decrease from that of the respective 8-benzoyl monoester **9** (4H, $\Delta\delta/\Delta C = -0.1821$), yet the 8-substituted quinoline ring of the unsymmetrical phthalate diester **11c** (4H, $\Delta\delta/\Delta C = -0.0982$) showed a 46% decrease from the benzoyl monoester **9a**. This is a significant reduction in $\Delta\delta/\Delta C$ when compared to the symmetrical 8- phthalate diester. This shows that the protons on the 6-substituted quinoline ring of the unsymmetrical diesters provide evidence for preferable stacking geometry slightly more than the symmetrical diesters, whereas the $\Delta\delta/\Delta C$ of the protons on the 8-substituted quinoline ring becomes greatly

reduced (Figure 14 – C), meaning the unsymmetrical diester diquinolines are able to take up lower energy conformations much more than their symmetrical 8-diester diquinoline counterparts. Comparatively, the 8-diester **4a** has only 5% less concentration dependence ($\Delta\delta/\Delta C = -0.1254$) than the 8-benzoate monoester **4** ($\Delta\delta/\Delta C = -0.1323$), making it less likely to self-associate in solution.

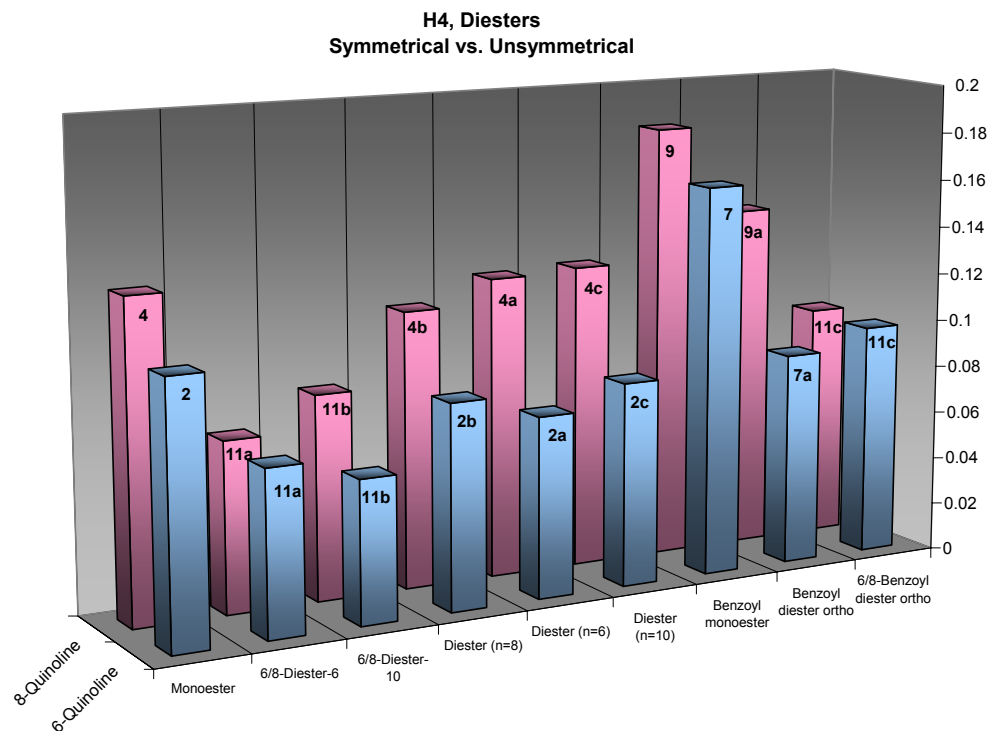
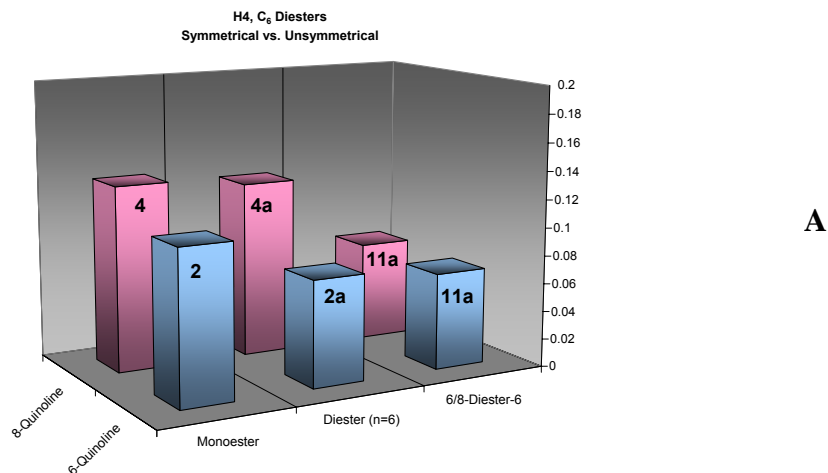
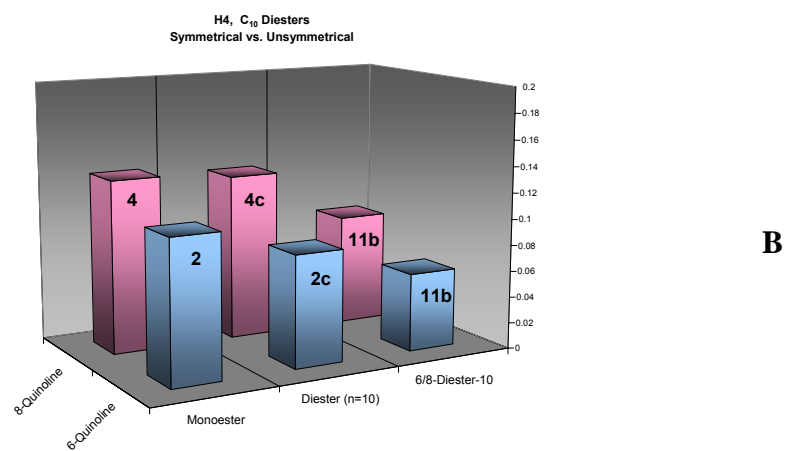


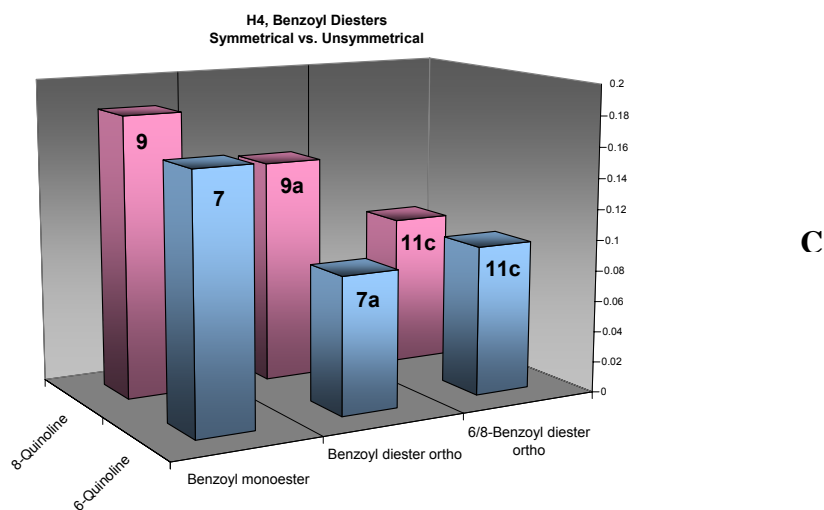
Figure 13: Concentration dependence for proton H4 of symmetrical and unsymmetrical diester quinoline derivatives. The H4 proton on the 6-quinoline rings are shown in blue (front) and H4 proton on the 8-quinoline ring are shown in red (back). For corresponding tethers with hydrocarbon tethers, the number of carbon atoms is shown (n). The absolute values are shown on the Z-axis for the scale of $\Delta\delta/\Delta C$.



A



B



C

Figure 14: Area specific plots of $\Delta\delta/\Delta C$ for proton H4 of symmetrical and unsymmetrical diester quinoline derivatives vs. the equivalent monomer. **(A)** C₆-tethered diesters. **(B)** C₁₀-tethered diesters. **(C)** Phthalate-tethered diesters. All plots show significantly reduced $\Delta\delta/\Delta C$ for 4H of the 8-quinoline ring on unsymmetrical products.

Monomers vs. Dimers

Through molecular modeling, it was proposed that quinoline derivatives tethered at the 6-position would be able to conform to the anti-parallel geometry when in the stacked conformation with opposing dipoles as the driving force behind the geometry. Quinoline dimers tethered at the 8-position would not be able to realize this conformation, yet may experience alternate or slightly offset geometries. The quinoline dimers that have a diester linkage support this model very well (Figure 14 – **2a**, **7a**) when compared with their respective monomers (**2**, **7**). When both the 6 and 8-aliphatic diesters are compared, it is evident that the 6-diester **2a** has 30% less concentration dependence ($\Delta\delta/\Delta C = -0.0755$) with respect to the corresponding monomer **2** ($\Delta\delta/\Delta C = -0.1082$) and, therefore more π - π stacking character. Comparatively, the 8-diester **4a** has only 5% less concentration dependence ($\Delta\delta/\Delta C = -0.1254$) than the 8-benzoyl monoester **4** ($\Delta\delta/\Delta C = -0.1323$), making it less likely to self associate in solution. It is difficult to distinguish between intermolecular and intramolecular interactions, especially with respect to the quinoline dimers, such as the case with ortho linked benzyl diethers (**8a**, **10a**) or phthalate diesters (**7a**, **9a**). Specifically, these two sets of compounds are torsionally constrained in a syn configuration so that the quinoline rings are more likely to see each other.

The initial investigation into quinoline dimers and their inter- and intramolecular stacking behavior was based on the comparison between a monoquinoline and its corresponding diquinoline. It was proposed that if the diquinoline products showed the same concentration dependence as the monomers, then their behavior should be alike, hence the chemical environments around the aromatic protons are experiencing the same

changes with concentration and the two quinoline rings of the dimers are acting independently of each other.

The changes for proton H4 of the alkyl diether compounds when compared to the monoether compounds are minimal (Figure 14) and in the case of the 6-benzyl diether **8a** ($\Delta\delta/\Delta C = -0.0747$), there is a 16% greater concentration dependence than proton H4 on the 6-benzyl monoether **8** ($\Delta\delta/\Delta C = -0.0640$), although the magnitude of the 6 benzyl ether is smaller than the alkyl ether, possibly due to steric constrain. Consistent with an anti-parallel stacking conformation, the 6-alkyl diester **2a** ($\Delta\delta/\Delta C = -0.0755$) and the 6-phthalate diester **7a** ($\Delta\delta/\Delta C = -0.0888$) show a large decrease in concentration dependence when compared to their monomers, **2** and **7**, respectively (**2** \rightarrow **2a**: 30% decrease, **7** \rightarrow **7a**: 45% decrease). This is proposed to be the result of favorable intramolecular stacking between the quinoline rings. The 8-diester diquinoline products (**4a-c**, **9a**), which are not proposed to intramolecularly stack into the anti-parallel conformation, show similar $\Delta\delta/\Delta C$ to that of the monomer (Figure 14). The 8-phthalate diester **9a** has smaller concentration dependence than that of the 8-benzoyl monoester **9**, but not as significant as the 6-phthalate diester **7a** compared to its monomer **7**. This slight reduction in concentration dependence for the 8-quinolines is likely due to being constrained by being tethered in the ortho position, yet not having a stacking conformation allowing opposing dipoles or as energetically favorable as that of the 6-phthalate diester diquinoline.

Meta and para benzyl diethers and phthalate diesters were synthesized for both 6 and 8-substituted quinolines. The benzyl diethers showed very little change in concentration dependence when compared with the benzyl monomer. The phthalate diester compounds

were not investigated due to solubility limits in CDCl_3 . There is no clear or obvious trend when making a comparison of all the 6-quinoline dimers, except to say that they experience very similar concentration dependence and exhibit more intramolecular π - π interactions than many of the 8-quinoline dimers (Figure 15). This strengthens the argument that there are many inter and intramolecular forces which can influence a compounds ability to π - π stack inter- or intramolecularly.

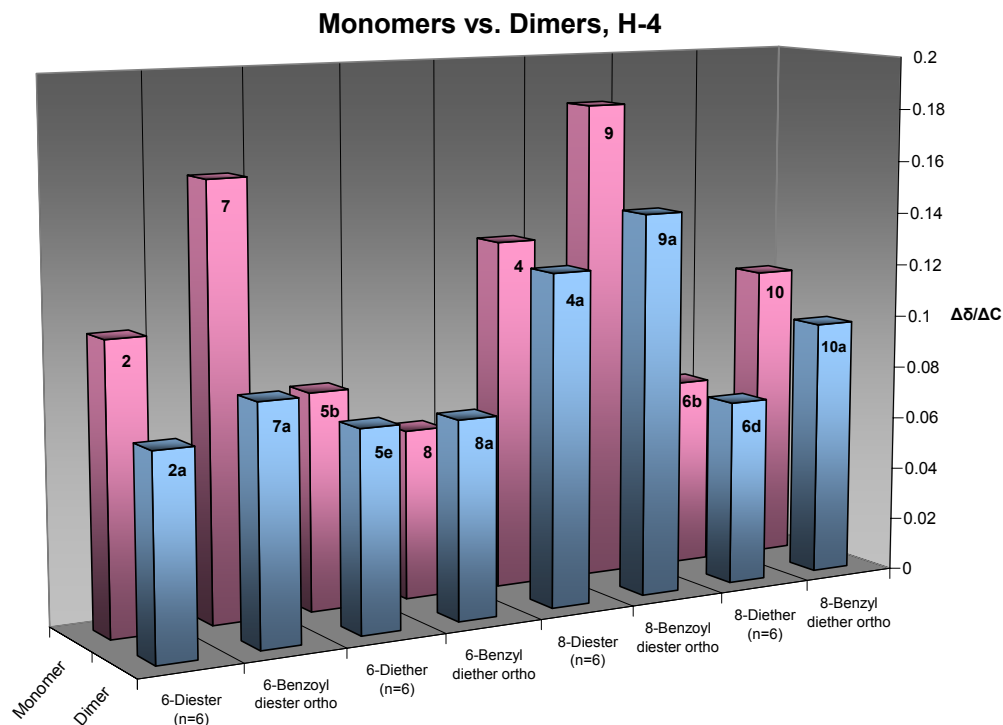


Figure 15: Concentration dependence for proton H4 of monoquinoline vs. diquinoline products. Dimers are shown in blue (front) and monomers are shown in red (back). For corresponding tethers with hydrocarbon tethers, the number of carbon atoms in the tether is shown (n). The absolute values are shown on the Z-axis for the scale of $\Delta\delta/\Delta C$.

Dimers, H4

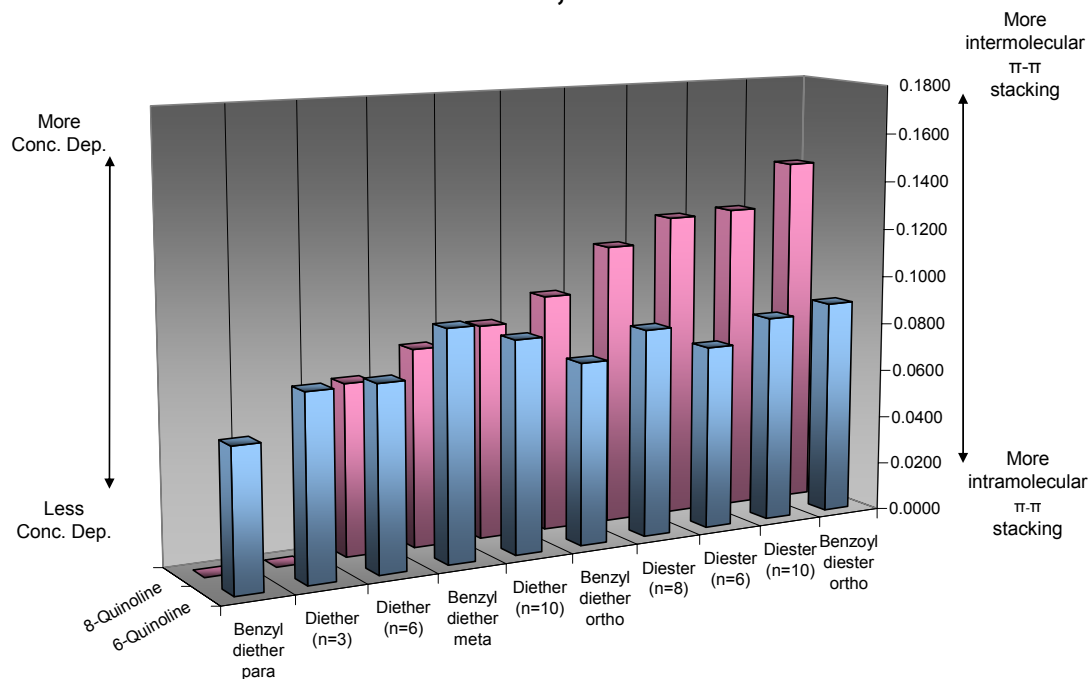
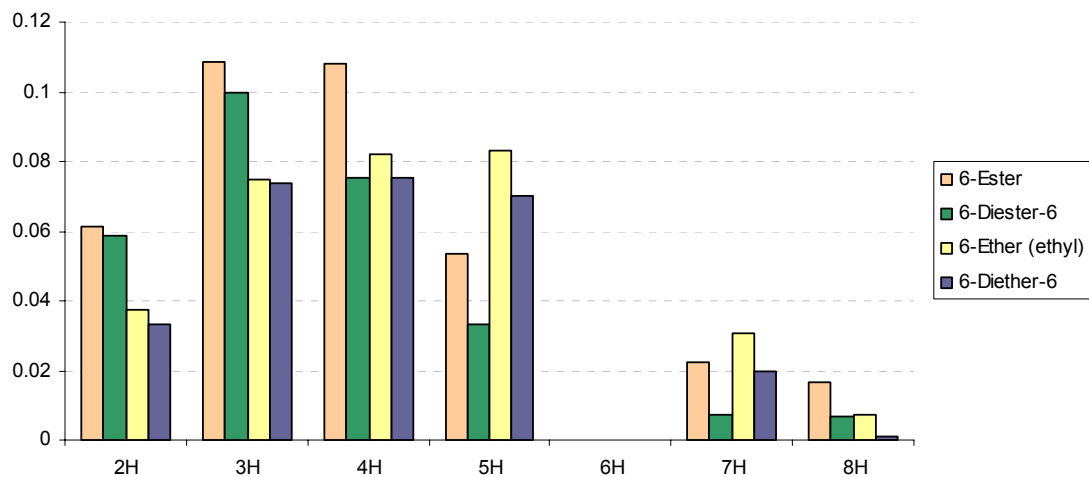


Figure 16: Concentration dependence for proton H4 of diquinoline derivatives. 6-Quinoline dimers are shown in blue (front) and 8-quinoline dimer are shown in red (back). For corresponding tethers with hydrocarbon tethers, the number of carbon atoms is shown (n). The absolute values are shown on the Z-axis for the scale of $\Delta\delta/\Delta C$. 8-Quinoline benzyl diether (para) and diether ($n=3$) could not be synthesized.

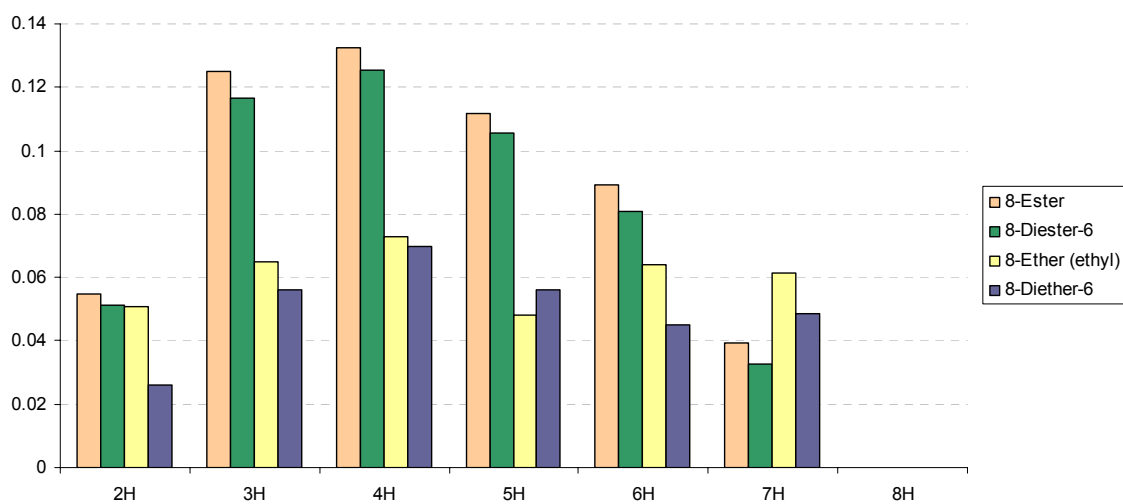
Functional Hinge Groups

This investigation focused mainly on ester and ether functional groups within all quinoline derivatives, although the initial work with amide monomers was very interesting because of the very large changes in concentration dependences observed. While the amide groups most likely incorporate hydrogen bonding into their interactions, the esters and ethers can not interact through classical hydrogen bonding. However, it was observed that the concentration dependence for the majority of ester linked compounds was greater than that of the ether linkages. When alkyl diesters and phthalate diesters are compared with their respective monomers, they are shown to fit the model proposed in this investigation based on the anti-parallel conformation and dipole-dipole stacking. This is evident by observing the difference in concentration dependence of the 6-diester diquinoline **2a** to that of the 6-monoester **2** (Figure 16 - **A**). Alternatively, the aromatic protons on the 8-diester diquinoline **4a** experience the same change in environment as the 8-monoester **4** as concentration changes (Figure 16 - **B**). This data supports that the dipole coupled anti-parallel model such that 8-diquinoline compounds would not be able to stack intramolecularly due to steric strain from the hydrocarbon linker.

The alkyl diether diquinolines attached at the 6 and 8 positions behave similarly to their respective monomers and deviate only slightly either positively or negatively. One explanation might be that the ether substituents significantly change the overall dipole to partially prevent π - π interactions either inter- or intramolecularly. It may also well be a matter of electrostatics, such that the ether groups are strongly electron donating to the quinoline making the ring too electron rich to interact with itself.



A



B

Figure 17: (A) Concentration dependence for aromatic protons on the 6-quinoline monomer and dimers: **2**, **2a**, **5b**, **5e**. (B) Concentration dependence for the aromatic protons on the 8-quinoline monomer and dimers: **4**, **4a**, **6b**, **6d**. The alkyl diesters and diethers have a C₆ linker and the absolute values are shown on the y-axis for the scale of $\Delta\delta/\Delta C$.

The quinoline dimers that have a benzene ring located in the tether are torsionally constrained so that the chances of intramolecular π - π interactions are greatly increased. All ortho benzyl or benzoyl tethered dimers that can π - π stack have a calculated intramolecular distance of 2-4 Å, which supports evidence of previous work^{28,30,32,34,37,38} done on π - π stacking distance. Calculations have been performed on host-guest complexes utilizing molecular tweezers and show the intramolecular host-host distance is optimized at about 7.5 Å. Likewise, benzyl dimers tethered in the meta position (**8b**, **10b**) are spatially separated so that they would not intramolecularly stack but could still accept guest molecules. Host-guest experiments were beyond the scope of this research.

Computational Dipoles

Using Titan software, semiempirical molecular orbital calculations were performed on simple monoester (**2**, **4**) and monoether quinolines (**5b**, **6b**) to observe the relationship between dipole moments and concentration dependence (Table 14). The structure of the molecule was also compared with the calculated results to distinguish between functional groups and ring position. At the AM1 level, the calculated dipoles of **2**, **4**, **5b**, **6b** were 1.161, 1.684, 1.431 and 1.602 Debye, respectively. From computation at the Hartree-Fock / 6-31G** level, the calculated dipoles of **2**, **4**, **5b**, **6b** were 2.937, 2.116, 1.713 and 2.383 Debye, respectively. There was close to 35% difference between calculated dipoles for monoesters **2** and **4** for the two levels of calculations, compared to the 28% difference found for the monoethers **5b** and **6b**. This could help explain why the concentration dependence for 8-monoester **4** is 20% higher than the 6-monoester **2**, yet the concentration dependence for 8-monoether **6b** is 13% less than the 6-monoether **5b** (Figure 11).

Table 14: Comparison of calculated dipoles as semi-empirical, molecular orbital and density functional theory, values shown for selected 6 and 8-substituted mono and diquinoline derivatives. Calculations were performed on Titan (ver 1.0.1., 1999) by Wavefunction and Schrodinger, Inc. Dipole units reported in Debyes.

#	Dipole (AM1)	Dipole (HF/6-31G**)	Dipole (B3LYP / 6-31G**)	#	Dipole (AM1)	Dipole (HF/6-31G**)	Dipole (B3LYP / 6-31G**)
2	1.161	2.937	1.732	4	1.684	2.116	2.242
7	2.264	2.461	2.788	9	1.531	2.481	1.947
5a	1.161	1.451	1.891	6a	1.789	2.566	1.968
5b	1.431	1.713	2.142	6b	1.602	2.383	1.724
5c	1.478	1.671	2.292	6c	1.602	2.490	1.691
8	1.258	1.753	2.315	10	2.486	2.558	1.680
9a	2.938	3.388	n/a	7a	2.778	2.133	n/a

The electrostatic potential map of these simple quinolines (**2**, **4**, **5b**, **6b**) was also calculated to help understand the relation between individual proton concentration dependent chemical shift and electrostatics (Figure 18). Throughout this study, there was a trend in concentration dependence of individual protons on the quinoline ring, with H2 having a small $\Delta\delta/\Delta C$, H4 having the largest $\Delta\delta/\Delta C$ and H7 having a small $\Delta\delta/\Delta C$ again, creating a common curve throughout each plot. Looking at the electrostatic potential map on these monoquinoline derivatives, it can be seen that there is more electron density over the benzene ring and less over the pyridine ring. Specifically, H4 is the most electropositive hydrogen on the quinoline ring and H7 being the least electropositive hydrogen. This could imply that there is a strong relation between electropositive atoms and concentration dependence. It is not known if the increase in quinoline concentration or the increase in π electrons in the system is causing the protons to experience less of the magnetic field producing lower chemical shifts. An accurate method to computationally determine dipole moments is needed if the relation between dipole-dipole interactions and concentration dependence is to be established. It is worth noting that these quinoline products may contain multiple dipole moments, or multipoles, which can affect their stacking behavior and influence the conformation of their solution state structure.

The NMR data is representative of the environment of the quinoline protons while in solution; however a look at the x-ray crystal structure of these compounds may provide further insight into their solution state conformation. The crystal structure of the 6-substituted diester **2c** (Figure 19) shows that the dimer is not folded, yet the quinoline rings interact intermolecularly with each other. Single crystal x-ray quality crystals of other quinoline products have not yet been produced.

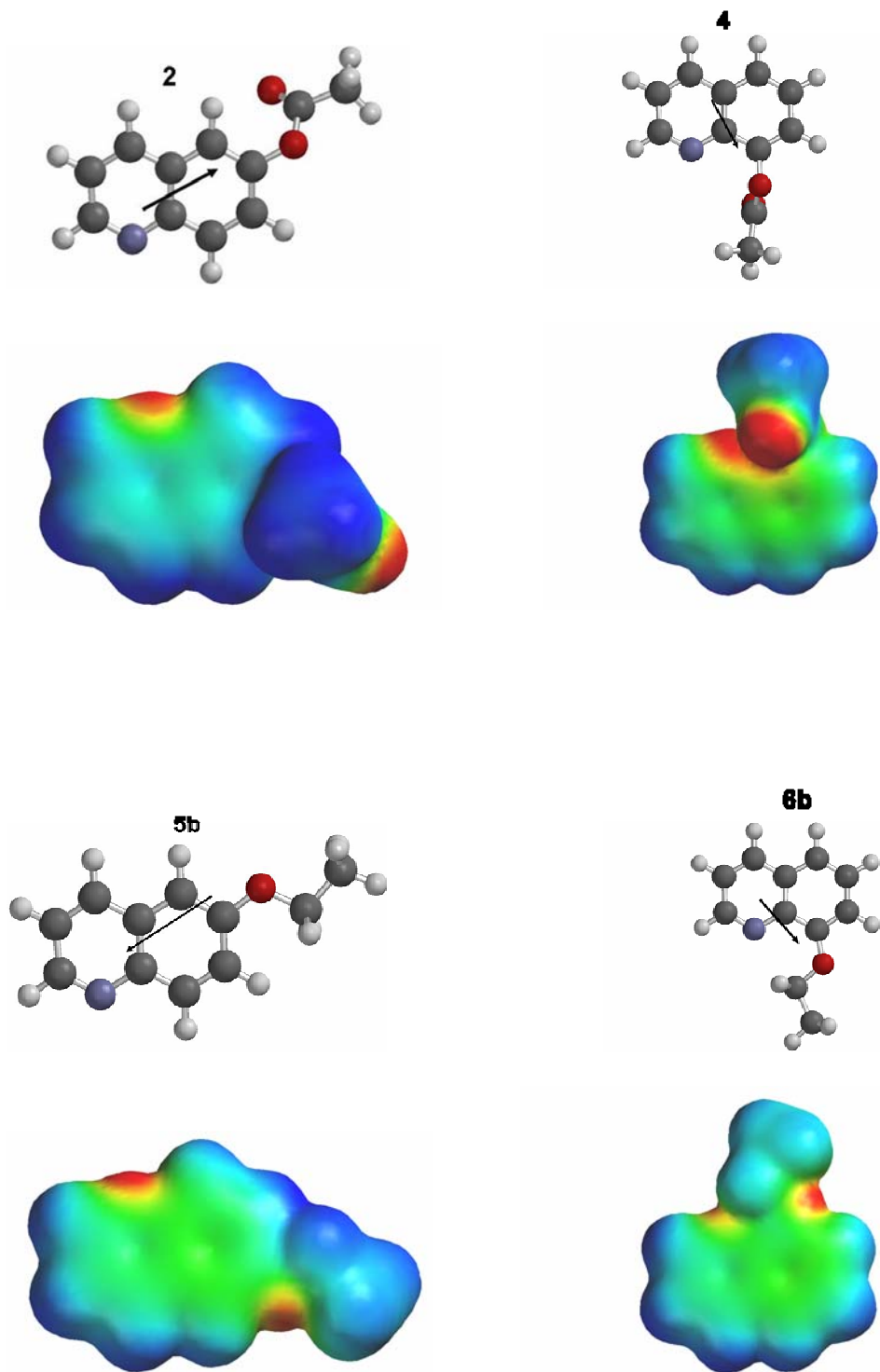


Figure 18: Electrostatic potential maps for 6 and 8-quinoline monomers (**2**, **4**, **5b**, **6b**). Structures were geometry optimized at the semi-empirical / AM1 level followed by a single point HF / 6-31G** calculation. Dipole calculations were recorded at both levels for comparison, indicated by arrows. Calculations were performed on Titan (ver 1.0.1., 1999) by Wavefunction and Schrodinger, Inc.

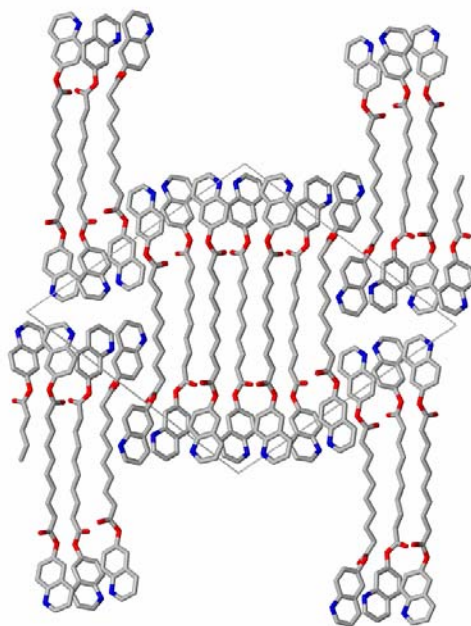
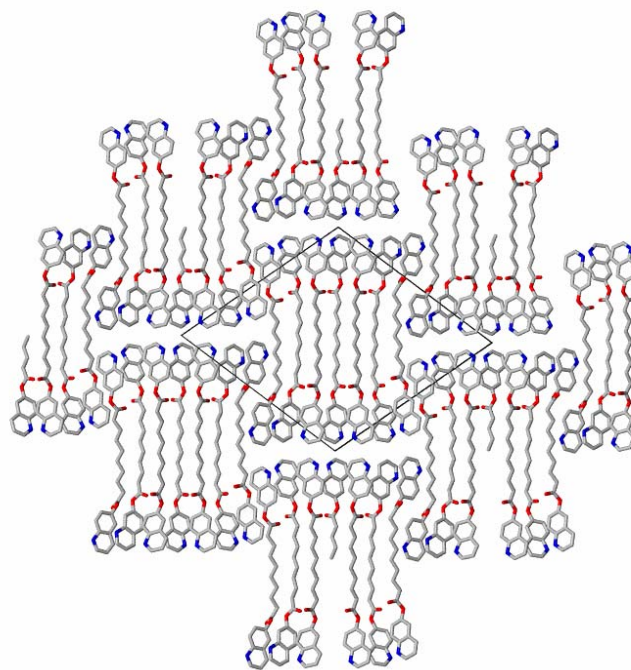


Figure 19: X-Ray crystal structures of 6-substituted diquinoline diester **2c**. Product is shown in a linear conformation. Recrystallized from vapor diffusion method with CHCl_3 / Pentane.

CONCLUSION

Since the understanding of aromatic π - π interactions and intermolecular stacking may provide a deeper insight into the behavior of a number of biologically important chemical structures, it is essential that we study these compounds with a focus on their dependence on concentration. The synthesis and comparisons of free vs. tethered quinolines have shown there is a strong tendency for aromatic rings to inter- and intramolecularly stack and partially overcome the electron repulsion from their π electrons. Through molecular modeling, one can predict the stacking behavior of diquinoline products and perhaps that of other aromatic ring systems at various concentrations. The understanding of this stacking effect in nonpolar solutions may help to elucidate the solution structure and explain activities of molecules containing π - π interactions, ranging from aspects of folding in proteins to multi-layer aromatic-metal complexes.

Our research has shown that there is support for predictions made about concentration dependent quinoline behavior based on molecular modeling and extensive NMR data. The ^1H -NMR behavior of the 6-substituted quinoline monoester and diester analogs provides further evidence consistent with the anti-parallel face to face conformational stacking (**i**, **ii**, **iii**, **iv** - Figure 7). Inverted conformations (**v**, **vi** - Figure 7) are not consistent with these results, based on the small change in $\Delta\delta/\Delta C$ between 8-substituted quinoline monoesters and diesters.

The length of the tethering chain and the position on the ring where it is attached also partially determined whether aromatic stacking was allowed or hindered. The hinge functional group adds to the total number of atoms located in the chain and affects the magnitude of chemical shift of neighboring protons. The C_{10} 8-diether compound, for

instance, did not show evidence of intramolecular stacking when compared to the 8-mono ether. However, the $\Delta\delta/\Delta C$ of the C₁₀ 8-diether **6e** ($\Delta\delta/\Delta C = -0.0877$) was almost 40% less than that of the C₁₀ 8-diester **4c** ($\Delta\delta/\Delta C = -0.1267$), which shows that ether hinge groups have smaller changes in chemical shifts than the ester hinge groups for the 8-substituted diquinolines, although chain length may also play a role.

The theory that 6-position analogs will be able to conform into a stacking arrangement is reinforced (Figure 17), such as in non-inverted conformations (**i-iv**, Figure 7), whereas the 8-diquinoline analogs would not be able to stack in anti-parallel conformations (**ii, iv, vi**). The lack of change for the 8-diquinoline diester analogs also rules out parallel conformations (**i, iii** and **vi**) for these dimers, since the tether at the 8-position should still allow the quinolines to stack intramolecularly. The data is consistent with anti-parallel stacking being dominant, where the nitrogens are opposite to each other and that both inverted conformations do not form under these conditions, in which the H-4 proton over the nitrogen shows the greatest change in chemical shifts.

The obstacles to understanding the solution state structure based on $\pi - \pi$ interactions arise from the number of experimental conditions that can vary with each molecule and solvent being investigated. The multitude of interactions involved can be limited to a few, but it is very difficult to isolate them and measure their individual contributions quantitatively. The NMR data represents an average of all the conformations experienced by each compound in which conformational stacking in π -electron rich aromatics is a dynamic process, where other geometrical variations are not excluded.³ The absence of absolute trends in the concentration dependence data suggest that the solution state structure in nonpolar, aprotic solvents is controlled by multiple forces,

including dipole-dipole, electrostatic interactions and London dispersion forces at the inter and intramolecular level.

EXPERIMENTAL

General. Solvents were purchased from Burdick & Jackson, while anhyd. DMF, anhydrous DCM, triethylamine and 1,4 dicyanobenzene was purchased from Acros. DMF, DCM and triethylamine were distilled over molecular sieves (3A, beads, 4.0-8.0 mesh, Aldrich). 8-Hydroxyquinoline (**3**) was purchased from Fisher Chemicals. K_2CO_3 , 6-hydroxyquinoline (**1**), 4-hydroxyquinoline, tetrabutylammonium-hydrosulfate, terephthaloyl chloride, 1,2,4,5-tetrakis (bromomethyl)benzene, α,α' -dibromo-*p*-xylene and NaH (60%, dispersion in mineral oil) were purchased from Aldrich. All flash column chromatography done using silica gel (0.04-0.063 mm, 230-430 mesh ASTM) purchased from EM Science. 1,3-dibromopropane was purchased from Eastman Organic Chemicals. Anthranilic acid and 1,10 – diiododecane were purchased from Avocado Research Chemicals. Acetyl chloride (98%), Sebacyl chloride (90-95%), 1-iodoethane and 1-iodopropane were purchased from Acros. TLC plates (Silica gel 60 F₂₅₄) and anhyd. THF (DriSolv) were purchased through EMD Chemicals. All solvents used for synthesis were distilled and stored over molecular sieves.

Instrumentation. NMR experiments were performed using a Bruker 400 MHz Avance DRX spectrometer. All NMR spectra taken in $CDCl_3$ and concentration dependence data can be found in Appendix 1. UV-Vis spectra obtained with a Varian Cary double-beam Bio 100 spectrometer and Ocean Optics USB2000. IR analysis performed on a Thermo Nicolet IR-100. GC-MS data was acquired with a Varian CP-3800 (GC) and Varian Saturn 2200 (GC-MS). Automated flash column samples were collected with a CombiFlash retriever by Isco. Samples were concentrated under vacuum with a Buchi Rotavapor R-3000 and a Welch 1400 vacuum pump. Computational results

calculated with HyperChem (ver. 5.11) by HyperCube and Titan (ver 1.0.1., 1999) by Wavefunction and Schrodinger, Inc.

Determination of concentration dependent chemical shifts ($\Delta\delta/\Delta C$). Serial dilutions were performed on mono or diquinoline solutions of known concentrations, giving 4-5 concentrations (0.250 – 0.016 M). The $^1\text{H-NMR}$ spectra were referenced to TMS at 0.00 ppm. The chemical shifts of the quinoline protons were plotted against the concentration of quinoline rings in solution. The $\Delta\delta/\Delta C$'s of diquinoline products were halved in order to maintain a 1:1 molar ratio of quinoline rings throughout mono and diquinoline products. The slope of the linear trend line was plotted as a bar chart and, in most cases, the absolute value was taken to enhance its visual representation.

Synthesis of Aliphatic Monoester and Diester Quinoline Analogs

Quinolin-6-yl acetate (2)

6-Hydroxyquinoline (0.7208 g, 5.0 mmol) was dissolved in CH_2Cl_2 (20 mL) and acetyl chloride (1 mL, 14.0 mol) and distilled triethylamine (1 mL, 7.0 mol) were added to the solution. The reaction was stirred at 25° C for 16 hours under N_2 . Sat. aq. NaHCO_3 (20 mL) and CH_2Cl_2 (5 mL) were added to the mixture and the organic layer was separated and dried over MgSO_4 . The organic layers was concentrated under reduced pressure and purified by FCC using a solvent gradient of 40 – 50 % EtOAc/hexanes. The fractions containing the desired product were combined and were concentrated to give **2**, (0.740 g, 79%) as light brown oil. UV-Vis [MeOH, λ_{max} , nm, (ϵ): 272 (3300), 302 (2400), 315 (2600). IR (neat, cm^{-1}): 1759.64, 1501.59, 1198.92, 1143.63. $^1\text{H-NMR}$ (0.500 M in CDCl_3): δ 8.88 (1H, *d*, J = 7.3 Hz, H-2), 8.12 (1H, *d*, J = 9.1 Hz, H-8), 8.08 (1H, *d*, J = 8.2 Hz, H-4), 7.55 (1H, *d*, J = 2.3 Hz, H-5), 7.46 (1H, *dd*, J = 9.1 and 2.5 Hz, H-7), 7.37

(1H, *dd*, $J = 8.2$ and 4.2 Hz, H-3), 2.30 (3H, *s*, H-2'). ^{13}C -NMR (CDCl_3): δ 31.52 (C2'), 118.57 (C5), 121.74 (C3), 124.88 (C7), 128.67 (C10), 131.21 (C4), 135.96 (C8), 146.44 (C9), 148.62 (C6), 150.41 (C2), 169.32 (C1').

Diquinolin-6-yl adipate (2a)

6-Hydroxyquinoline (0.720 g, 5.0 mmol) was stirred in CH_2Cl_2 (10 mL) in the presence of triethylamine (0.698 mL, 5.0 mmol), adipoyl chloride (0.297 mL, 2.0 mmol) was added slowly over 1 hour under Ar and stirred at room temperature for 20 h. Sat. aq. NaHCO_3 solution (15 mL) and CH_2Cl_2 (5 mL) were added to the mixture and the organic layer was separated, dried over anhyd. Na_2SO_4 and concentrated under reduced pressure. The reaction mixture was purified by FCC using a solvent gradient from 60% EtOAc/Hexanes to 5% MeOH/EtOAc. Fractions containing pure product were combined, concentrated under reduced pressure to yield **2a** (0.471 g, 60%) as a light brown solid (m.p. 100-107° C). UV-Vis [MeOH, λ_{max} , nm, (ϵ): 271 (8260), 301 (5880), 314 (6580). IR (KBr, cm^{-1}): 1754.95, 1637.87, 1502.88, 1211.39, 1148.25. ^1H -NMR (0.250 M in CDCl_3): δ 8.88 (1H, *dd*, $J = 4.0$ and 1.2 Hz, H-2), 8.12 (1H, *d*, $J = 8.0$ Hz, H-8), 8.07 (1H, *d*, $J = 8.4$ Hz, H-4), 7.56 (1H, *d*, $J = 2.4$ Hz, H-5), 7.47 (1H, *dd*, $J = 9.2$ and 2.4 Hz, H-7), 7.36 (1H, *dd*, $J = 8.4$ and 4.4 Hz, H-3), 2.72 (2H, *t*, $J = 5.6$ Hz, H-2'), 1.95 (2H, *p*, $J = 2.8$, Hz, H-3'). ^{13}C -NMR (CDCl_3): δ 24.26 (C3'), 34.01 (C2'), 118.41 (C5), 121.62 (C3), 124.71 (C7), 128.53 (C10), 131.07 (C8), 135.79 (C4), 146.29 (C9), 148.45 (C6), 150.28 (C2), 171.71 (C1').

Diquinolin-6-yl suberate (2b)

6-Hydroxyquinoline (0.506 g, 3.5 mmol) was stirred in distilled CH_2Cl_2 (8 mL) in the presence of triethylamine (0.487 mL, 3.5 mmol) and suberoyl chloride (0.252 mL, 1.4

mmol) was added slowly over 2 hours under Ar. The mixture was stirred at room temperature for 22 h. Sat. aq. NaHCO₃ (15 mL) and CH₂Cl₂ (10 mL) were added to the mixture and the organic layer was separated, dried over anhyd. Na₂SO₄ and concentrated under reduced pressure. The reaction mixture was purified by FCC using a solvent gradient from 50% EtOAc/Hexanes to 5% MeOH/EtOAc. Fractions containing pure product were combined, concentrated under reduced pressure to give **2b** (0.334 g, 55% yield) as a light brown solid (m.p. 100-103° C). UV-Vis [MeOH, λ_{max}, nm, (ε)]: 312 (9940), 323 (10400). IR (KBr, cm⁻¹): 2934.59, 1753.95, 1501.70, 1164.94, 731.37. ¹H-NMR (0.250 M in CDCl₃): δ 8.88 (1H, *dd*, *J* = 4.4 and 1.6 Hz, H-2), 8.12 (1H, *d*, *J* = 9.2 Hz, H-8), 8.07 (1H, *dd*, *J* = 8.4 and 0.8 Hz, H-4), 7.55 (1H, *d*, *J* = 2.4 Hz, H-5), 7.46 (1H, *dd*, *J* = 9.2 and 2.4 Hz, H-7), 7.36 (1H, *dd*, *J* = 8.4 and 4.0 Hz, H-3), 2.65 (2H, *t*, *J* = 7.6 Hz, H-2'), 1.83 (2H, *p*, *J* = 6.6 Hz, H-3'), 1.53 (2H, *p*, *J* = 4.0 Hz, H-4'). ¹³C-NMR (CDCl₃): δ 24.69 (C3'), 28.74 (C4'), 34.29 (C2'), 118.40 (C5), 121.59 (C3), 124.77 (C7), 128.54 (C10), 131.02 (C8), 135.79 (C4), 146.25 (C9), 148.52 (C6), 150.21 (C2), 172.12 (C1').

Diquinolin-6-yl sebecate (2c)

6-Hydroxyquinoline (0.720 g, 5.0 mmol) was stirred CH₂Cl₂ (20 mL) with sebacyl chloride (0.426 mL, 2.0 mmol) in the presence of distilled triethylamine (0.698 mL, 5.0 mmol) under Ar at room temperature for 25 h. Sat. aq. NaHCO₃ solution (20 mL) and CH₂Cl₂ (5 mL) were added to the mixture and the organic layer was separated, dried over anhyd. Na₂SO₄ and concentrated under reduced pressure. The reaction mixture was purified by FCC using a solvent gradient from 50 – 60 % EtOAc / Hexanes. Fractions containing pure product were combined, concentrated under reduced pressure and

recrystallized from CHCl_3/n -heptane to give **2c** (0.76 g, 83% yield) as white crystals (m.p. 102-104° C). UV-Vis [MeOH, λ_{max} , nm, (ϵ): 225 (43500), 272 (5800), 302 (4200), 315 (4700). IR (KBr, cm^{-1}): 2924.95, 1751.93, 1569.70, 1164.33. HRMS (FAB⁺): Calculated for $\text{C}_{28}\text{H}_{28}\text{N}_2\text{O}_4$: 457.5493 ($\text{M} + \text{H}^+$), found 457.2118 ($\text{M} + \text{H}^+$). ¹H-NMR (0.125 M in CDCl_3): δ 8.90 (1H, *dd*, $J = 4.2$ and 1.7 Hz, H-2), 8.13 (1H, *d*, $J = 9.0$ Hz, H-8), 8.12 (1H, *dd*, $J = 8.1$ and 1.5 Hz, H-4), 7.56 (1H, *d*, $J = 2.5$ Hz, H-5), 7.47 (1H, *dd*, $J = 9.1$ and 2.6 Hz, H-7), 7.41 (1H, *dd*, $J = 8.3$ and 4.2 Hz, H-3), 2.66 (2H, *t*, $J = 7.5$ Hz, H-2'), 1.85 (2H, *p*, $J = 7.3$ Hz, H-3'), 1.49 (4H, *m*, $J = 7.5$ Hz, H-4' and H-5'). ¹³C-NMR (CDCl_3): δ 24.92 (C3'), 29.08 (C4'), 29.13 (C5'), 34.43 (C2'), 118.46 (C5), 121.62 (C3), 124.85 (C7), 128.58 (C10), 131.06 (C8), 135.80 (C4), 146.30 (C14), 148.30 (C9), 150.25 (C2), 172.29 (C1').

Quinolin-8-yl acetate (4)

8-Hydroxyquinoline (0.7283 g, 5.0 mmol) was dissolved in CH_2Cl_2 (20 mL) and acetyl chloride (1.00 mL, 14.0 mmol) and triethylamine (1.00 mL, 7.0 mmol) were added to the solution. The reaction was stirred at 25° C for 24 hours under N_2 . Sat. NaHCO_3 (20 mL) and CH_2Cl_2 (4 mL) were added to the mixture and the organic layer was separated and dried over MgSO_4 . The organic layers were concentrated under reduced pressure. The reaction mixture was purified by FCC using a solvent gradient of 50 – 60 % EtOAc/hexanes. The fractions containing the desired product were combined and concentrated under reduced pressure to yield **4** (0.40 g, 43%) as a pale yellow oil. UV-Vis [MeOH, λ_{max} , nm, (ϵ): 282 (4700), 313 (2800), 315 (4700). IR (neat, cm^{-1}): 1762.76, 1502.01, 1368.86, 1207.72, 791.06. ¹H-NMR (0.250 M in CDCl_3): δ 8.91 (1H, *dd*, $J = 4.4$ and 1.7 Hz, H-2), 8.15 (1H, *dd*, $J = 8.3$ and 1.7 Hz, H-4), 7.70 (1H, *dd*, $J = 8.2$ and

1.4 Hz, H-5), 7.52 (1H, *t*, *J* = 7.5 Hz, H-6), 7.44 (1H, *dd*, *J* = 7.5 and 1.4 Hz, H-7), 7.41 (1H, *dd*, *J* = 8.3 and 4.2 Hz, H-3), 2.50 (3H, *s*, H-2'). ¹³C-NMR (CDCl₃): δ 30.43 (C2'), 121.63(C3), 121.78 (C7), 125.95 (C5), 126.26 (C6), 129.56 (C10), 136.17 (C4), 141.15 (C9), 147.30 (C8), 150.51 (C2), 169.86 (C1').

Diquinolin-8-yl adipate (4a)

8-Hydroxyquinoline (0.720 g, 5.0 mmol) was stirred in CH₂Cl₂ (5 mL) in the presence of triethylamine (0.698 mL, 5.0 mmol). Adipoyl chloride (0.297 mL, 2.0 mmol) was added slowly over 1 hour under Ar and stirred at room temperature for 32 h. Sat. aq. NaHCO₃ solution (15 mL) and CH₂Cl₂ (5 mL) were added to the mixture and the organic layer was separated and dried over anhyd. Na₂SO₄ and concentrated under reduced pressure. The reaction mixture was purified by FCC using a solvent gradient from 85-100%

EtOAc/Hexanes. Fractions containing pure product were combined, concentrated under reduced pressure to give **4** (0.293 g, 36% yield) as a light yellow solid (m.p. 150-154° C). UV-Vis [MeOH, λ_{max}, nm, (ε)]: 287 (18600), 300 (16600), 313 (12900). IR (KBr, cm⁻¹): 2943.61, 1766.02, 1503.22, 1113.76. ¹H-NMR (0.032 M in CDCl₃): δ 8.91 (1H, *dd*, *J* = 4.0 and 1.6 Hz, H-2), 8.17 (1H, *dd*, *J* = 8.2 and 2.0 Hz, H-4), 7.72 (1H, *dd*, *J* = 8.0 and 1.2 Hz, H-5), 7.53 (1H, *t*, *J* = 7.6 Hz, H-6), 7.45 (1H, *dd*, *J* = 7.2 and 1.2 Hz, H-7), 7.41 (1H, *dd*, *J* = 8.4 and 4.0 Hz, H-3), 2.93 (2H, *t*, *J* = 2.0 Hz, H-2'), 2.13 (2H, *p*, *J* = 1.2 Hz, H-3'). ¹³C-NMR (CDCl₃): δ 24.59 (C3'), 34.04 (C2'), 121.92(C3), 126.00 (C7), 126.43 (C5), 126.55 (C6), 129.75 (C10), 136.37 (C4), 141.21 (C9), 147.46 (C8), 150.63 (C2), 172.46 (C1').

Diquinolin-8-yl suberate (4b)

8-Hydroxyquinoline (0.720 g, 5.0 mmol) was stirred in CH₂Cl₂ (10 mL) in the presence of triethylamine (0.698 mL, 5.0 mmol). Adipoyl chloride (0.297 mL, 2.0 mmol) was added slowly over 1.5 hour under Ar and stirred at room temperature for 22 h. Sat. aq. NaHCO₃ solution (15 mL) and CH₂Cl₂ (5 mL) were added to the mixture and the organic layer was separated, dried over anhyd. Na₂SO₄ and concentrated under reduced pressure. The reaction mixture was purified by FCC using a solvent gradient from 50-100% EtOAc/Hexanes. Fractions containing pure product were combined, concentrated under reduced pressure to give **4** (0.577 g, 67% yield) as a pale yellow solid (m.p. 118-121° C). UV-Vis [MeOH, λ_{max}, nm, (ε)]: 288 (9850), 300 (8320), 313 (6120). IR (KBr, cm⁻¹): 2936.43, 1758.59, 1500.19, 1123.49. ¹H-NMR (0.250 M in CDCl₃): δ 8.89 (1H, *dd*, *J* = 4.0 and 1.6 Hz, H-2), 8.11 (1H, *dd*, *J* = 8.4 and 1.6 Hz, H-4), 7.67 (1H, *dd*, *J* = 8.0 and 1.2 Hz, H-5), 7.49 (1H, *t*, *J* = 7.6 Hz, H-6), 7.43 (1H, *dd*, *J* = 7.2 and 1.2 Hz, H-7), 7.36 (1H, *dd*, *J* = 8.2 and 4.4 Hz, H-3), 2.84 (2H, *t*, *J* = 7.2 Hz, H-2'), 1.92 (2H, *p*, *J* = 4.8 Hz, H-3'), 1.64 (2H, *p*, *J* = 4.8 Hz, H-4'). ¹³C-NMR (CDCl₃): δ 24.92 (C3'), 28.86 (C4'), 34.18 (C2'), 121.55 (C7), 121.72 (C3), 125.82 (C5), 126.62 (C6), 129.53 (C10), 136.02 (C4), 141.28 (C9), 147.49 (C8), 150.48 (C2), 172.60 (C1').

Diquinolin-8-yl sebecate (4c)

8-Hydroxyquinoline (0.7228 g, 5.0 mmol) was dissolved in distilled CH₂Cl₂ (20 mL). Sebacyl chloride (0.430 mL, 2.0 mmol) and distilled triethylamine (0.700 mL, 5.0 mmol) were added to the solution. The reaction was stirred at 25° C for 26 hours under N₂. Sat. NaHCO₃ (20 mL) and CH₂Cl₂ (5 mL) were added to the mixture and the organic layer was separated. The organic layers were concentrated under reduced pressure and purified by FCC using a solvent gradient of 50 – 60 % EtOAc/hexanes. The fractions containing

the desired product were combined, concentrated under reduced pressure and recrystallized with CHCl_3 / hexanes to give **4c** (0.56 g, 83%) as white crystals (m.p. 122-126° C). UV-Vis [MeOH, λ_{max} , nm, (ϵ): 290 (8800), 306 (8450), 319 (6220). IR (KBr, cm^{-1}): 1748.13, 1592.68, 1115.39. $^1\text{H-NMR}$ (0.250 M in CDCl_3): δ 8.89 (1H, *dd*, $J = 4.2$ and 1.7 Hz, H-2), 8.14 (1H, *dd*, $J = 8.4$ and 1.7 Hz, H-4), 7.69 (1H, *dd*, $J = 8.2$ and 1.3 Hz, H-5), 7.51 (1H, *t*, $J = 7.5$ Hz, H-6), 7.43 (1H, *dd*, $J = 7.5$ and 1.4 Hz, H-7), 7.40 (1H, *dd*, $J = 8.3$ and 4.2 Hz, H-3), 2.81 (2H, *t*, $J = 7.4$ Hz, H-2'), 1.87 (2H, *p*, $J = 7.6$ Hz, H-3'), 1.51 (2H, *m*, $J = 5.3$ Hz, H-4'), 1.42 (2H, *m*, $J = 6.6$ Hz, H-5'). $^{13}\text{C-NMR}$ (CDCl_3): δ 25.19 (C3'), 29.30 (C4'), 29.42 (C5'), 34.40 (C2'), 121.77 (C7), 121.89 (C3), 125.96 (C5), 126.41 (C6), 129.70 (C10), 136.25 (C4), 141.42 (C9), 147.62 (C8), 150.62 (C2), 172.86 (C1').

Synthesis of Aliphatic Monoether and Diether Quinoline Analogs

6-Methoxyquinoline (5a)

6-Hydroxyquinoline (0.29 g, 2.0 mmol) was dissolved in 20% DCM/DMF (6 mL) and iodomethane (0.124 mL, 2.0 mmol) and NaH (0.072 g, 3.0 mmol) were added to the solution. The reaction was stirred at 25° C for 24 hours under N_2 . EtOAc (12 mL) and water (15 mL) and 10% NaOH (10 mL) were added to the mixture and the organic layer was separated and dried over MgSO_4 . The organic layers were combined and concentrated under reduced pressure and purified by FCC with 60% EtOAc/hexanes. The fractions containing the desired product were combined and concentrated to yield **5a** (0.239 g, 69%) as a light brown oil. UV-Vis [MeOH, λ_{max} , nm, (ϵ): 240 (18650), 270 (5200), 320 (6330), 335 (6780). IR (neat, cm^{-1}): 2982.13, 1721.17, 1618.43, 1501.22, 1360.01, 1220.45. $^1\text{H-NMR}$ (0.125 M in CDCl_3): δ 8.75 (1H, *dd*, $J = 4.3$ and 2.0 Hz, H-

2), 8.04 (1H, *dd*, $J = 8.4$ and 1.2 Hz, H-4), 7.99 (1H, *d*, $J = 9.2$ Hz, H-8), 7.37 (1H, *dd*, $J = 9.2$ and 2.8 Hz, H-7), 7.34 (1H, *dd*, $J = 8.2$ and 4.2 Hz, H-3), 7.05 (1H, *d*, $J = 2.8$ Hz, H-5), 3.97 (3H, *s*, H-1'). ^{13}C -NMR (CDCl_3): δ 55.80 (C1'), 106.33 (C5), 121.98 (C3), 123.01 (C7), 129.12 (C10), 130.94 (C8), 134.44 (C4), 145.22(C9), 148.45 (C2), 157.21 (C6).

6-Ethoxyquinoline (5b)

6-Hydroxyquinoline (0.29 g, 2.0 mmol) was dissolved in DMF (4 mL). Iodoethane (0.162 mL, 2.0 mmol) and NaH (0.072 g, 3.0 mmol) were added to the solution. The reaction was stirred at 25° C for 24 hours under N_2 . EtOAc (12 mL) and water (15 mL) and 10% NaOH (10 mL) were added to the mixture and the organic layer was separated and dried over MgSO_4 . The organic layers were concentrated and purified by FCC eluding with 60% EtOAc/hexanes. The fractions containing the desired product were combined and concentrated under reduced pressure to yield **5b** (0.239 g, 69%) as a tan oil. UV-Vis [MeOH, λ_{max} , nm, (ϵ): 268 (7300), 330 (10600). IR (neat, cm^{-1}): 2984.24, 1711.17, 1622.18, 1502.11, 1362.31, 1225.16. ^1H -NMR (0.125 M in CDCl_3): δ 8.75 (1H, *dd*, $J = 4.2$ and 1.7 Hz, H-2), 8.03 (1H, *dd*, $J = 8.4$ and 1.3 Hz, H-4), 7.99 (1H, *d*, $J = 9.2$ Hz, H-8), 7.37 (1H, *dd*, $J = 9.1$ and 2.8 Hz, H-7), 7.34 (1H, *dd*, $J = 8.2$ and 4.2 Hz, H-3), 7.05 (1H, *d*, $J = 2.7$ Hz, H-5), 4.15 (2H, *q*, $J = 6.9$ Hz, H-1'), 1.49 (3H, *t*, $J = 6.9$ Hz, H-2'). ^{13}C -NMR (CDCl_3): δ 22.34 (C2'), 69.87 (C1'), 105.77 (C5), 121.11 (C3), 123.03 (C7), 129.55 (C10), 131.22 (C8), 134.56 (C4), 144.58 (C9), 147.99 (C2), 157.23 (C6).

6-Propoxyquinoline (5c)

6-Hydroxyquinoline (0.29 g, 2.0 mmol) was dissolved in DMF (4 mL). Iodopropane (0.195 mL, 2.0 mmol) and NaH (0.072 g, 3.0 mmol) was added to the solution. The

reaction was stirred at 25° C for 18 hours under N₂. Et₂O (10 mL) and water (15 mL) and 10% NaOH (10 mL) were added to the mixture and the organic layer was separated and dried over MgSO₄. The organic layers were concentrated and purified by FCC with a gradient solvent system of 60% EtOAc/hexane to 100% EtOAc. The fractions containing the desired product were combined and concentrated to yield **5c** (0.374 g, 72%) as a light brown oil. UV-Vis [MeOH, λ_{max}, nm, (ε)]: 242 (20430), 268 (4830), 319 (6670), 331 (6930). IR (neat, cm⁻¹): 2965.34, 1621.58, 1500.89, 1227.86, 884.54. ¹H-NMR (0.125 M in CDCl₃): δ 8.75 (1H, *dd*, *J* = 4.4 and 2.0 Hz, H-2), 8.03 (1H, *dd*, *J* = 8.4 and 1.2 Hz, H-4), 7.99 (1H, *d*, *J* = 9.2 Hz, H-8), 7.37 (1H, *dd*, *J* = 9.2 and 2.8 Hz, H-7), 7.34 (1H, *dd*, *J* = 8.2 and 4.2 Hz, H-3), 7.05 (1H, *d*, *J* = 2.8 Hz, H-5), 4.03 (2H, *t*, *J* = 6.4 Hz, H-1'), 1.88 (2H, *p*, *J* = 6.8 Hz, H-2'), 1.08 (3H, *t*, *J* = 7.2 Hz, H-3'). ¹³C-NMR (CDCl₃): δ 10.77 (C3'), 22.71 (C2'), 69.99 (C1'), 106.00 (C5), 121.49 (C3), 122.78 (C7), 129.54 (C10), 130.96 (C8), 134.94 (C4), 144.52 (C9), 148.01 (C2), 157.44 (C6).

6,6'-[Propane-1,3-diylbis(oxy)]diquinoline (5d)

6-Hydroxyquinoline (0.29 g, 2.0 mmol) was dissolved in DMF (4 mL) and K₂CO₃ (0.249 g, 1.8 mmol) while stirring for 10 minutes. 1, 3-dibromopropane (0.092 mL, 0.9 mmol) was added to the solution in two portions 30 minutes apart. The reaction continued to stir at 97° C for 24 hours under N₂. Et₂O (15 mL) and water (20 mL) and 10% NaOH (8 mL) were added to the mixture and the organic layer was separated and dried over MgSO₄. The organic layers were concentrated under reduced pressure and purified by FCC using a gradient solvent of 60-100% EtOAc/hexanes. The fractions containing the desired product were combined and concentrated under reduced pressure to yield **5d** (0.14 g, 47.1%) as a light brown solid (m.p. 109-114° C). UV-Vis [MeOH, λ_{max}, nm, (ε)]: 268

(5100), 330 (7200), 349 (400). IR (KBr, cm^{-1}): 2937.61, 1621.52, 1501.31, 1226.90, 833.93. $^1\text{H-NMR}$ (0.250 M in CDCl_3): δ 8.75 (1H, *dd*, $J = 4.2$ and 1.7 Hz, H-2), 8.00 (1H, *d*, $J = 9.1$ Hz, H-8), 7.99 (1H, *dd*, $J = 7.9$ and 1.2 Hz, H-4), 7.38 (1H, *dd*, $J = 9.1$ and 2.8 Hz, H-7), 7.31 (1H, *dd*, $J = 8.2$ and 4.2 Hz, H-3), 7.08 (1H, *d*, $J = 2.7$ Hz, H-5), 4.30 (2H, *t*, $J = 6.1$ Hz, H-1'), 2.40 (1H, *p*, $J = 6.0$ Hz, H-2'). $^{13}\text{C-NMR}$ (CDCl_3): δ 29.36 (C2'), 69.84 (C1'), 106.14 (C5), 121.58 (C3), 122.61 (C7), 129.47 (C10), 131.06 (C8), 134.99 (C4), 144.57 (C9), 148.18 (C2), 157.09 (C6).

6,6'-[Hexane-1,2-diylbis(oxy)]diquinoline (5e)

6-Hydroxyquinoline (0.29 g, 2.0 mmol) was dissolved in DMF (4 mL) and K_2CO_3 (0.249 g, 1.8 mmol) while stirring for 10 minutes. 1,6-dibromohexane (0.139 mL, 0.9 mmol) was added in four portions 15 minutes apart. The reaction was stirred at 25°C for 24 hours under N_2 . Et₂O (15 mL) and water (20 mL) and 10% NaOH (5 mL) were added to the mixture and the organic layer was separated and dried over MgSO_4 . The organic layers were concentrated and purified by FCC using a gradient solvent of 40-100% EtOAc/hexanes. The fractions containing the desired product were combined and concentrated under reduced pressure to yield **5e** (0.12 g, 36%) as a tan solid (m.p. 107 - 115°C). UV-Vis [MeOH, λ_{max} , nm, (ϵ): 267 (5500), 331 (7800), 349 (600). IR (KBr, cm^{-1}): 2942.82, 1622.33, 1500.16, 1231.33, 840.13. $^1\text{H-NMR}$ (0.032 M in CDCl_3): δ 8.76 (1H, *dd*, $J = 4.2$ and 1.7 Hz, H-2), 8.03 (1H, *dd*, $J = 6.9$ and 1.2 Hz, H-4), 7.99 (1H, *d*, $J = 9.2$ Hz, H-8), 7.37 (1H, *dd*, $J = 9.1$ and 2.8 Hz, H-7), 7.34 (1H, *dd*, $J = 8.2$ and 4.2 Hz, H-3), 7.06 (1H, *d*, $J = 2.7$ Hz, H-5), 4.11 (2H, *t*, $J = 6.4$ Hz, H-1'), 1.92 (2H, *m*, $J = 6.8$ Hz, H-2'), 1.64 (2H, *m*, $J = 6.0$ Hz, H-3'). $^{13}\text{C-NMR}$ (0.100 M in CDCl_3): δ 26.10

(C3'), 29.29 (C2'), 68.27 (C1'), 105.98 (C5), 121.51 (C3), 122.74 (C7), 129.51 (C10), 130.92 (C4), 134.98 (C8), 144.43 (C9), 147.98 (C2), 157.37 (C6).

6,6'-[Decane-1,2-diylbis(oxy)]diquinoline (5f)

6-Hydroxyquinoline (0.29 g, 2.0 mmol) and K₂CO₃ (0.207 g, 1.5 mmol) was dissolved in DMF (4 mL) while stirring for 10 minutes. 1, 10-diiododecane (0.151 mL, 0.9 mmol) was added dropwise over 1 hour. The reaction was stirred at 90° C for 20 hours under N₂. Et₂O (15 mL) and water (10 mL) and 10% NaOH (5 mL) were added to the mixture and the organic layer was separated and dried over MgSO₄. The organic layers were concentrated under reduced pressure and purified by FCC using a gradient solvent of 60-100% EtOAc/hexanes. The fractions containing the desired product were combined and concentrated under reduced pressure to yield **5f** (0.099 g, 24%) as a light brown solid (m.p. 104-106 ° C). UV-Vis [MeOH, λ_{max}, nm, (ε)]: 238 (16990), 318 (2910), 331 (3110). IR (KBr, cm⁻¹): 2942.75, 1622.09, 1500.54, 1228.42, 841.23. ¹H-NMR (0.032 M in CDCl₃): δ 8.76 (1H, *dd*, *J* = 4.0 and 1.2 Hz, H-2), 8.02 (1H, *d*, *J* = 8.0 Hz, H-4), 7.99 (1H, *d*, *J* = 9.2 Hz, H-8), 7.37 (1H, *dd*, *J* = 9.1 and 2.8 Hz, H-7), 7.34 (1H, *dd*, *J* = 8.1 and 4.2 Hz, H-3), 7.06 (1H, *d*, *J* = 2.4 Hz, H-5), 4.07 (2H, *t*, *J* = 6.4 Hz, H-1'), 1.86 (2H, *m*, *J* = 6.8 Hz, H-2'), 1.51 (2H, *m*, *J* = 6.2 Hz, H-3'), 1.37 (2H, *m*, *J* = 6.2 Hz, H-3'). ¹³C-NMR (0.100 M in CDCl₃): δ 26.25 (C3'), 29.34 (C4'), 29.55 (C2'), 68.45 (C1'), 105.97 (C5), 121.48 (C3), 122.76 (C7), 129.52 (C10), 130.89 (C4), 134.94 (C8), 144.45 (C9), 147.95 (C2), 157.42 (C6).

8-Methoxyquinoline (6a)

8-Hydroxyquinoline (0.200 g, 1.3 mmol) was dissolved in anhyd. THF (10 mL) and NaH (0.052 g, 1.3 mmol) and 1-iodomethane (0.081 mL, 1.3 mmol) in two portions 30

minutes apart. The reaction was stirred at 25° C for 16 hours under Ar. EtOAc (10 mL), water (10 mL) and sat. NaCl (5 mL) were added to the mixture and the organic layer was separated and dried over MgSO₄. The organic layer was concentrated under reduced pressure and purified by FCC with 100% EtOAc/hexane. The fractions containing the desired product were combined and concentrated under reduced pressure to yield **6a** (0.080 g, 38%) a pale yellow oil . UV-Vis [MeOH, λ_{max}, nm, (ε)]: 209 (4010), 241 (12760), 305 (1110). IR (neat, cm⁻¹): 2927.97, 1757.73, 1579.70, 1174.73. ¹H-NMR (0.125 M in CDCl₃): δ 8.93 (1H, *dd*, *J* = 4.0 and 1.6 Hz, H-2), 8.13 (1H, *dd*, *J* = 8.2 and 1.7 Hz, H-4), 7.47 (1H, *t*, *J* = 8.1 Hz, H-6), 7.43 (1H, *dd*, *J* = 8.2 and 4.0 Hz, H-3), 7.39 (1H, *dd*, *J* = 8.0 and 1.2 Hz, H-5), 7.06 (1H, *dd*, *J* = 7.8 and 1.2 Hz, H-7), 4.11 (3H, *s*, H-1'). ¹³C-NMR (CDCl₃): δ 59.78 (C1'), 108.73 (C7), 119.55 (C5), 121.75 (C3), 126.88 (C6), 129.75 (C10), 135.98 (C4), 140.53 (C9), 149.56 (C2), 150.08 (C8).

8-Ethoxyquinoline (6b)

8-Hydroxyquinoline (0.300 g, 2.0 mmol) was dissolved in THF (20 mL) and NaH (0.080 g, 2.0 mmol). 1-iodoethane (0.162 mL, 2.0 mmol) was added in two portions 20 minutes apart. The reaction was stirred at 25° C for 12 hours under Ar. EtOAc (15 mL) and water (10 mL) and sat. NaCl (5 mL) were added to the mixture and the organic layer was separated and dried over MgSO₄. The organic layer was concentrated under reduced pressure and purified by FCC with 100% EtOAc/hexanes. The fractions containing the desired product were combined and concentrated under reduced pressure to yield **6b** (0.135 g, 39%) as a light yellow oil. UV-Vis [MeOH, λ_{max}, nm, (ε)]: 212 (10190), 241 (15000), 305 (1430). IR (neat, cm⁻¹): 1637.67, 912.31, 743.39. ¹H-NMR (0.125 M in CDCl₃): δ 8.96 (1H, *dd*, *J* = 4.2 and 1.7 Hz, H-2), 8.13 (1H, *dd*, *J* = 8.2 and 1.6 Hz, H-4),

7.45 (1H, *t*, *J* = 8.0 Hz, H-6), 7.42 (1H, *dd*, *J* = 8.1 and 4.2 Hz, H-3), 7.38 (1H, *dd*, *J* = 8.0 and 1.2 Hz, H-5), 7.06 (1H, *dd*, *J* = 8.0 and 1.6 Hz, H-7), 4.33 (2H, *q*, *J* = 7.2 Hz, H-1'), 1.64 (3H, *t*, *J* = 7.2 Hz, H-2'). ¹³C-NMR (CDCl₃): δ 14.80 (C2'), 64.99 (C1'), 108.77 (C7), 119.54 (C5), 121.63 (C3), 126.88 (C6), 129.63 (C10), 136.21 (C4), 140.49 (C9), 149.54 (C2), 150.05 (C8).

8-Propoxyquinoline (6c)

8-Hydroxyquinoline (0.29 g, 2.0 mmol) was dissolved in DMF (4.5 mL) and NaH (0.072 g, 3.0 mmol). 1-iodopropane (0.195 mL, 2.0 mmol) was added in four portions 15 minutes apart. The reaction was stirred at 25° C for 16 hours under N₂. Et₂O (20 mL) and water (15 mL) and sat. NaCl (5 mL) were added to the mixture and the organic layer was separated and dried over MgSO₄. The organic layer was concentrated under reduced pressure and purified by FCC with 60% EtOAc/hexanes. The fractions containing the desired product were combined under reduced pressure and concentrated to yield **6c** (0.22 g, 58.8%) as a pale yellow oil. UV-Vis [MeOH, λ_{max}, nm, (ε)]: 306 (4500), 349 (600). IR (neat, cm⁻¹): 1764.87, 1500.30, 1367.90, 1208.18, 791.01. ¹H-NMR (0.125 M in CDCl₃): δ 8.95 (1H, *dd*, *J* = 4.2 and 1.7 Hz, H-2), 8.11 (1H, *dd*, *J* = 8.3 and 1.7 Hz, H-4), 7.44 (1H, *t*, *J* = 8.0 Hz, H-6), 7.41 (1H, *dd*, *J* = 8.2 and 4.2 Hz, H-3), 7.36 (1H, *dd*, *J* = 9.3 and 1.2 Hz, H-5), 7.06 (1H, *dd*, *J* = 7.7 and 1.1 Hz, H-7), 4.18 (2H, *t*, *J* = 7.0 Hz, H-1'), 2.04 (2H, *p*, *J* = 7.2 Hz, H-2'), 1.10 (3H, *t*, *J* = 7.4 Hz, H-3'). ¹³C-NMR (CDCl₃): δ 14.91 (C3'), 20.72 (C2'), 70.62 (C1'), 108.79 (C7), 119.56 (C5), 121.70 (C3), 126.89 (C6), 129.69 (C10), 136.11 (C4), 140.57 (C9), 149.57 (C2), 150.03 (C8).

8,8'-[Hexane-1,2-diylbis(oxy)]diquinoline (6d)

8-Hydroxyquinoline (0.29 g, 2.0 mmol) and K₂CO₃ (0.249 g, 1.8 mmol) were dissolved in DMF (4 mL) and stirred for 15 minutes. 1,6-diiodohexane (0.074 mL, 0.45 mmol) was added dropwise over 1 hour to the solution. The reaction was stirred at 95° C for 21 hours under N₂. Et₂O (2.5 mL), water (15 mL) and 10% NaOH (10 mL) were added to the mixture and the organic layer was separated and dried over MgSO₄. The organic layers were concentrated under reduced pressure under reduced pressure and purified by FCC with 100% EtOAc/hexanes. The fractions containing the desired product were combined and concentrated under reduced pressure to yield **6d** (0.042 g, 25%) as a light yellow solid (m.p. 136-139° C). UV-Vis [MeOH, λ_{max}, nm, (ε)]: 236 (34420), 310 (5182), 349 (664). IR (KBr, cm⁻¹): 1655.13, 1543.53, 1500.12, 1383.05, 1106.34, 791.15. ¹H-NMR (0.250 M in CDCl₃): δ 8.93 (1H, *dd*, *J* = 4.2 and 1.7 Hz, H-2), 8.08 (1H, *dd*, *J* = 8.2 and 1.7 Hz, H-4), 7.42 (1H, *t*, *J* = 8.0 Hz, H-6), 7.38 (1H, *dd*, *J* = 8.2 and 4.2 Hz, H-3), 7.34 (1H, *dd*, *J* = 8.1 and 1.2 Hz, H-5), 7.06 (1H, *dd*, *J* = 6.9 and 1.2 Hz, H-7), 4.23 (2H, *t*, *J* = 4.9 Hz, H-1'), 2.04 (2H, *p*, *J* = 6.4 Hz, H-2'), 1.66 (2H, *m*, *J* = 6.4 Hz, H-3'). ¹³C-NMR (CDCl₃): δ 25.53 (C3'), 28.94 (C2'), 68.81 (C1'), 108.65 (C7), 119.37 (C5), 121.49 (C3), 126.68 (C6), 129.48 (C10), 135.86 (C4), 140.39 (C9), 149.27 (C2), 154.80 (C8).

8,8'-[Decane-1,2-diylbis(oxy)]diquinoline (6e)

8-Hydroxyquinoline (0.261 g, 1.8 mmol) and K₂CO₃ (0.221 g, 1.6 mmol) were dissolved in DMF (4 mL). 1,10-diiododecane (0.316 g, 0.8 mmol) was added to the solution in two portions 30 minutes apart. The reaction was stirred in the dark at 95° C for 16 hours under N₂. Et₂O (25 mL), water (20 mL) and 10% NaOH (8 mL) were added to the mixture and the organic layer was separated and dried over MgSO₄. The organic layer

was concentrated under reduced pressure and purified by FCC with a gradient solvent of 20-100% EtOAc/hexanes. The fractions containing the desired product were combined and concentrated under reduced pressure to yield **6e** (0.138 g, 40.3%) as a light yellow solid (m.p. 96-98 ° C). UV-Vis [MeOH, λ_{max} , nm, (ϵ): 236 (35440), 309 (6384), 236 (770). IR (KBr, cm^{-1}): 2925.73, 1570.41, 1501.06, 1379.91, 1317.42, 1262.03, 1106.04, 791.64. $^1\text{H-NMR}$ (0.064 M in CDCl_3): δ 8.95 (1H, *dd*, $J = 4.2$ and 1.7 Hz, H-2), 8.11 (1H, *dd*, $J = 8.2$ and 1.7 Hz, H-4), 7.44 (1H, *t*, $J = 8.0$ Hz, H-6), 7.42 (1H, *dd*, $J = 8.2$ and 4.2 Hz, H-3), 7.36 (1H, *dd*, $J = 8.0$ and 1.2 Hz, H-5), 7.06 (1H, *dd*, $J = 7.0$ and 1.2 Hz, H-7), 4.23 (2H, *t*, $J = 4.9$ Hz, H-1'), 2.04 (2H, *p*, $J = 5.4$ Hz, H-2'), 1.52 (2H, *p*, $J = 6.4$ Hz, H-3'), 1.38 (4H, *m*, $J = 5.5$ Hz, H-4' and H-5'). $^{13}\text{C-NMR}$ (CDCl_3): δ 26.21 (C3'), 29.11 (C5'), 29.58 (C4'), 29.63 (C2'), 69.15 (C1'), 108.74 (C7), 119.47 (C5), 121.66 (C3), 126.85 (C6), 129.65 (C10), 136.03 (C4), 140.57 (C9), 149.44 (C2), 155.03 (C8).

Synthesis of Benzyl Monoether and Diether Quinoline Analogs

6-(Benzyloxy)quinoline (8)

6-Hydroxyquinoline (0.435 g, 3.0 mmol) and K_2CO_3 (0.373 g, 2.7 mmol) were dissolved in DMF (10 mL) and stirred for 10 minutes. Benzyl bromide (0.339 μL , 2.7 mmol) was added to the solution and reacted at 25° C for 18 hours under Ar. Et_2O (25 mL), water (20 mL) and 10% NaOH (8 mL) were added to the mixture and the organic layer was separated and dried over MgSO_4 . The organic layers were concentrated under reduced pressure and purified by FCC with 100% EtOAc. The fractions containing the desired product were combined, concentrated under reduced pressure and purified by recrystallization with EtOAc / Heptane to yield **8** (0.227 g, 36%) as a light brown oil. UV-Vis [MeOH, λ_{max} , nm, (ϵ): 243 (21290), 267 (6480), 318 (7760), 329 (8330). IR

(neat, cm^{-1}): 1622.30, 1501.23, 1382.38, 1227.23, 1023.53, 833.93, 731.16. $^1\text{H-NMR}$ (0.125 M in CDCl_3): δ 8.78 (1H, *dd*, $J = 4.0$ and 1.6 Hz, H-2), 8.04 (1H, *dd*, $J = 8.0$ and 1.6 Hz, H-4), 8.03 (2H, *d*, $J = 8.6$ Hz, H-8), 7.48 (2H, *d*, $J = 8.0$ Hz, H-4'), 7.60 (1H, *dd*, $J = 9.2$ and 4.2 Hz, H-7), 7.41 (1H, *tt*, $J = 8.4$ and 2.0 Hz, H-5'), 7.36 (2H, *d*, $J = 8.4$ Hz, H-3'), 7.36 (1H, *dd*, $J = 6.0$ and 2.4 Hz, H-3), 7.16 (1H, *d*, $J = 2.0$ Hz, H-5), 5.20 (2H, *s*, H-1'). $^{13}\text{C-NMR}$ (CDCl_3): δ 70.31 (C1'), 106.53 (C5), 121.43 (C3), 122.72 (C7), 127.57 (C4'), 128.21 (C3'), 128.72 (C5'), 129.31 (C10), 130.81 (C8), 135.02 (C4), 136.46 (C2'), 144.38 (C9), 147.99 (C2), 156.90 (C6).

6,6'-[1,2-Phenylenebis(methyleneoxy)]diquinoline (8a)

6-Hydroxyquinoline (0.435 g, 3.0 mmol) and K_2CO_3 (0.373 g, 2.7 mmol) were dissolved in DMF (10 mL) and stirred for 10 minutes. *o*-Xylylene dibromide (0.351 mg, 1.35 mmol) was added to the solution and reacted at 25°C for 12 hours under Ar. Et_2O (25 mL) and water (20 mL) were added to the mixture and the organic layer was separated and dried over MgSO_4 . The organic layers were concentrated under reduced pressure and purified by FCC with a solvent gradient of 100% EtOAc to 10% MeOH / EtOAc. The fractions containing the desired product were concentrated under reduced pressure and recrystallized to yield **8a** (0.148 g, 28%) as a light brown oil. UV-Vis [MeOH, λ_{max} , nm, (ϵ): 238 (20240), 266 (3003), 318 (3320), 329 (3620). IR (neat, cm^{-1}): 1622.26, 1501.69, 1381.10, 1224.73, 1166.37, 833.79, 754.78. $^1\text{H-NMR}$ (0.016 M in CDCl_3): δ 8.76 (1H, *dd*, $J = 4.2$ and 1.6 Hz, H-2), 8.00 (1H, *d*, $J = 9.2$ Hz, H-8), 7.96 (1H, *dd*, $J = 8.4$ and 1.0 Hz, H-4), 7.60 (1H, *dd*, $J = 7.2$ and 6.4 Hz, H-3'), 7.43 (1H, *dd*, $J = 7.2$ and 6.4 Hz, H-4'), 7.42 (1H, *dd*, $J = 4.8$ and 1.2 Hz, H-7), 7.31 (1H, *dd*, $J = 8.0$ and 1.6 Hz, H-3). 7.13 (1H, *d*, $J = 2.4$ Hz, H-5), 5.33 (2H, *s*, H-1'). $^{13}\text{C-NMR}$ (CDCl_3): δ 68.30 (C1'), 106.53

(C5), 121.41 (C3), 122.35 (C7), 128.77 (C4'), 129.16 (C10), 129.28 (C3'), 130.97 (C8), 134.76 (C4), 134.83 (C2'), 144.42 (C9), 148.12 (C2), 156.60 (C6).

6,6'-[1,3-Phenylenebis(methyleneoxy)]diquinoline (8b)

6-Hydroxyquinoline (0.435 g, 3.0 mmol) and K₂CO₃ (0.373 g, 2.7 mmol) were dissolved in DMF (15 mL) and stirred for 15 minutes. *m*-Xylylene dibromide (0.351 mg, 1.35 mmol) was added to the solution and reacted at 25° C for 14 hours under Ar. Et₂O (25 mL) and water (20 mL) were added to the mixture and the organic layer was separated and dried over MgSO₄. The organic layer was concentrated under reduced pressure and purified by FCC with 100% EtOAc. The fractions containing the desired product were concentrated under reduced pressure to yield **8b** (0.215 g, 40%) a light brown oil. UV-Vis [MeOH, λ_{max}, nm, (ε)]: 243 (21920), 266 (7150), 318 (8150), 329 (8550). IR (neat, cm⁻¹): 3027.78, 2934.20, 1622.29, 1501.49, 1380.71, 1224.61, 834.10, 752.83. ¹H-NMR (0.016 M in CDCl₃): δ 8.78 (1H, *dd*, *J* = 4.2 and 1.6 Hz, H-2), 8.03 (1H, *d*, *J* = 8.8 Hz, H-8), 8.01 (1H, *dd*, *J* = 8.0 and 1.6 Hz, H-4), 7.63 (0.5H, *s*, H-5'), 7.48 (1H, *s*, H-3'), 7.48 (0.5H, *s*, H-4'), 7.45 (1H, *dd*, *J* = 9.6 and 2.8 Hz, H-7), 7.35 (1H, *dd*, *J* = 8.0 and 4.0 Hz, H-3). 7.16 (1H, *d*, *J* = 2.8 Hz, H-5), 5.23 (2H, *s*, H-1'). ¹³C-NMR (CDCl₃): δ 70.06 (C1'), 106.53 (C5), 121.44 (C3), 122.56 (C7), 126.56 (C5'), 127.32 (C4'), 129.11 (C3'), 131.01 (C8), 134.89 (C4), 137.06 (C10), 144.05 (C9), 148.16 (C2), 156.73 (C6).

6,6'-[1,4-Phenylenebis(methyleneoxy)]diquinoline (8c)

6-Hydroxyquinoline (0.200 g, 1.3 mmol) and K₂CO₃ (0.193 g, 1.4 mmol) were dissolved in anhyd. DMF (10 mL) and stirred for 5 minutes. α,α-Dibromo-*p*-xylene (0.185 mg, 0.7 mmol) was added to the solution and reacted at 25° C for 10 hours under Ar. Et₂O (15 mL) and water (15 mL) were added to the mixture and the organic layer was separated

and dried over Na₂SO₄. The reaction mixture was purified by FCC with 100 % EtOAc. Fractions containing pure product were concentrated under reduced pressure to yield **8c** (0.048 g, 20%) as a light brown oil. UV-Vis [MeOH, λ_{max}, nm, (ε)]: 239 (15860), 269 (2080), 318 (2170), 330 (2260). IR (neat, cm⁻¹): 3023.18, 1625.31, 1498.89, 1385.11, 1220.95, 755.13. ¹H-NMR (0.125 M in CDCl₃): δ 8.78 (1H, *dd*, *J* = 4.0 and 1.2 Hz, H-2), 8.04 (1H, *dd*, *J* = 8.0 and 1.2 Hz, H-4), 8.03 (1H, *d*, *J* = 9.2 Hz, H-8), 7.54 (2H, *s*, H-3'), 7.46 (1H, *dd*, *J* = 9.2 and 2.8 Hz, H-7), 7.35 (1H, *dd*, *J* = 8.0 and 4.0 Hz, H-3). 7.16 (1H, *d*, *J* = 2.8 Hz, H-5), 5.18 (2H, *s*, H-1'). ¹³C-NMR (CDCl₃): δ 70.16 (C1'), 106.74 (C5), 121.64 (C3), 122.77 (C7), 128.07 (C3'), 129.45 (C1'), 131.19 (C4), 135.10 (C8), 136.69 (C10), 144.69 (C9), 148.32 (C2), 156.96 (C6).

8-(Benzyloxy)quinoline (10)

8-Hydroxyquinoline (0.435 g, 3.0 mmol) and K₂CO₃ (0.373 g, 2.7 mmol) were dissolved in anhyd. DMF (12 mL) and stirred for 15 minutes. Benzyl bromide (0.339 μL, 2.7 mmol) was added to the solution and reacted at 50° C for 72 hours under Ar. Et₂O (15 mL) and 1M NaOH (15 mL) were added to the mixture and the organic layer was separated and dried over MgSO₄. The reaction mixture was purified by FCC using 80 % EtOAc. Fractions containing pure product were concentrated under reduced pressure to yield **10** (0.407 g, 64%) as a pale yellow oil. UV-Vis [MeOH, λ_{max}, nm, (ε)]: 243 (21950), 304 (7530). IR (neat, cm⁻¹): 3034.52, 1569.01, 1499.96, 1375.73, 1318.15, 1263.43, 1104.74, 750.50 ¹H-NMR (0.125 M in CDCl₃): δ 8.98 (1H, *dd*, *J* = 4.0 and 1.6 Hz, H-2), 8.12 (1H, *dd*, *J* = 8.4 and 1.6 Hz, H-4), 7.52 (2H, *d*, *J* = 7.8 Hz, H-3'), 7.43 (1H, *dd*, *J* = 8.4 and 4.4 Hz, H-3), 7.36 (4H, *m*, H-5, H-6, H-4'), 7.28 (1H, *d*, *J* = 8.0 Hz, H-7), 7.03 (1H, *dd*, *J* = 5.6 and 2.8 Hz, H-5') , 5.45 (2H, *s*, H-1'). ¹³C-NMR (CDCl₃): δ

70.92 (C1'), 110.06 (C5'), 120.04 (C5), 121.81 (C3), 126.77 (C6), 127.31 (C3'), 128.21 (C3'), 128.01 (C7), 128.83 (C4'), 129.71 (C10), 136.10 (C4), 137.16 (C2'), 140.70 (C9), 149.60 (C2), 154.53 (C8).

8,8'-[1,2-Phenylenebis(methyleneoxy)]diquinoline (10a)

8-Hydroxyquinoline (0.435 g, 3.0 mmol) and K₂CO₃ (0.373 g, 2.7 mmol) were dissolved in anhyd. DMF (15 mL) and stirred for 10 minutes. *o*-Xylylene dibromide (0.351 mg, 1.35 mmol) was added to the solution and reacted at 50° C for 72 hours under Ar. Et₂O (15 mL) and 1M NaOH (15 mL) were added to the mixture and the organic layer was separated and dried over MgSO₄. The reaction mixture was purified by FCC with a solvent gradient of 50 % EtOAc / Hexanes to 100% EtOAc to 10% MeOH / EtOAc.

Fractions containing pure product were concentrated under reduced pressure to yield **10a** (0.067 g, 12.5%) as a pale yellow oil. UV-Vis [MeOH, λ_{max}, nm, (ε)]: 211 (10190), 240 (12440), 304 (1280). IR (neat, cm⁻¹): 1569.06, 1500.15, 1317.61, 1100.84, 730.26. ¹H-NMR (0.125 M in CDCl₃): δ 8.93 (1H, *dd*, *J* = 4.0 and 1.6 Hz, H-2), 8.10 (1H, *dd*, *J* = 8.4 and 1.6 Hz, H-4), 7.59 (1H, *dd*, *J* = 5.2 and 2.4 Hz, H-3'), 7.41 (1H, *dd*, *J* = 8.4 and 4.4 Hz, H-3), 7.32 (3H, *m*, H-5, H-6, H-7), 7.13 (1H, *dd*, *J* = 5.6 and 2.8 Hz, H-4'), 5.63 (2H, *s*, H-1'). ¹³C-NMR (CDCl₃): δ 69.18 (C1'), 110.05 (C4'), 119.88 (C5), 121.55 (C3), 126.57 (C6), 128.27 (C7), 128.76 (C3'), 129.41 (C10), 134.98 (C2'), 135.81 (C4), 140.48 (C9), 149.29 (C2), 154.20 (C8).

8,8'-[1,3-phenylenebis(methyleneoxy)]diquinoline (10b)

8-Hydroxyquinoline (0.435 g, 3.0 mmol) and K₂CO₃ (0.373 g, 2.7 mmol) were dissolved in anhyd. DMF (15 mL) and stirred for 10 minutes. *m*-Xylylene dibromide (0.351 mg, 1.35 mmol) was added to the solution and reacted at 50° C for 72 hours under Ar. Et₂O

(15 mL) and 1M NaOH (15 mL) were added to the mixture and the organic layer was separated and dried over MgSO₄. The reaction mixture was purified by FCC with a solvent gradient of 50 % EtOAc / Hexanes to 100% EtOAc. Fractions containing pure product were concentrated under reduced pressure to yield **10b** (0.124 g, 23%) as a light yellow oil. UV-Vis [MeOH, λ_{max}, nm, (ε)]: 216 (12180), 242 (20800), 307 (3110). IR (neat, cm⁻¹): 3060.22, 1569.88, 1500.41, 1376.19, 1317.72, 1104.87, 790.93. ¹H-NMR (0.125 M in CDCl₃): δ 8.95 (1H, *dd*, *J* = 4.0 and 1.6 Hz, H-2), 8.10 (1H, *dd*, *J* = 8.4 and 1.6 Hz, H-4), 7.65 (0.5H, *s*, H-5'), 7.46 (0.5H, *d*, *J* = 8.0 Hz, H-4'), 7.41 (1H, *dd*, *J* = 8.0 and 4.0 Hz, H-3), 7.35 (3H, *m*, H-3', H-6, H-7), 6.98 (1H, *dd*, *J* = 7.2 and 1.6 Hz, H-5), 5.44 (2H, *s*, H-1'). ¹³C-NMR (CDCl₃): δ 70.74 (C1'), 110.11 (C5), 120.03 (C3'), 121.75 (C3), 125.89 (C5'), 126.74 (C7), 126.78 (C6), 129.63 (C10), 129.65 (C4'), 136.09 (C4), 137.53 (C2'), 140.55 (C9), 149.48 (C2), 154.38 (C8).

Synthesis of Benzoyl Monoester and Diester Quinoline Analogs

Quinolin-6-yl benzoate (7)

6-Hydroxyquinoline (0.300 g, 2.0 mmol) and triethylamine (0.279 mL, 2.0 mmol) were dissolved in 50 % DCM / DMF (12 mL) and stirred for 20 minutes. Benzoyl chloride (0.220 mL, 1.9 mmol) was added to the solution dropwise and reacted at 25° C for 18 hours under Ar. The reaction mixture was concentrated under reduced pressure and purified by FCC with 50% EtOAc / Hexanes. The fractions containing the desired product were concentrated under reduced pressure and purified by recrystallization with EtOAc / Heptane to yield **7** (0.425 g, 90%) as a light brown solid (m.p. 106-111° C). UV-Vis [MeOH, λ_{max}, nm, (ε)]: 232 (12060), 301 (1070), 314 (1090). IR (KBr, cm⁻¹): 3031.62, 2929.98, 1622.30, 1501.23, 1382.38, 1227.23, 1167.13, 833.97, 731.16. ¹H-

NMR (0.250 M in CDCl₃): δ 8.93 (1H, *dd*, $J = 4.4$ and 2.0 Hz, H-2), 8.25 (2H, *dd*, $J = 8.0$ and 2.0 Hz, H-3'), 8.19 (1H, *d*, $J = 6.0$ Hz, H-8), 8.14 (1H, *dd*, $J = 8.4$ and 1.2 Hz, H-4), 7.70 (1H, *d*, $J = 5.6$ Hz, H-5), 7.66 (1H, *tt*, $J = 7.2$ and 1.2 Hz, H-5'), 7.60 (1H, *dd*, $J = 8.8$ and 2.4 Hz, H-7), 7.53 (2H, *t*, $J = 6.0$ Hz, H-4'), 7.42 (1H, *dd*, $J = 8.0$ and 4.4 Hz, H-4). ¹³C-NMR (CDCl₃): δ 118.63 (C5), 121.64 (C3), 124.92 (C7), 128.62 (C10), 128.70 (C4'), 129.24 (C2'), 130.26 (C3'), 131.03 (C8), 133.87 (C5'), 135.92 (C4), 146.27 (C9), 148.80 (C6), 150.23 (C2), 165.13 (C1').

Diquinolin-6-yl phthalate (7a)

6-Hydroxyquinoline (0.300 g, 2.0 mmol) and triethylamine (0.279 mL, 2.0 mmol) were dissolved in 80% anhyd. DCM / DMF (12 mL) and stirred for 15 minutes. Phthaloyl chloride (0.144 mL, 0.95 mmol) was added to the solution dropwise and reacted at 25° C for 14 hours under Ar. The reaction mixture was concentrated under reduced pressure and purified by FCC with 100% EtOAc / Hexanes. The fractions containing the desired product were concentrated under reduced pressure to yield **7a** (0.095 g, 24%) as a tan solid (m.p. 135-145° C). UV-Vis [MeOH, λ_{\max} , nm, (ϵ): 209 (87800), 224 (80533), 301 (6400), 314 (6533). IR (KBr, cm⁻¹): 3027.94, 2933.28, 1622.26, 1501.69, 1381.10, 1224.73, 833.79, 754.78. ¹H-NMR (0.016 M in CDCl₃): δ 8.92 (1H, *dd*, $J = 4.4$ and 1.6 Hz, H-2), 8.15 (1H, *d*, $J = 9.2$ Hz, H-8), 8.10 (1H, *dd*, $J = 7.8$ and 1.2 Hz, H-4), 8.08 (1H, *dd*, $J = 5.6$ and 3.2 Hz, H-3'), 7.78 (1H, *dd*, $J = 5.6$ and 3.2 Hz, H-4'), 7.71 (1H, *d*, $J = 4.2$ Hz, H-5), 7.62 (1H, *dd*, $J = 9.2$ and 4.2 Hz, H-7), 7.41 (1H, *dd*, $J = 8.2$ and 4.4 Hz, H-3). ¹³C-NMR (CDCl₃): δ 118.78 (C5), 121.86 (C3), 124.71 (C7), 128.74 (C10), 129.86 (C3'), 131.43 (C8), 131.68 (C2'), 132.30 (C4'), 136.10 (C4), 146.62 (C9), 148.70 (C6), 150.61 (C2), 166.03 (C1').

Quinolin-8-yl benzoate (9)

8-Hydroxyquinoline (0.300 g, 2.0 mmol) and triethylamine (0.279 mL, 2.0 mmol) were dissolved in 50 % anhyd. DCM / DMF (12 mL) and stirred for 20 minutes. Benzoyl chloride (0.220 μ L, 1.9 mmol) was added to the solution and reacted at 25° C for 18 hours under Ar. The reaction mixture was concentrated under reduced pressure to give **9** (0.431 g, 91%) as a bright yellow solid (m.p. 112-116° C). UV-Vis [MeOH, λ_{max} , nm, (ϵ): 230 (10690), 280 (1730), 300 (1130), 314 (760). IR (KBr, cm^{-1}): 3034.52, 2934.12, 1569.01, 1499.96, 1375.73, 1318.15, 1263.43, 1104.74, 750.50. $^1\text{H-NMR}$ (0.250 M in CDCl_3): δ 8.86 (1H, *dd*, $J = 4.4$ and 2.0 Hz, H-2), 8.35 (2H, *dd*, $J = 8.0$ and 2.0 Hz, H-3'), 8.17 (1H, *dd*, $J = 8.4$ and 1.6 Hz, H-4), 7.74 (1H, *dd*, $J = 4.4$ and 4.0 Hz, H-6), 7.64 (1H, *tt*, $J = 7.2$ and 2.0 Hz, H-5'), 7.55 (2H, *dd*, $J = 8.0$ and 1.2 Hz, H-5 and H-7), 7.52 (2H, *t*, $J = 8.0$ Hz, H-4'), 7.40 (1H, *dd*, $J = 8.6$ and 4.4 Hz, H-3). $^{13}\text{C-NMR}$ (CDCl_3): δ 121.66 (C5), 121.76 (C3), 126.06 (C6), 126.27 (C7), 128.61 (C4'), 129.53 (C10), 129.62 (C2'), 130.60 (C3'), 133.60 (C5'), 136.04 (C4), 141.43 (C9), 147.75 (C8), 150.65 (C2), 165.54 (C1').

Diquinolin-8-yl phthalate (9a)

8-Hydroxyquinoline (0.300 g, 2.0 mmol) and triethylamine (0.279 mL, 2.0 mmol) were dissolved in 80 % anhyd. DCM / DMF (12 mL) and stirred for 15 minutes. Phthaloyl chloride (0.144 mL, 0.95 mmol) was added to the solution and reacted at 25° C for 14 hours under Ar. The reaction mixture was concentrated under reduced pressure and purified by FCC with 50% EtOAc / Hexanes. The fractions containing the desired product were concentrated under reduced pressure to yield **9a** (0.180 g, 47%) as a light yellow solid (m.p. 178-181° C). UV-Vis [MeOH, λ_{max} , nm, (ϵ): 228 (8330), 281 (1560),

313 (700). IR (KBr, cm^{-1}): 1742.03, 1500.01, 1265.15, 1230.59, 1106.60. $^1\text{H-NMR}$ (0.125 M in CDCl_3): δ 8.89 (1H, *dd*, $J = 4.4$ and 1.6 Hz, H-2), 8.35 (2H, *dd*, $J = 8.0$ and 2.0 Hz, H-3'), 8.15 (1H, *dd*, $J = 8.0$ and 1.6 Hz, H-4), 7.74 (1H, *dd*, $J = 5.6$ and 3.2 Hz, H-4'), 7.70 (1H, *dd*, $J = 8.4$ and 1.2 Hz, H-5), 7.55 (1H, *dd*, $J = 8.0$ and 1.2 Hz, H-7 and H-7'), 7.46 (1H, *t*, $J = 8.0$ Hz, H-6), 7.40 (1H, *dd*, $J = 8.6$ and 4.4 Hz, H-3). $^{13}\text{C-NMR}$ (CDCl_3): δ 121.92 (C7), 121.93 (C3), 126.20 (C5), 126.46 (C6), 129.72 (C10), 130.37 (C3'), 131.96 (C4'), 132.16 (C2'), 136.08 (C4), 141.59 (C9), 147.58 (C8), 150.81 (C2), 166.28 (C1').

Synthesis of Unsymmetrical Diesters

Quinolin-6-yl quinolin-8-yl adipate (11a)

6-Hydroxyquinoline (0.100 g, 0.6 mmol) and 8-hydroxyquinoline (0.100 mg, 0.6 mmol) was stirred in CH_2Cl_2 (15 mL) in the presence of triethylamine (0.167 mL, 1.2 mmol), adipoyl chloride (0.073 mL, 0.5 mmol) was added slowly over 1 hour under Ar and stirred at room temperature for 24 h. Reaction was extracted with EtOAc (10 mL) and 1M NaOH solution (10 mL) and the organic layer was separated, dried over anhyd. Na_2SO_4 and concentrated under reduced pressure. The reaction mixture was purified by FCC using a solvent of 100% EtOAc. Fractions containing pure product were combined, concentrated under reduced pressure to yield **11a** (0.040 g, 20%) as a light brown solid (m.p. 134-137° C). UV-Vis [MeOH, λ_{max} , nm, (ϵ): 252 (7860), 322 (4790), 331 (6330). IR (KBr, cm^{-1}): 1746.85, 1621.79, 1513.44, 1203.30, 1131.22. $^1\text{H-NMR}$ (0.125 M in CDCl_3): δ 8.90 (2H, *m*, H-2, H-2'), 8.17 (1H, *dd*, $J = 8.0$ and 1.6 Hz, H-4'), 8.12 (2H, *d*, $J = 9.2$ Hz, H-4, H-8), 7.72 (1H, *dd*, $J = 8.0$ and 1.2 Hz, H-5'), 7.56 (1H, *d*, $J = 2.4$ Hz, H-5), 7.53 (1H, *t*, $J = 8.0$ Hz, H-6'), 7.47 (1H, *d*, $J = 2.4$ Hz, H-7), 7.45 (1H, *d*, $J = 2.0$ Hz,

H-7'), 7.42 (2H, *m*, H-3, H-3'), 2.92 (2H, *t*, $J = 8.0$ Hz, H-2''), 2.70 (2H, *t*, $J = 8.0$ Hz, H-9''), 2.04 (4H, *m*, H-3'', H-8''). ^{13}C -NMR (CDCl_3): δ 24.57 (C3'', C4''), 34.06 (C6''), 34.29 (C2''), 118.62 (C5), 121.68 (C3, C3'), 121.94 (C7'), 124.99 (C7), 126.01 (C10'), 126.09 (C5'), 126.40 (C6'), 129.71 (C10), 131.18 (C4), 135.99 (C8), 136.21 (C4'), 141.36 (C9), 146.43 (C9'), 147.60 (C8), 148.70 (C6), 150.37 (C2'), 150.65 (C2), 172.07 (C10''), 172.47 (C1'').

Quinolin-6-yl quinolin-8-yl sebecate (11b)

6-Hydroxyquinoline (0.145 g, 1.0 mmol) and 8-hydroxyquinoline (0.145 g, 1.0 mmol) was stirred in CH_2Cl_2 (20 mL) in the presence of triethylamine (0.279 mL, 2.0 mmol), sebacoyl chloride (0.241 mL, 0.9 mmol) was added slowly over 1 hour under Ar and stirred at room temperature for 24 h. Reaction was extracted with EtOAc (10 mL) and 1M NaOH solution (10 mL) and the organic layer was separated, dried over anhyd. Na_2SO_4 and concentrated under reduced pressure. The reaction mixture was purified by FCC using a solvent of 100% EtOAc. Fractions containing pure product were combined, concentrated under reduced pressure to yield **11b** (0.051 g, 12% yield) as light brown solid (m.p. 120-124° C). UV-Vis [MeOH, λ_{max} , nm, (ϵ): 234 (23400), 279 (5600), 318 (3200), IR (KBr, cm^{-1}): 2931.93, 1749.74, 1562.55, 1151.31. ^1H -NMR (0.125 M in CDCl_3): δ 8.90 (2H, *m*, H-2, H-2'), 8.17 (1H, *dd*, $J = 8.0$ and 1.6 Hz, H-4'), 8.12 (2H, *d*, $J = 9.2$ Hz, H-4, H-8), 7.72 (1H, *dd*, $J = 8.0$ and 1.2 Hz, H-5'), 7.56 (1H, *d*, $J = 2.4$ Hz, H-5), 7.53 (1H, *t*, $J = 8.0$ Hz, H-6'), 7.47 (1H, *d*, $J = 2.4$ Hz, H-7), 7.45 (1H, *d*, $J = 2.0$ Hz, H-7'), 7.42 (2H, *m*, H-3, H-3'), 2.80 (2H, *t*, $J = 8.0$ Hz, H-2''), 2.64 (2H, *t*, $J = 8.0$ Hz, H-9''), 1.83 (4H, *m*, H-3'', H-8''), 1.49 (8H, *m*, H-4'' \rightarrow H-7''). ^{13}C -NMR (CDCl_3): δ 25.10 (C3'', C8''), 29.28 (C4'' \rightarrow C7''), 34.36 (C9''), 34.459 (C3''), 118.59 (C5), 121.81

(C3, C3'), 121.88 (C7'), 125.05 (C7), 125.98 (C5'), 126.39 (C6'), 128.73 (C10), 129.70 (C10'), 131.05 (C4), 136.06 (C8), 136.23 (C4'), 141.42 (C9), 146.32 (C9'), 147.62 (C8), 148.77 (C6), 150.28 (C2'), 150.60 (C2), 172.43 (C10''), 172.82 (C1'').

Quinolin-6-yl quinolin-8-yl phthalate (11c)

6-Hydroxyquinoline (0.150 g, 1.0 mmol) and 8-hydroxyquinoline (0.150 g, 1.0 mmol) was stirred in 10 % DMF / CH₂Cl₂ (20 mL) in the presence of triethylamine (0.279 mL, 2.0 mmol), phthaloyl chloride (0.144 mL, 0.95 mmol) was added slowly over 1 hour under Ar and stirred at room temperature for 24 h. Reaction was extracted with EtOAc (10 mL) and 1M NaOH solution (10 mL) and the organic layer was separated, dried over anhyd. Na₂SO₄ and concentrated under reduced pressure. The reaction mixture was purified by FCC using a solvent of 100% EtOAc. Fractions containing pure product were combined, concentrated under reduced pressure to yield **11c** (0.047 g, 11%) as a tan solid (m.p. 112-118° C). UV-Vis [MeOH, λ_{max}, nm, (ε)]: 211 (34500), 312 (9300), 308 (6210). IR (KBr, cm⁻¹): 3020.33, 1603.98, 1511.77, 1323.12, 1245.69, 812.45, ¹H-NMR (0.125 M in CDCl₃): δ 8.91 (1H, *dd*, *J* = 4.0 and 1.6 Hz, H-2), 8.84 (1H, *dd*, *J* = 4.0 and 1.6 Hz, H-2'), 8.30 (1H, *dd*, *J* = 8.0 and 1.6 Hz, H-3''), 8.18 (1H, *dd*, *J* = 8.0 and 1.6 Hz, H-4'), 8.11 (1H, *d*, *J* = 9.2 Hz, H-8), 8.06 (1H, *d*, *J* = 9.2 Hz, H-4), 8.01 (1H, *dd*, *J* = 6.4 and 2.0 Hz, H-6''), 7.75 (3H, *m*, H-4'', H-5'', H-5'), 7.69 (1H, *d*, *J* = 2.4 Hz, H-5), 7.62 (1H, *d*, *J* = 2.0 Hz, H-7), 7.59 (1H, *dd*, *J* = 7.2 and 1.2 Hz, H-7'), 7.52 (1H, *t*, *J* = 8.0 Hz, H-6'), 7.39 (2H, *dd*, *J* = 8.0 and 4.0 Hz, H-3, H-3'). ¹³C-NMR (CDCl₃): δ 118.86 (C5), 121.77 (C3'), 121.88 (C3), 122.06 (C7'), 125.06 (C7), 126.47 (C5'), 126.56 (C6'), 128.89 (C10), 129.77 (C6''), 129.98 (C10'), 130.72 (C3''), 131.20 (C8), 131.96 (C7''), 132.01 (C2''),

132.14 (C5''), 132.21 (C4''), 136.23 (C4'), 136.27 (C4), 141.65 (C8'), 146.72 (C9'), 147.48 (C6), 148.92 (C9), 150.43 (C2'), 150.89 (C2), 166.54 (8''), 166.67 (1'').

Synthesis of Aliphatic Monoamides

***N*-Quinolin-6-ylacetamide (13)**

6-Aminoquinoline (0.200 g, 1.4 mmol) and distilled triethylamine (2mL, 1.4 mmol) were dissolved in CH₂Cl₂ (20 mL). Acetyl chloride (0.171 mL, 1.4 mmol) was added to the solution dropwise. The reaction was stirred at 25° C for 26 hours under N₂. Sat.

NaHCO₃ (23 mL) and CH₂Cl₂ (5 mL) were added to the mixture and the organic layer was separated and dried over MgSO₄. The organic layer was concentrated under reduced pressure and purified by FCC with a solvent gradient of 40 – 50 % Acetone/hexanes.

The fractions containing the desired product were combined and concentrated under reduced pressure to yield **13** (0.230 g, 50.6%) as a light brown solid (m.p. 102-104 ° C).

UV-Vis [MeOH, λ_{max}, nm, (ε)]: 225 (43500), 272 (5800), 302 (4200), 315 (4700). IR (KBr, cm⁻¹): 2924.95, 1751.93, 1569.70, 1164.33. ¹H-NMR (0.125 M in CDCl₃): δ 8.81 (1H, *dd*, *J* = 4.0 and 1.2 Hz, H-2), 8.55 (1H, *s*, NH), 8.39 (1H, *d*, *J* = 2.0 Hz, H-5), 8.08 (1H, *d*, *J* = 8.4, H-4), 7.99 (1H, *d*, *J* = 8.8, H-8), 7.58 (1H, *dd*, *J* = 8.8 and 2.0 Hz, H-5), 7.37 (1H, *dd*, *J* = 8.4 and 4.0 Hz, H-3), 2.24 (1H, *s*, H-2'). ¹³C-NMR (CDCl₃): δ 24.82 (C2'), 116.29 (C5), 121.82 (C3), 123.39 (C7), 129.10 (C10), 130.12 (C8), 136.15 (C6, C4), 145.57 (C9), 149.47 (C2), 169.08 (C1').

***N*-quinolin-8-ylacetamide (15)**

8-Aminoquinoline (0.200 g, 1.4 mmol) and distilled triethylamine (2mL, 1.4 mmol) were dissolved in CH₂Cl₂ (15 mL). Acetyl chloride (0.171 mL, 1.4 mmol) was added to the solution dropwise. The reaction was stirred at 25° C for 24 hours under N₂. Sat.

NaHCO₃ (23 mL) and CH₂Cl₂ (5 mL) were added to the mixture and the organic layer was separated and dried over MgSO₄. The organic layer was concentrated under reduced pressure and purified by FCC with a solvent gradient of 40 – 50 % Acetone/hexanes. The fractions containing the desired product were combined and concentrated under reduced pressure to yield **15** (0.116 g, 25%) as a off-white solid (m.p. 106-109 ° C). UV-Vis [MeOH, λ_{max}, nm, (ε)]: 234 (9500), 252 (5100), 310 (4200). IR (KBr, cm⁻¹): 2920.91, 1732.91, 1599.72, 1132.22. ¹H-NMR (0.125 M in CDCl₃): δ 9.78 (1H, *s*, NH), 8.80 (1H, *dd*, *J* = 4.0 and 1.6 Hz, H-2), 8.76 (1H, *dd*, *J* = 7.2 and 1.6 Hz, H-7), 8.15 (1H, *dd*, *J* = 8.0 and 1.6 Hz, H-4), 7.53 (1H, *t*, *J* = 8.0 Hz, H-6), 7.49 (1H, *dd*, *J* = 8.0 and 1.6 Hz, H-5), 7.44 (1H, *dd*, *J* = 8.0 and 4.0 Hz, H-3), 2.35 (1H, *s*, H-2'). ¹³C-NMR (CDCl₃): δ 25.32 (C2'), 116.60 (C7), 121.64 (C5), 121.77 (C3), 127.59 (C6), 128.11 (C10), 134.72 (C8), 136.56 (C4), 138.43 (C9), 148.30 (C2), 168.96 (C1').

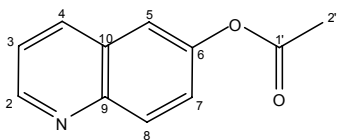
REFERENCES

- (1) Chen, R. J.; Zhang, Y.; Wang, D.; Dai, H. *J. Am. Chem. Soc.* **2001**, *123*, 3838-3839.
- (2) Magistrato, A.; Pregosin, P. S.; Albinati, A.; Rothlisberger, U. *Organometallics* **2001**, *20*, 4178-4184.
- (3) Cubberley, M. S.; Iverson, B. L. *J. Am. Chem. Soc.* **2001**, *123*, 7560-7563.
- (4) Tanaka, S.-y.; Yasuda, M.; Baba, A. *J. Org. Chem.* **2006**, *71*, 800-803.
- (5) Reisch, J.; Mueller, M. *Pharmazie* **1983**, *38*, 631-2.
- (6) Reisch, J. *Pharmazie* **1967**, *26*, 420-2.
- (7) Zamble, A.; Hennebelle, T.; Sahpaz, S.; Bailleul, F. *Chemical & Pharmaceutical Bulletin* **2007**, *55*, 643-645.
- (8) Fokialakis, N.; Magiatis, P.; Chinou, I.; Mitaku, S.; Tillequin, F. *Chemical & Pharmaceutical Bulletin* **2002**, *50*, 413-414.
- (9) Shea, R., *Synthesis, NMR and Bioactivities of Substituted Quinolines*, University of North Carolina Wilmington, 1998.
- (10) Srivastava, S.; Tewari, S.; Chauhan, P. M. S.; Puri, S. K.; Bhaduri, A. P.; Pandey, V. C. *Bioorganic & Medicinal Chemistry Letters* **1999**, *9*, 653-658.
- (11) Foley, M.; Tilley, L. *International Journal for Parasitology* **1997**, *27*, 231-240.
- (12) Graves, P. R.; Kwiek, J. J.; Fadden, P.; Ray, R.; Hardeman, K.; Coley, A. M.; Foley, M.; Haystead, T. A. *J. Mol. Pharmacol* **2002**, *62*, 1364-1372.
- (13) Fahrni, C.; O'Halloran, T. **1999**.
- (14) Nasir, S.; Fahrni, C.; Suhy, D.; Kolodsick, K.; Singer, C.; O'Halloran, T. *J. Biol. Inorg. Chem.* **1999**, *6*, 775-83.
- (15) Mitra, A.; Seaton, P.; Assarpour, R.; Williamson, T. *Tetrahedron* **1998**, *54*, 15489-15498.
- (16) Guan, L.; Hu, Y.; Kaback, H. R. *Biochemistry* **2003**, *42*, 1377-1382.
- (17) Mignon, P.; Loverix, S.; Steyaert, J.; Geerlings, P. *Nucleic Acids Research* **2005**, *33*, 1779-1789.
- (18) McKay, S. L.; Haptonstall, B.; Gellman, S. H. *J. Am. Chem. Soc.* **2001**, *123*, 1244-1245.
- (19) Soundararajan, S. *Z. phys. Chem. Bd.* **1963**, *226*, 303-308.
- (20) Tumambac, G. E.; Wolf, C. *J. Org. Chem.* **2005**, *70*, 2930-2938.
- (21) Huang, F.; Zhou, L.; Jones, J. W.; Gibson, H. W.; Ashraf-Khorassani, M. *Chem. Commun.* **2004**, 2670 - 2671.
- (22) Jijun, Z.; Jian Ping, L.; Jie, H.; Chih-Kai, Y. *Applied Physics Letters* **2003**, *82*, 3746-3748.
- (23) Munakata, M.; Wu, L. P.; Takayoshi, K.-S.; Maekawa, M.; Suenaga, Y.; Ohta, T.; Konaka, H. *Inorg. Chem.* **2003**, *42*, 2553-2558.
- (24) Ewing, D. F. *Organic Magnetic Resonance* **1973**, *5*, 321-325.
- (25) Yanuka, Y.; Superstine, S. Y.; Superstine, E. *Journal of Pharmaceutical Sciences* **1979**, *68*, 1400-1403.
- (26) Lapytov, S.; Fakhfakh, M. A.; Julian, J.-C.; Franck, X.; Hocquemiller, R.; Figadere, B. *Bull. Chem. Soc. Jpn.* **2005**, *78*, 1296-1301.

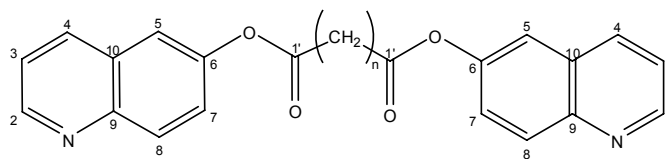
- (27) Kishikawa, K.; Tsubokura, S.; Kohmoto, S.; Yamamoto, M. *J. Org. Chem.* **1999**, *64*, 7568-7578.
- (28) Hunter, C. A.; Sanders, J. K. M. *J. Am. Chem. Soc.* **1990**, *112*, 5525-34.
- (29) Lee, E. C.; Kim, D.; Jurecka, P.; Tarakeshwar, P.; Hobza, P.; Kim, K. S. *J. Phys. Chem. A* **2007**, *111*, 3446-3457.
- (30) Chen, C. W.; H.W. Whitlock, J. *J. Am. Chem. Soc.* **1978**, *100*, 4921-4922.
- (31) Klärner, F.-G.; Kahlert, B.; Boese, R.; Blaser, D.; Juris, A.; Marchioni, F. *Chem. Eur. J.* **2005**, *11*, 3363-3374.
- (32) Harmata, M. *Acc. Chem. Res.* **2004**, *37*, 862-873.
- (33) Zhao, F.; Zhao, M. *Recent Res. Devel. Physics*, **2005**, 6.
- (34) Kurebayashi, H.; Haino, T.; Usui, S.; Fukazawa, Y. *Tetrahedron* **2001**, *57*, 8667-8674.
- (35) Abraham, R. J.; Mobil, M. *Spectroscopy Europe*, 16-21.
- (36) Mishra, B. K.; Sathyamurthy, N. *J. Phys. Chem. A.* **2005**, *109*, 6-8.
- (37) Chen, C. W.; Whitlock, H. W. J. *J. Am. Chem. Soc.* **1978**, *100*, 4921-4922.
- (38) Nemeto, H.; Kawano, T.; Ueji, N.; Bando, M.; Kido, M.; Suzuki, I.; Shibuya, M. *Organic Letters* **2000**, *2*, 1015-1017.

APPENDIX

Appendix 1: Structures and H-NMR data for 6-substituted mono and diester products.



2



2a-c

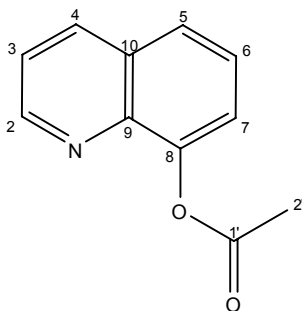
a: n=6

b: n=8

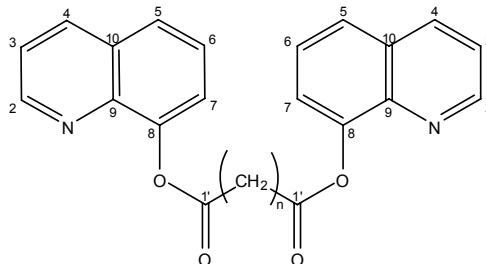
c: n=10

	C (M)	H-2	H-3	H-4	H-5	H-6	H-7	H-8
2	0.016	-	-	-	-	-	-	-
	0.031	8.918	7.439	8.147	7.578	x	7.483	8.142
	0.062	8.917	7.435	8.143	7.577	x	7.482	8.122
	0.125	8.913	7.429	8.140	7.574	x	7.481	8.118
	0.250	8.906	7.416	8.138	7.567	x	7.478	8.116
	0.500	8.890	7.388	8.134	7.553	x	7.472	8.096
2a	0.016	-	-	-	-	x	-	-
	0.031	8.915	7.426	8.109	7.584	x	7.489	8.128
	0.062	8.911	7.419	8.096	7.584	x	7.489	8.127
	0.125	8.905	7.407	8.094	7.584	x	7.489	8.126
	0.250	8.889	7.382	8.072	7.570	x	7.486	8.125
2b	0.016	8.912	7.424	8.102	7.571	x	7.475	8.135
	0.031	8.911	7.421	8.099	7.570	x	7.475	8.135
	0.062	8.907	7.414	8.093	7.568	x	7.474	8.134
	0.125	8.900	7.400	8.081	7.564	x	7.474	8.133
	0.250	8.889	7.377	8.062	7.557	x	7.474	8.133
2c	0.016	8.909	7.424	8.134	7.568	x	7.471	8.112
	0.031	8.908	7.421	8.133	7.566	x	7.471	8.111
	0.062	8.904	7.415	8.134	7.565	x	7.471	8.111
	0.125	8.898	7.402	8.133	7.561	x	7.470	8.092
	0.250	8.885	7.376	8.132	7.553	x	7.470	8.088

Appendix 2: Structures and H-NMR data for 8-substituted mono and diester products.



4



4a-c

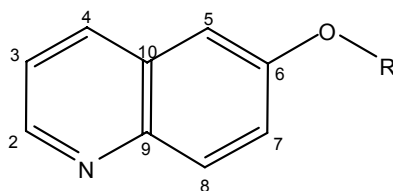
a: n=6

b: n=8

c: n=10

	C (M)	H-2	H-3	H-4	H-5	H-6	H-7	H-8
4	0.016	8.934	7.448	8.202	7.564	7.747	7.466	x
	0.031	8.932	7.446	8.199	7.561	7.745	7.465	x
	0.062	8.930	7.444	8.195	7.558	7.741	7.464	x
	0.125	8.928	7.445	8.187	7.554	7.735	7.462	x
	0.250	8.921	7.438	8.170	7.542	7.720	7.456	x
	0.500	8.907	7.428	8.138	7.520	7.692	7.447	x
4a	0.016	-	-	-	-	-	-	x
	0.031	8.928	7.435	8.186	7.734	7.551	7.467	x
	0.062	8.926	7.428	8.178	7.728	7.547	7.466	x
	0.125	8.910	7.413	8.162	7.714	7.536	7.461	x
	0.250	8.906	7.384	8.131	7.688	7.516	7.453	x
4b	0.016	8.928	7.434	8.188	7.733	7.552	7.438	x
	0.031	8.925	7.433	8.182	7.728	7.548	7.433	x
	0.062	8.921	7.425	8.173	7.721	7.543	7.433	x
	0.125	8.915	7.410	8.156	7.707	7.532	7.429	x
	0.250	8.903	7.382	8.127	7.682	7.513	7.422	x
4c	0.016	8.918	7.439	8.186	7.451	7.550	7.730	x
	0.031	8.916	7.432	8.183	7.451	7.548	7.727	x
	0.062	8.913	7.429	8.175	7.448	7.543	7.720	x
	0.125	8.906	7.426	8.159	7.445	7.533	7.707	x
	0.250	8.891	7.419	8.126	7.437	7.512	7.678	x

Appendix 3: Structures and H-NMR data for 6-substituted monoether products.



5a-c

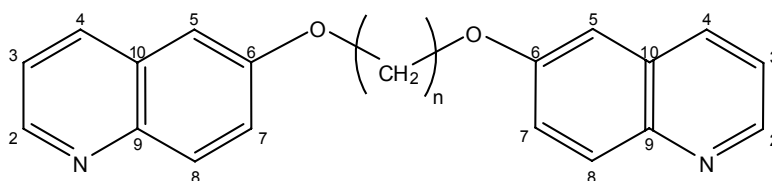
a: R=methyl

b: R=ethyl

c: R=propyl

	<u>C (M)</u>	H-2	H-3	H-4	H-5	H-6	H-7	H-8
5a	0.016	8.765	7.345	8.051	7.076	x	7.394	7.992
	0.031	8.764	7.343	8.049	7.074	x	7.393	7.992
	0.062	8.763	7.340	8.045	7.071	x	7.391	7.992
	0.125	8.760	7.334	8.039	7.064	x	7.389	7.991
	0.250	8.755	7.324	8.026	7.053	x	7.385	7.989
5b	0.016	8.769	7.365	8.051	7.067	x	7.388	8.009
	0.031	8.767	7.363	8.049	7.065	x	7.386	8.008
	0.062	8.766	7.362	8.047	7.062	x	7.386	8.008
	0.125	8.764	7.356	8.041	7.057	x	7.384	8.008
	0.250	8.759	7.347	8.031	7.047	x	7.380	8.007
5c	0.016	8.752	7.332	8.046	7.063	x	7.395	7.984
	0.031	8.752	7.331	8.046	7.062	x	7.395	7.984
	0.062	8.750	7.329	8.046	7.060	x	7.394	7.984
	0.125	8.748	7.324	8.038	7.055	x	7.393	7.984
	0.250	8.744	7.314	8.030	7.045	x	7.389	7.983

Appendix 4: Structures and H-NMR data for 6-substituted diether products.



5d-f

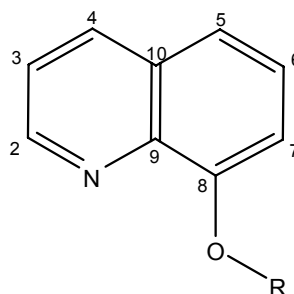
d: n=3

e: n=6

f: n=10

	<u>C (M)</u>	H-2	H-3	H-4	H-5	H-6	H-7	H-8
5d	0.016	8.776	7.363	8.039	7.122	x	7.408	8.035
	0.031	8.775	7.361	8.037	7.120	x	7.407	8.034
	0.062	8.773	7.357	8.032	7.116	x	7.406	8.030
	0.125	8.768	7.348	8.023	7.107	x	7.402	8.015
	0.25	8.760	7.328	8.004	7.086	x	7.396	8.013
5e	0.016	8.768	7.360	8.043	7.071	x	7.390	8.007
	0.031	8.768	7.360	8.041	7.069	x	7.390	8.007
	0.062	8.766	7.358	8.038	7.066	x	7.388	8.007
	0.125	8.763	7.350	8.031	7.060	x	7.386	8.007
	0.250	8.759	7.340	8.022	7.051	x	7.385	8.019
5f	0.016	8.765	7.358	8.043	7.063	x	7.387	8.005
	0.031	8.763	7.344	8.039	7.060	x	7.386	8.005
	0.062	8.757	7.348	8.032	7.054	x	7.385	8.005
	0.125	8.753	7.335	8.019	7.043	x	7.372	8.002
	0.250	8.744	7.316	8.002	7.025	x	7.372	8.002

Appendix 5: Structures and H-NMR data for 8-substituted monoether products.



6a-c

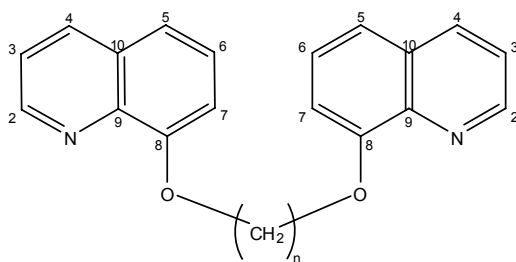
a: R=methyl

b: R=ethyl

c: R=propyl

	<u>C (M)</u>	H-2	H-3	H-4	H-5	H-6	H-7	H-8
6a	0.016	8.932	7.425	8.131	7.390	7.500	7.059	x
	0.031	8.931	7.424	8.130	7.389	7.499	7.058	x
	0.062	8.931	7.422	8.129	7.388	7.498	7.057	x
	0.125	8.929	7.419	8.124	7.385	7.495	7.054	x
	0.250	8.926	7.413	8.116	7.379	7.490	7.048	x
6b	0.016	8.965	7.421	8.130	7.379	7.477	7.069	x
	0.031	8.964	7.420	8.129	7.375	7.476	7.067	x
	0.062	8.962	7.418	8.128	7.371	7.472	7.064	x
	0.125	8.959	7.413	8.124	7.369	7.468	7.061	x
	0.250	8.953	7.406	8.113	7.366	7.462	7.054	x
6c	0.016	-	-	-	-	-	-	x
	0.031	8.965	7.424	8.137	7.389	7.471	7.077	x
	0.062	8.964	7.423	8.136	7.384	7.474	7.076	x
	0.125	8.961	7.416	8.128	7.380	7.465	7.070	x
	0.250	8.954	7.408	8.114	7.377	7.455	7.060	x

Appendix 6: Structures and H-NMR data for 8-substituted diether products.



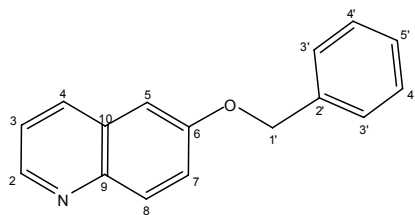
6d-e

d: n=6

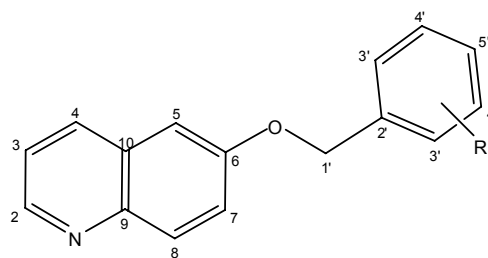
e: n=10

	<u>C (M)</u>	H-2	H-3	H-4	H-5	H-6	H-7	H-8
6d	0.016	8.956	7.398	8.132	7.384	7.465	7.072	x
	0.031	8.955	7.396	8.130	7.382	7.463	7.070	x
	0.062	8.953	7.392	8.126	7.379	7.460	7.068	x
	0.125	8.949	7.382	8.116	7.371	7.454	7.061	x
	0.250	8.944	7.372	8.100	7.358	7.444	7.049	x
6e	0.016	8.959	7.425	8.126	7.377	7.466	7.072	x
	0.031	8.959	7.425	8.126	7.377	7.465	7.072	x
	0.062	8.958	7.419	8.120	7.373	7.462	7.069	x
	0.125	8.955	7.408	8.109	7.364	7.455	7.062	x
	0.250	8.949	7.387	8.086	7.347	7.440	7.049	x

Appendix 7: Structures and H-NMR data for 6-substituted benzyl mono and diether products.



8



8a-c

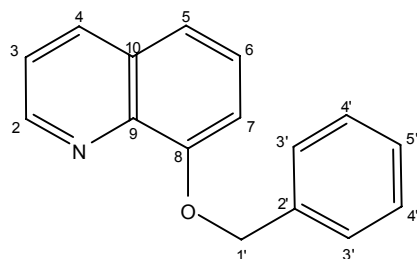
a: R=ortho

b: R=meta

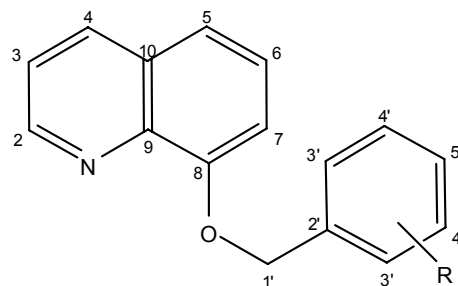
c: R=para

	C (M)	H-2	H-3	H-4	H-5	H-6	H-7	H-8
8	0.016	8.786	7.342	8.061	7.1694	x	7.42	8.038
	0.031	8.788	7.338	8.060	7.170	x	7.420	8.041
	0.062	8.786	7.337	8.058	7.168	x	7.418	8.043
	0.125	8.784	7.336	8.056	7.164	x	7.414	8.046
	0.250	8.778	7.330	8.046	7.155	x	7.408	8.044
8a	0.016	8.768	7.337	7.971	7.143	x	7.416	8.016
	0.031	8.766	7.335	7.969	7.142	x	7.415	8.016
	0.062	8.762	7.328	7.963	7.137	x	7.412	8.016
	0.125	8.757	7.319	7.954	7.131	x	7.409	8.015
	0.25	8.743	7.299	7.936	7.117		7.402	8.013
8b	0.016	8.79	7.365	8.005	7.16	x	-	8.038
	0.031	8.787	7.362	8.002	7.157	x	-	8.038
	0.062	8.783	7.354	7.994	7.149	x	-	8.036
	0.125	8.776	7.340	7.981	7.137	x	-	8.035
	0.250	8.764	7.317	7.961	7.116	x	-	8.032
8c	0.016	8.782	7.348	8.035	7.163	x	7.450	8.043
	0.031	8.778	7.348	8.034	7.162	x	7.449	8.043
	0.062	8.777	7.345	8.031	7.159	x	7.448	8.043
	0.125	8.776	7.345	8.031	7.159	x	7.448	8.044
	0.250	8.765	7.316	8.007	7.133	x	7.436	8.040

Appendix 8: Structures and H-NMR data for 8-substituted benzyl mono and diether products.



10



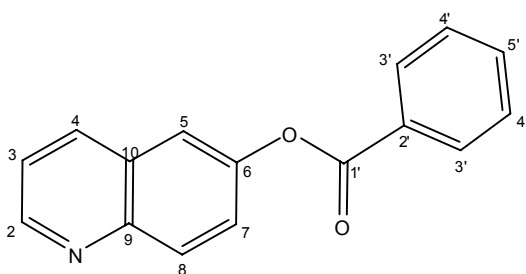
10a-c

a: R=ortho

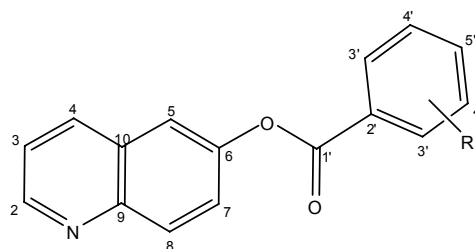
b: R=meta

	<u>C (M)</u>	H-2	H-3	H-4	H-5	H-6	H-7	H-8
10	0.016	8.975	7.426	8.122	7.024	-	7.533	x
	0.031	8.973	7.424	8.119	7.022	-	7.533	x
	0.062	8.972	7.420	8.115	7.020	-	7.532	x
	0.125	8.970	7.413	8.108	7.016	-	7.530	x
	0.250	8.965	7.401	8.095	7.009	-	7.526	x
10a	0.016	8.924	7.394	8.086	7.141	-	7.606	x
	0.031	8.923	7.393	8.085	7.140	-	7.606	x
	0.062	8.922	7.391	8.084	7.140	-	7.605	x
	0.125	8.920	7.388	8.080	7.138	-	7.605	x
	0.25	8.917	7.381	8.073	7.136	-	7.603	x
10b	0.016	8.957	7.419	8.115	6.983	-	7.450	x
	0.031	8.954	7.416	8.112	6.981	-	7.449	x
	0.062	8.950	7.410	8.106	6.979	-	7.446	x
	0.125	8.941	7.399	8.095	6.973	-	7.439	x
	0.250	8.929	7.380	8.077	6.966	-	7.430	x

Appendix 9: Structures and H-NMR data for 6-substituted benzoyl monoester and phthalate diester products.



7

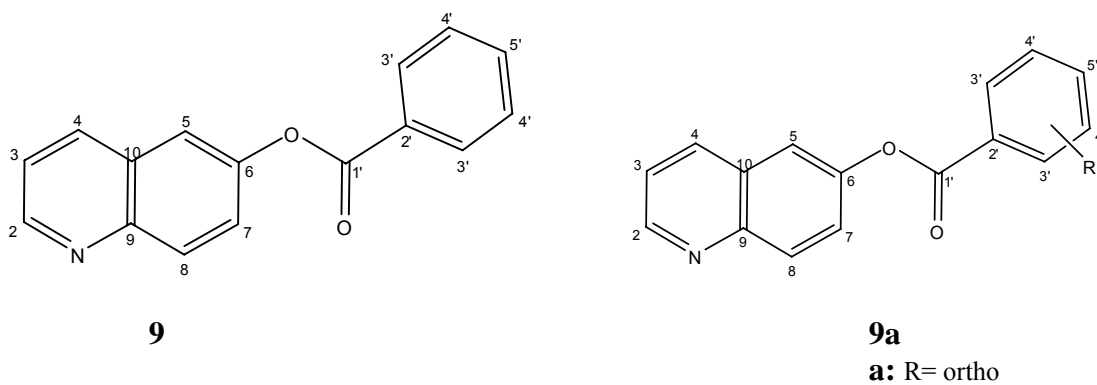


7a

a: R= ortho

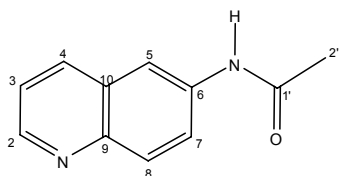
	<u>C (M)</u>	H-2	H-3	H-4	H-5	H-6	H-7	H-8
7	0.016	8.939	7.438	8.167	7.726	x	7.624	8.204
	0.031	8.940	7.436	8.165	7.725	x	7.623	8.208
	0.062	8.934	7.429	8.157	7.719	x	7.619	8.206
	0.125	8.930	7.419	8.147	7.713	x	7.617	8.204
	0.250	8.922	7.402	8.129	7.704	x	7.612	8.202
7a	0.016	8.914	7.398	8.101	7.715	x	7.612	8.160
	0.031	8.912	7.395	8.098	7.715	x	7.610	8.160
	0.062	8.910	7.391	8.095	7.713	x	7.610	8.159
	0.125	8.902	7.378	8.086	7.709	x	7.608	8.157
	0.25	8.891	7.359	8.059	7.704	x	7.588	8.155

Appendix 10: Structures and H-NMR data for 8-substituted benzoyl monoester and phthalate diester products.

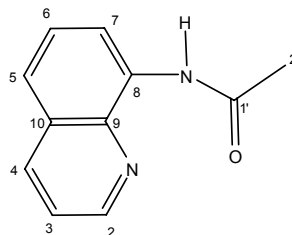


	<u>C (M)</u>	H-2	H-3	H-4	H-5	H-6	H-7	H-8
9	0.016	8.891	7.423	8.199	7.596	7.791	7.582	x
	0.031	8.891	7.420	8.197	7.594	7.788	7.580	x
	0.062	8.889	7.415	8.191	7.590	7.783	7.578	x
	0.125	8.884	7.403	8.178	7.581	7.773	7.565	x
	0.250	8.874	7.383	8.157	7.567	7.755	7.553	x
9a	0.016	8.902	7.420	8.182	7.730	7.516	7.583	x
	0.031	8.898	7.413	8.174	7.723	7.510	7.578	x
	0.062	8.892	7.402	8.163	7.714	7.502	7.575	x
	0.125	8.881	7.382	8.142	7.695	7.486	7.572	x
	0.250	8.868	7.353	8.113	7.670	7.463	7.563	x

Appendix 11: Structures and H-NMR data for 6-substituted monoamide products.



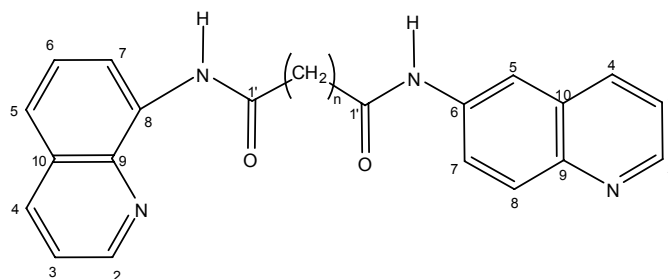
13



15

	C (M)	H-2	H-3	H-4	H-5	H-6	H-7	H-8
13	0.016	-	-	-	-	-	-	-
	0.031	8.841	7.404	8.139	8.369	x	7.553	8.052
	0.062	8.834	7.400	8.131	8.375	x	7.562	8.042
	0.125	8.829	7.393	8.116	8.385	x	7.576	8.026
	0.25	8.816	7.379	8.092	8.404	x	7.603	7.999
	0.5	8.793	7.349	8.046	8.428	x	7.670	7.965
15	0.016	8.733	7.465	8.220	8.417	x	7.757	7.981
	0.031	8.732	7.461	8.216	8.422	x	7.759	7.980
	0.062	8.731	7.462	8.208	8.421	x	7.764	7.980
	0.125	8.728	7.452	8.195	8.419	x	7.773	7.980
	0.250	-	-	-	-	-	-	-

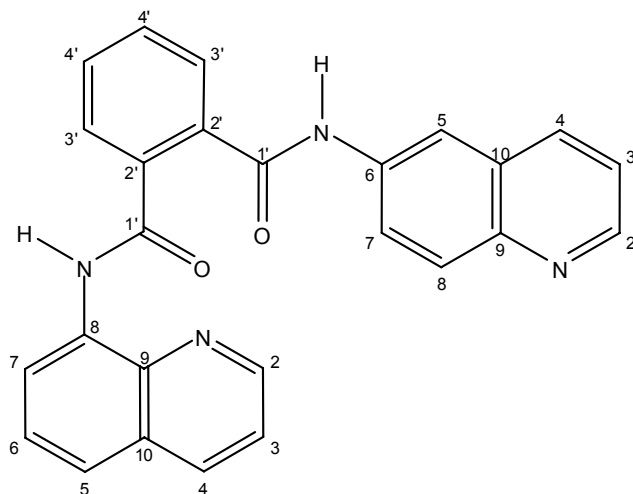
Appendix 12: Structures and H-NMR data for 6,8-unsymmetrical aliphatic and benzoyl diester products.



11a: n=6

11b: n=10

		6-Substituted quinoline ring							
		<u>C (M)</u>	H-2	H-3	H-4	H-5	H-6	H-7	H-8
11a	0.016	8.930	x	8.110	7.587	x	7.489	8.132	
	0.031	8.925	x	8.110	7.586	x	7.489	8.132	
	0.062	8.928	x	8.102	7.585	x	7.489	8.134	
	0.125	8.923	x	8.092	7.580	x	7.488	8.134	
	0.25	8.916	x	8.079	7.575	x	7.486	8.135	
11b	0.016	8.906	x	8.111	7.568	x	7.473	8.111	
	0.031	8.906	x	8.109	7.568	x	7.473	8.113	
	0.062	8.905	x	8.105	7.567	x	7.473	8.115	
	0.125	8.902	x	8.098	7.563	x	7.473	8.117	
	0.25	x	x	x	x	x	x	x	
		8-Substituted quinoline ring							
		<u>C (M)</u>	H-2	H-3	H-4	H-5	H-6	H-7	H-8
11a	0.016	8.930	x	8.201	7.749	7.544	7.467	x	
	0.031	8.925	x	8.199	7.748	7.543	7.467	x	
	0.062	8.928	x	8.194	7.743	7.540	7.466	x	
	0.125	8.923	x	8.182	7.730	7.532	7.464	x	
	0.25	8.916	x	8.166	7.717	7.522	7.463	x	
11b	0.016	8.906	x	8.188	7.730	7.532	7.451	x	
	0.031	8.906	x	8.186	7.729	7.532	7.450	x	
	0.062	8.905	x	8.180	7.723	7.527	7.450	x	
	0.125	8.902	x	8.167	7.712	7.519	7.448	x	
	0.25	x	x	x	x	x	x	x	



11c

		6-Substituted quinoline ring							
		<u>C (M)</u>	H-2	H-3	H-4	H-5	H-6	H-7	H-8
11c	0.016	8.930	x	8.110	7.587	x	7.489	8.132	
	0.031	8.925	x	8.110	7.586	x	7.489	8.132	
	0.062	8.928	x	8.102	7.585	x	7.489	8.134	
	0.125	8.923	x	8.092	7.580	x	7.488	8.134	
	0.25	8.916	x	8.079	7.575	x	7.486	8.135	
		8-Substituted quinoline ring							
		<u>C (M)</u>	H-2	H-3	H-4	H-5	H-6	H-7	H-8
11c	0.016	8.930	x	8.201	7.749	7.544	7.467	x	
	0.031	8.925	x	8.199	7.748	7.543	7.467	x	
	0.062	8.928	x	8.194	7.743	7.540	7.466	x	
	0.125	8.923	x	8.182	7.730	7.532	7.464	x	
	0.25	8.916	x	8.166	7.717	7.522	7.463	x	